The Investigation of Reactions of Atomic Metal Anions with Small Hydrocarbons and Alcohols in the Gas Phase

Thesis submitted to the

Faculty of Graduate & Postdoctoral Studies

University of Ottawa

in partial fulfillment of the requirements for the

M.Sc. degree in the

Ottawa-Carleton Chemistry Institute

August 2013

Candidate:

Jaleh Halvachizadeh

Supervisor:

Dr. Paul M. Mayer

To my father,

who taught me the love and value of studying

when he was among us

Acknowledgments

I would like to give special thanks to those who have helped me while I was working towards my Masters. I would not have been able to complete this project without them.

Firstly, I thank my supervisor Dr. Paul M. Mayer. Not only has he guided me along the way and shared his exceptional knowledge of chemistry, but he is also one of my role models. He has showed me that it is still possible to be successful even while managing dozens of tasks at the same time. I thank him for giving me the opportunity to live my dream as a chemist.

I thank Dr. John L. Holmes for teaching me about gas phase chemistry and for his constant patience and generosity in helping me when I needed it most.

I thank Dr. Sander Mommers and Dr. Sharon Curtis for their great knowledge about instruments.

I thank the professors for my graduate courses at the University of Ottawa who taught me the core knowledge of chemistry, Dr. John Holmes, Dr. Clem Kazakoff, Dr. Paul Mayer and Dr. Darrin Richeson.

I thank the administrative staff of the Chemistry Department at the University of Ottawa, especially Annette, Josée and Linda.

I thank members of Dr. Mayer's research group including Dr. Ameneh Gholami, Justin Renaud, Brandi West, Jeffery Butson, Mélanie Ouellette, Jenna Hamilton, Alex Mungham and Dhiya Hassan.

An important thank you goes to Ms. Jennifer Waterman for assistance with my English that enabled me to continue and complete my studies.

Lastly, but most importantly I thank my dear husband, Mehdi and my sweet boys, Siavash and Keyvan, for their love and constant support.

Table of Contents

List of Figures

List of tables

List of schemes

List of equations

List of abbreviations

amu: atomic mass unit
˚c: degree centigrade, a temperature unit
CID: collision induced dissociation
EA: electron affinity
ESI: electrospray ionization
eV: electron volt, an energy unit
$\Delta_{acid}H$: the gas phase acidity of a fragment
Δ_fH: the heat of formation of a fragment
Δ_rH: the enthalpy of a reaction
kJ/mol: kilojoules per mole, an energy unit
kV: kilo volt, an energy unit
mbar: milli bar, a pressure unit
min.: minutes
MS: mass spectroscopy
m/z: mass up on charge
sec.: seconds
V: volt, an energy unit

Abstract

Hydrocarbons are an abundant resource of carbon and hydrogen. For example, fossil can be used to produce useful organic compounds. However hydrocarbons seem to be inert. Thus, the activation of the C-H bond is a popular research area. Metals play the main role in most catalysts that convert hydrocarbons to starting materials in industry. The study of metals is important because the properties of the metal core greatly influences the reactivity of a catalyst.[1]

The study of the chemistry of metals in the gas phase provides valuable information about the properties of metals. This information can be expanded to the chemistry of metals in the condensed phase. Furthermore, it is often both more accurate and more manageable to study the profile of a reaction in the gas phase than in the condensed phase.[2,3]

There are many studies about metal cations in the gas phase due to ease of their production. However metals have low electronegativity, limiting the study of gas phase metal anions. Recently, a simple and efficient method to generate atomic metal anions was developed at the University of Ottawa in Dr. Mayer's research laboratory.[4-6] Atomic metal anions of Fe^-, Co^-, Cu^-, Ag^-, Cs^- and K^- were generated in an electrospray ionization (ESI) source of a mass spectrometer (MS).

In this thesis study generated metal anions were reacted with small hydrocarbons of pentane, 1-pentene, 2-pentene and 1-pentyne to investigate the role of different metal anions in the activation of the C-H bond. Also metal anions were reacted with small alcohols of 1-butanol, 2-butanol and 2-methyl-2-propanol to compare the results.

Metal anions showed a variety of reactions with these hydrocarbons and alcohols. Fe^- was the only metal anion to show the electron transfer reaction, indicating that alcohols are more electronegative than Fe^- and less electronegative than other metal anions. Fe^-, Co^- and Ag^- showed the complex formation reaction. All metal anions showed the deprotonation reaction. A deprotonation reaction follows the harpoon mechanism, the long range proton abstraction[7], and depends on the gas phase acidity of fragments. The most informative reaction observed was the dehydrogenation reaction because a metal-containing fragment is observed as a product in the spectrum of this reaction. The observation of a metal-containing fragment in the spectrum is significant because it emphasizes the important role that metal anions play in this reaction. This suggests that a dehydrogenation reaction involves metal insertion into a C-H bond. Among the transition metal anions, it was observed that Fe^- and Cu^- are more reactive than Co^- and Ag^- with regards to the dehydrogenation reaction, probably because Fe^- and Cu^- have a greater hydrogen affinity than Co^- and Ag^- that facilitates the hydrogen abstraction reaction. Another reason could be that Fe^- and Cu^- have a greater gas phase acidity that leads to a more stable intermediate in the course of the reaction. The results of this thesis study revealed that Cs^- and K^- could not abstract H from these substrates, probably due to the absence of occupied d orbitals that would facilitate insertion into a C-H bond.

Some metal anions not only can insert into a C-H bond of alcohols but also can insert into a C-O bond of alcohols to form metal hydroxide anions. Alcohols are more reactive than hydrocarbons with regards to reactions with metal anions because they contain a functional group.

This thesis study shows that some atomic metal anions are able to activate the C-H bond and abstract two hydrogens to form a double bond in hydrocarbons. It is probable that the electronic configuration, gas phase acidity and hydrogen affinity of the metal anions governs their reactivity.

Chapter 1: Introduction

1.1: The activation of the C-H bond by metal-containing cations

There are abundant sources of hydrocarbons in the earth that could be used to produce several useful starting materials to synthesis a variety of organic compounds. The main step in converting hydrocarbons to more valuable compounds is the activation of the C-H bond. Although methane is more abundant than other hydrocarbons, the activation of the C-H bond of methane is more challenging than the activation of the C-H bond of other hydrocarbons. Studies exist on converting methane to more valuable compounds such as methanol as a source of starting material in the fuel industry.[8] Too, Metals and metal-containing compounds can be used as catalysts to convert hydrocarbons to more useful products. There are also studies on the reactivity of metals and metal-containing compounds with hydrocarbons, focusing on the properties of the metal core.[1]

A variety of reactions of bare or ligated as well as neutral or charged metal atoms or metal-containing compounds, shown as [M], with C-H bond have been summarized by Dr. Schroder and Dr. Schwarz.[8] Their study indicates that five types of reactions can take place in those reactions (reactions 1 to 5).

a) Deprotonation $H_3C\text{-}H + [M] \rightarrow CH_3^- + [MH]^+$ (1)

b) Hydride trasfer $H_3C\text{-}H + [M] \rightarrow CH_3^+ + [MH]^-$ (2)

c) H-atom abstraction $H_3C\text{-}H + [M] \rightarrow CH_3^{\cdot} + [MH]$ (3)

d) Insertion $H_3C\text{-}H + [M] \rightarrow CH_3\text{-}[M]\text{-}H$ (4)

e) Carbene formation $H_3C\text{-}H + [M] \rightarrow [M]{=}CH_3 + H_2$ (5)

Dr. Schroder and Schwarz suggested that bare metal cations are more reactive than metal-containing cations. Through the investigation of the effect of the ligand on the reactivity of metal-containing cations, they found that closed-shell ligands, such as CO and H_2O, lower the reactivity of metal-containing cations and increase the selectivity. $Fe(H_2O)^+$ inserts into a C-H bond and $Fe(CO)^+$ inserts into a C-C bond. Pt^+ is seven times more reactive than $PtAr^+$ in the dehydrogenation reaction with methane while $PtAr_n^+$ does not activate methane. Furthermore, open-shell ligands, such as F and OH, increase the reactivity of metal-containing cations. Cr^+ is less reactive than $CrCl^+$ in regards to the activation of the C-H bond. CrF^+ dehydrogenates propane whereas CrF_3^+ and CrF_4^+ can activate methane.

The structure of intermediates in reactions of metals with alkanes has been reviewed by Dr. Hall and Dr. Perutz.[9] They investigated the bond lengths and bond energies of metal alkane complexes and suggested that a metal can be reactive when the complex between the metal and alkane is stable.

1.2: The activation of the C-H bond by bare metal cations

Dr. Gross and his coworkers showed that Fe^+ and Mo^+ are highly reactive cations in the reaction with aliphatic alcohols whereas Cr^+ is less reactive.[10]

Dr. Weisshaar showed that Sc^+, Ti^+, V^+, Fe^+, Co^+, and Ni^+ can activate a C-H bond and show the dehydrogenation reaction, whereas Cr^+, Mn^+, Cu^+ and Zn^+ are not able to activate a C-H bond.[1] His study suggests that the electronic configuration of the metal

cations governs their reactivity. In the condensed phase, the insertion of a metal center into a C-H bond is known as the oxidative addition reaction.

Dr. Roithova and Dr. Schroder reviewed the activation of alkanes by metal cations and suggested that 3d and 4d transition metal cations are not able to activate methane in thermal energy.[11] Their study suggests that in the reaction of the metal cation with methane, the metal cation inserts into the C-H bond to form an intermediate. Then an α-H shift, α-H elimination, takes place allowing a molecular hydrogen to leave the intermediate. Subsequently, a metal-carbene cation, MCH_2^+, will be produced. During this reaction the formal oxidation state of the metal will increase by two. Thus, only metals that are able to change their oxidation number can activate methane. Furthermore, the reaction should be exothermic. In other words, the amount of energy that is produced by the formation of M-C and H-H bonds should be more than the amount of energy used to break two C-H bonds. However, in reactions of alkanes other than methane with metal cations, a β-H shift, β-H elimination, takes place.

Dr. Blomberg and his coworkers performed AB initio quantum chemical calculations for reactions of methane with second-row transition metals and metal cations.[12] Results of these calculations show that at the left and in the middle of the periodic table metal cations have lower barrier for activation of a C-H bond, whereas on the right of the periodic table neutral metals have a lower barrier for activation of a C-H bond. The barrier or activation energy is the energy required to form an intermediate complex from starting materials in a reaction.

1.3: The activation of the C-H bond by metal-containing anions

There have been a limited number of studies investigating the reactions of metal anions and metal-containing anions with neutral substrates. Dr. Squires reviewed the chemistry of metal-containing anions including methods of generation, thermochemistry and reactivity of metal anions and metal-containing anions.[13] His study suggests that metal-containing anions show three kinds of reactions: ligand substitution, reactions with dioxygen and oxidative insertion/reductive elimination. Below are several examples of such reactions:

$CpCo(CO)_2^-$ and $CpCo(CO)^-$ react with NO and PF_3 to form substituted products (reactions 6 to 9):

$$CpCo(CO)_2^- + NO \rightarrow CpCo(NO)^- + 2CO \quad (6)$$

$$CpCo(CO)_2^- + PF_3 \rightarrow CpCo(CO)PF_3^- + CO \quad (7)$$

$$CpCo(CO)^- + NO \rightarrow CpCo(NO)^- + CO \quad (8)$$

$$CpCo(CO)^- + PF_3 \rightarrow CpCo(PF_3)^- + CO \quad (9).$$

The following example shows that oxygen can substitute ligands in a metal carbonyl anion (reaction 10):

$$M(CO)_n^- + O_2 \rightarrow M(CO)_xO_2^- + (n-x)CO \quad (10).$$

Metal-containing anions react with a variety of organic compounds by oxidative addition/reductive elimination (reactions 11 to 17):

$$(CO)_4Fe^- + ICF_3 \rightarrow (CO)_4FeI^- + CF_3 \quad (11)$$

$$(CO)_3Fe^- + H_2 \rightarrow (CO)_3FeH_2^- \quad (12)$$

$(CO)_2Fe^- + 2H_2O \rightarrow (CO)Fe(OH)_2^- + H_2 + CO$ (13)

$(CO)Fe^- + H_2S \rightarrow (CO)FeS^- + CO + H_2$ (14)

$(CO)_3Mn^- + NH_3 \rightarrow (CO)_3Mn(NH_3)^-$ (15)

$Mn(CO)_3^- + CH_3OH \rightarrow (CO)_3Mn(H_2CO)^- + H_2$ (16)

$M(CO)_n^- + RCl \rightarrow ClM(CO)_{n-m}^- + R + mCO$ (17).

Dr. McElvany and Dr. Allison show that metal-containing anions such as $Fe(CO)_{3,4}^-$, $Cr(CO)_{3\text{-}5}^-$ and $Co(CO)_{2,3}^-$ are not able to insert into a C-H bond and only insert into a C-X bond, where X is a functional group.[14] The predominate reaction between metal carbonyl anions and neutral organic molecules is the ligand substitution reaction. In order to investigate the effect of ligand on the reactivity, metal-containing anions that were containing different numbers of ligands were tested. The result shows that 17-electron anions ($M(CO)_{n-1}^-$), are unreactive in the gas phase, whereas 15-electron anions ($M(CO)_{n-2}^-$) are reactive. Thus, the more reactive anions of metal carbonyls, such as $Fe(CO)_3^-$ from $Fe(CO)_5$ and $Cr(CO)_4^-$ from $Cr(CO)_6$, were generated and were reacted with n-chloroalkanes. These experiments show that metal carbonyl anions can insert into the C-X bond and then undergo a β-hydrogen shift rearrangement. Metal-carbonyl anions show three types of reactions with alcohols and chloroalkanes: ligand substitution, chlorine abstraction and HCl abstraction (Scheme 1).

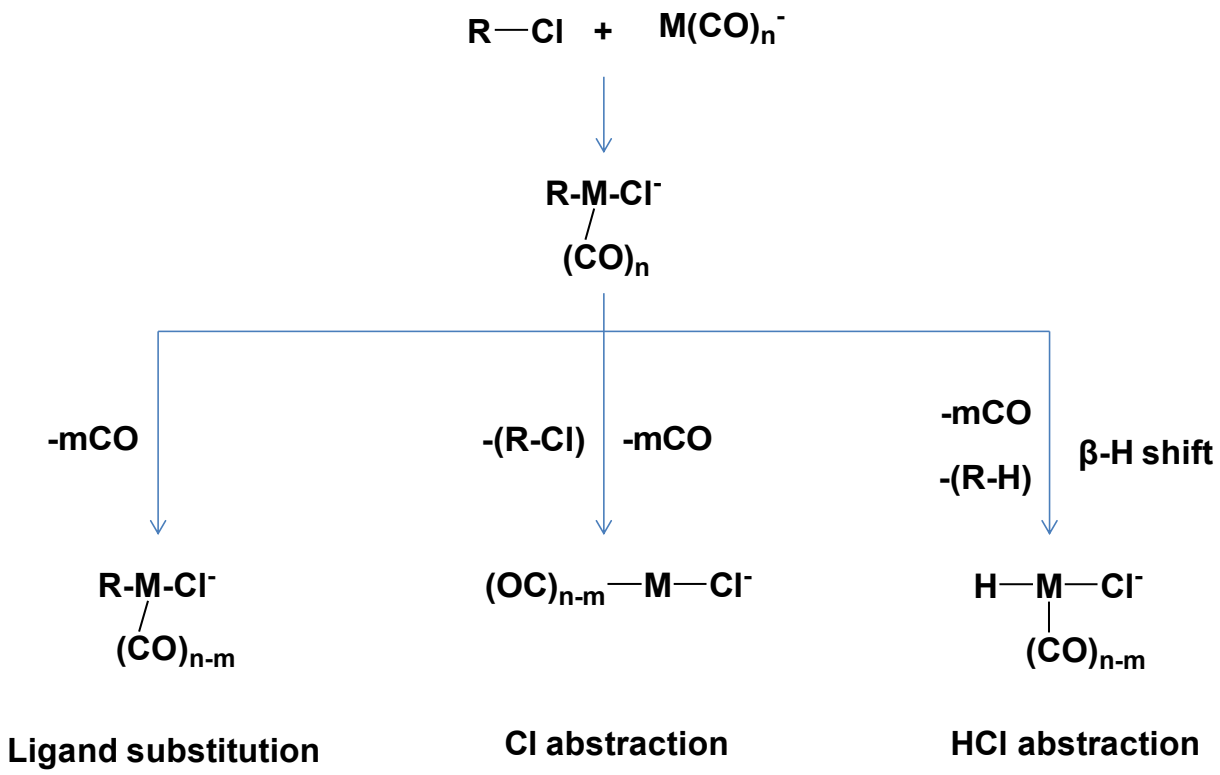

Scheme 1: Products of the reaction of metal-carbonyl anions with chloroalkanes

In the first step of this mechanism, the metal carbonyl anion makes a three centre-two electron bond with the σ halide-carbon bond of the haloalkane to form the intermediate complex. Next, the negative charge of the metal transfers to the halide atom because the halide is more electronegative than the metal. This step is the rate determining step of the mechanism and leads to the breakage of the halide-carbon bond and forms the intermediate. Finally, the intermediate of the metal insertion reaction can dissociate into products in such a way that the weakest bond will cleave and the negative charge will remain on the more electronegative fragment of the dissociation.

1.4: The formation of atomic metal anions

There are many studies on the chemistry of metal cations due to the ease of their production. Metals are the most electropositive elements in the periodic table. In contrast, there are only a few methods to generate metal anions such as FT-ICR, FA and the Knudson cell.[13] In the Fourier transform ion cyclotron resonance mass spectroscopy (FT-ICR or FT-MS), ions are generated in a trap by the electron impact ionization method and are separated according to their resonance frequency in the magnetic field surrounding the trap. Selected ions may remain in the trap for a longer period of time for further investigation, while the rest of the ions will leave the trap. In flowing afterglow (FA), ions are generated by the electron impact method and are carried by a buffer gas, such as helium, through the flow tube. Ions with the desired charge are separated at the end of the flow tube and focused into a quadrupole mass spectrometer. In the Knudsen cell method, metal-containing compounds such as K_2CrO_4 are heated to 1000 ˚k to produce a saturated vapor of ions and neutrals. For production of anions with this method, alkali metals can be mixed with the metal-containing compound as a reduction agent. Desired ions are transferred into a single-focusing mass spectrometer.

1.5: The formation of atomic metal anions by ESI

Previous methods of the generation of atomic metal anions are not readily implemented. In this thesis study, metal anions were generated by a simple and efficient method recently developed in Dr. Mayer's laboratory.[4-6] First, a solution of oxalic acid in

methanol (solution 1) and a solution of metal salt in methanol (solution 2) are made (Scheme 2).

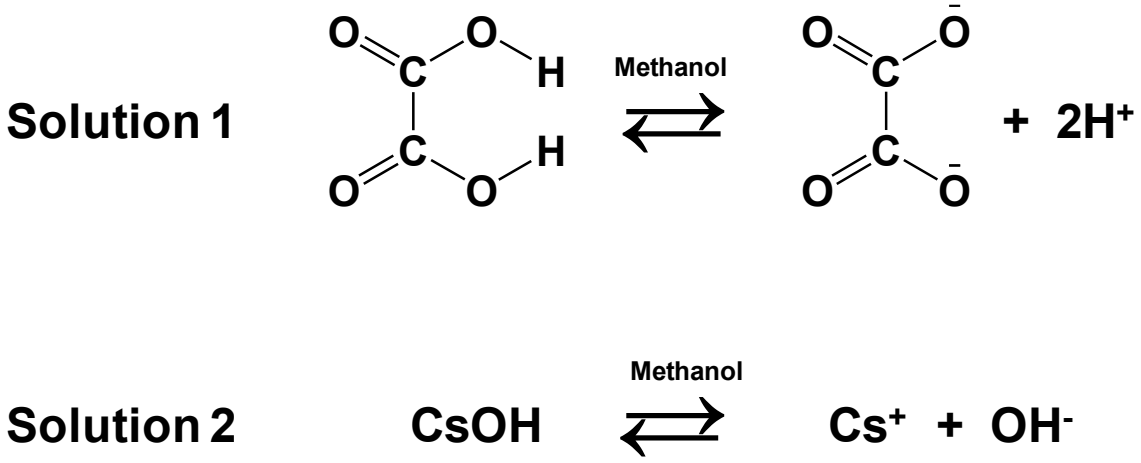

Scheme 2: Solution 1) Produced ions in a solution of oxalic acid in methanol; Solution 2) Produced ions in a solution of cesium hydroxide in methanol

These two solutions were then mixed by one-to-one ratio and diluted to the concentration of 10^{-5} molar. A metal oxalate complex forms in the mixture of these two solutions. With singly charged metals, the complex contains one oxalate. With triply charged metals, the complex contains two oxalates. With triply charged metals a two-to-one ratio of oxalic acid solution is mixed with metal salt solution. With doubly charged metals, instead of oxalic acid, tricarbalilic acid ($C_6O_6H_8$) is used to make solutions. Tricarbalylic acid has three carboxilate sites. All these complexes carry one negative charge (Scheme 3).

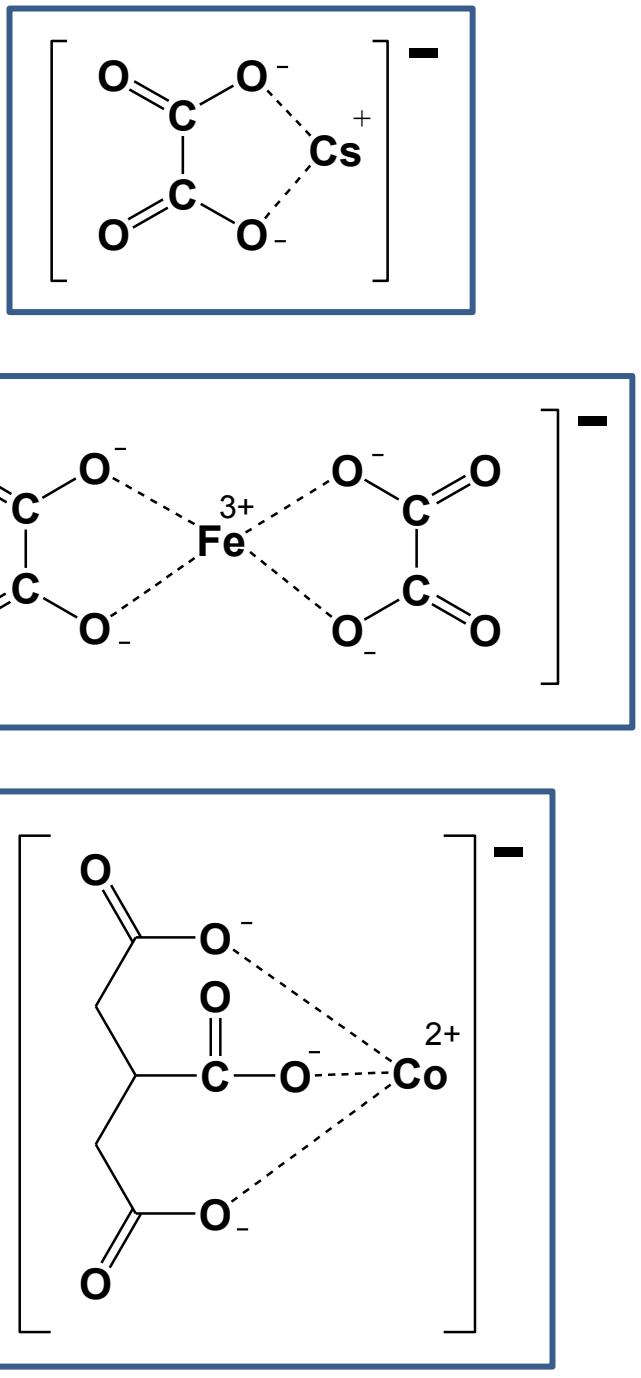

Scheme 3: Examples of formed complexes in the mixture of the solution of oxalic acid or tricarbalilic acid and the solution of metal salt

The diluted solution is injected into an electrospray ionization (ESI) source of a mass spectrometer. The complex will dissociate upon collision with atmospheric gas in the source region (CID) to two neutral CO_2 molecules and the metal anion (Scheme 4)[4,5].

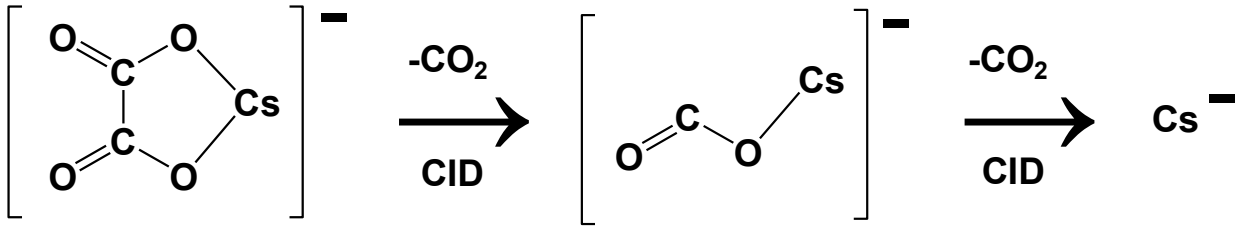

Scheme 4: The decomposition pattern of the cesium oxalate complex anion in the ESI source

The negative charge of the complex will remain on the metal because metals have higher electron affinity than CO_2, leading to the formation of metal anions (Table 1).[4]

Table 1: Electron affinity values for metals and CO_2

Fragment	CO_2	Fe	Co	Cu	Ag	Cs	K
Electron Affinity, eV	-0.104	0.151	0.6633	1.236	1.304	0.472	0.501

1.6: Ion molecule reactions

Reactions in a mass spectrometer take place by ion- neutral collisions. Thus, it is important to study the nature of a collision.[2,3] Reactive collisions in the mass spectrometer are assumed to occur via the formation of an encounter complex: $[M\ldots AB]^-$ (reaction 18).

$$M^- + AB \rightarrow [M\ldots AB]^- \rightarrow \text{products} \qquad (18)$$

In a mass spectrometer, ions move, so they have translational energy. This energy is called the laboratory-frame translational energy. Only part of the translational energy of the ion can be converted into the internal energy of the ion-neutral complex formed upon a collision. The center-of-mass translational energy is the maximum amount of laboratory-frame translational energy that can be transferred to internal (vibrational and rotational) energy in a collision. The laboratory-frame and the center-of-mass translational energies are related by the following equation:

Equation 1: The relationship between the laboratory-frame and the center-of-mass translational energies

$$E_{com} = E_{lab}\left(\frac{m_{target}}{m_{target} + m_{ion}}\right)$$

In an elastic collision, the internal energy of the ion and the neutral fragment will not change. In other words the translational energy of the ion will not be transferred to atoms or bonds in the encounter complex.

In an inelastic collision, the translational energy of the projectile ion will be transferred to the internal energy of the encounter complex. This process will form a collisionally activated complex that can lead to products. There are generally three kinds of processes that can take place in an inelastic collision:

1-Electronic excitation

2-Impulsive collision

3-Sticky collision

Electronic excitation is only important for collisions in the KeV range, while impulsive collisions (the ones investigated here) produce translational to vibrational energy transfer at eV collision energies. Sticky collisions are generally defined as when a long-lasting encounter complex is formed.

Reactions outlined in this thesis study take place by an impulsive collision. The internal energy of the formed complex distributes to some degree among the bonds to raise the vibrational energy of bonds. The bonds receiving a sufficient vibrational energy will break.

1.7: Objectives

In the present study, metal anions were allowed to react with neutral target gases in the collision cell of an ESI triple quadrupole mass spectrometer. Abundant sources of hydrocarbons can be used for the production of more industrially valuable compounds; thus, the activation of a C-H bond is a popular research area. Metal-containing anions cannot activate the C-H bond. In addition, metal anions might be more reactive than metal-containing anions due to their lower coordination number. Therefore, metal anions might be able to activate the C-H bond.

The goal of this thesis study was to compare the reactivity of the first row transition metal anions with each other. However, it was limited to experiments only with metal anions that can be generated in an ESI source, such as Fe^-, Co^-, Cu^-, Ag^-, Cs^- and K^-. So far, other metal anions cannot be generated in an ESI source because either the production of metal oxide anions are energetically more favorable than the production of

metal anions or an ESI source cannot provide suitable amount of energy for the production of these metal anions.

Small hydrocarbons were chosen to study the activation of the C-H bond. Hydrocarbons with five carbon atoms are the optimum size to experiment with because they are liquid and more readily implemented in the instrument than gases or solids. Furthermore, these hydrocarbons have enough vapor pressure to flow into the collision cell spontaneously. Comparing the result of reactions of hydrocarbons with the result of reactions of alcohols helps the investigation of the functional group effect on the reactivity. Same sized primary, secondary and tertiary alcohols with high enough vapor pressure to flow into the collision cell were selected to react with metal anions. The following substances were used as organic samples: pentane, 1-pentene, 2-pentene, 1-pentyne, 1-butanol, 2-butanol and 2-methyl-2-propanol.

Chapter 2: Experimental procedures

2.1: The schema of the ESI-MS

All experiments were performed in the negative mode of a Micromass electrospray ionization triple quadrupole mass spectrometer (Figures 1 and 2).[15]

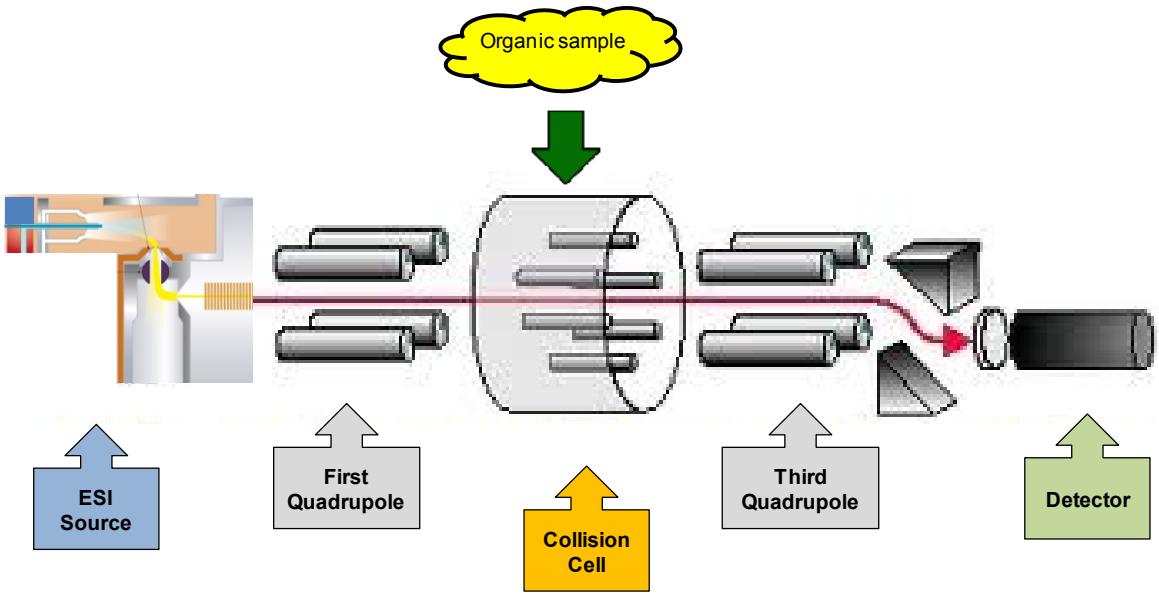

Figure 1: Schematic diagram of an electrospray ionization (ESI) triple quadrupole mass spectrometer; The prepared solution is injected into the ESI source where metal anions and other ions are generated; Metal anions are separated in the first quadrupole and are allowed to travel inside the instrument as a beam until they reach the detector; Organic samples are introduced into the collision cell to react with metal anions; Products are separated in the third quadrupole; The detector counts the ions

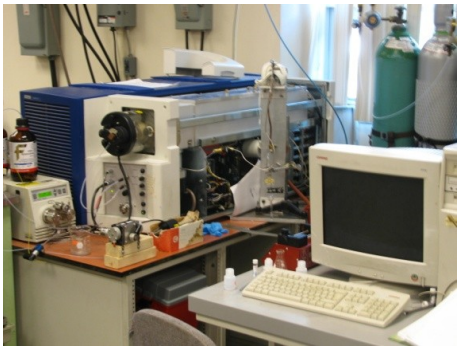

Figure 2: The electrospray ionization (ESI) triple quadrupole mass spectrometer used to perform indicated experiments in this thesis study

2.2: Preparing solutions

A 0.01 molar solution of oxalic acid in methanol was prepared (solution 1). A 0.01 molar solution of metal salt in methanol was prepared (solution 2). 10 µl of solution 1 and 10 µl of solution 2 and 980 µl of methanol were mixed to form a 10^{-4} molar mixture solution. The latter mixed solution can be diluted to form a 10^{-5} molar or a 10^{-6} molar metal oxalate solution (solution 3). When the metal has the oxidation number of 1, the solution 1 and the solution 2 were mixed with one-to-one ratio. When the metal has the oxidation number of 3, the solution 1 and the solution 2 were mixed with two-to-one ratio. For metals with the oxidation number of 2, instead of oxalic acid, tricarbalilic acid was used to prepare solutions.

To produce higher yields of metal anion in the ESI source, a three-fold molar excess of acid to the metal salt was typically used, in order to push the equilibrium toward metal oxalate complex formation (reaction 19).

$$Cs^+ + C_2O_4^{2-} \xrightleftharpoons{\text{Methanol}} [CsC_2O_4]^- \qquad (19)$$

2.3: Introducing the organic sample into the collision cell

In a reaction experiment, the organic sample needs to be placed in the instrument without a considerable increase in the internal pressure of the instrument. Also, the oxygen in the air can interfere with the result of experiments. About 0.2 ml of the organic sample is placed in the related vial and then the vial containing the organic sample is frozen with liquid nitrogen. The tubing is pumped by a roughing pump to empty it from air. The Granville-Phillips (GP) variable leak valve is gradually opened between the organic compound vial and the collision cell until enough pressure of the target gas is established in the collision cell (Figure 3).

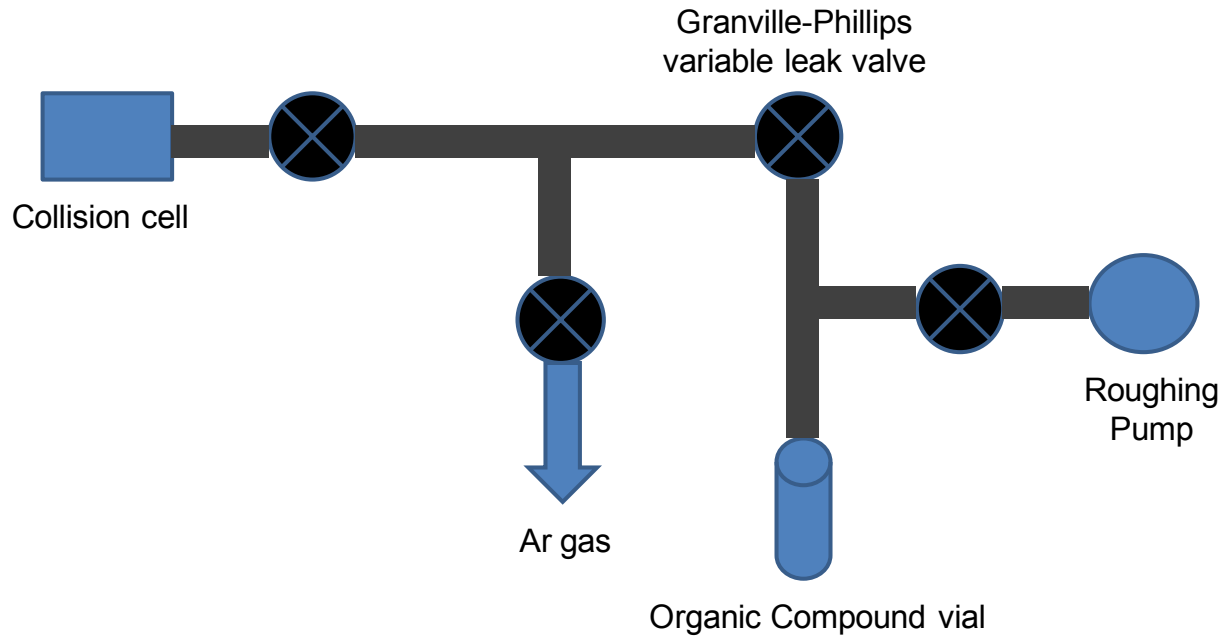

Figure 3: The schematic diagram of the designed tubing to introduce the organic sample into the collision cell

The roughing pump is not very powerful. As a consequence, even after three freeze-thaw cycles some air will still remain in the tubing. This researcher chose to use the help of the more powerful turbo pump of the instrument to lower the amount of air remaining in the tubing. This was done by leaving the GP valve open for five minutes while keeping the organic sample vial in the liquid nitrogen container. Then the GP valve was left half open to prevent air entering into the tubing until the organic sample in the vial had melted. Then the valve was optimized to maintain the desired pressure of the target gas in the collision cell.

2.4: The types of experiments

One can perform three types of experiments with an ESI triple quadrupole MS instrument, depending on the goal of the experiment.

2.4.1: All RF experiments

In an all RF experiment, all ions made in the source are allowed to travel through the instrument to reach the detector. This was done to determine whether the desired ions were made in the source. For example, the existence of m/z of 232 $(Fe(C_2O_4)_2)^-$ in a solution of iron oxalate can be checked in the mass spectrum of this solution to test the suitability of the prepared solution of iron oxalate to generate the iron anion.

2.4.2: Collision induced dissociation experiments (CID)

In these experiments an ion with the desired m/z is selected in the first quadrupole which is then allowed to travel through the instrument. One can select the m/z of the desired metal anion in order to perform further experiments on it. Meanwhile, in the collision cell, one can introduce the Ar gas as a collision gas. For example, one can choose the m/z of a metal anion (63 for Cu^-) in the first quadrupole and collide it with Ar in the collision cell at different voltages to check the purity of the metal anion beam. All selected ions have m/z 63 which could be Cu^-, the metal anion, or $C_2H_7O_2^-$, a deprotonated dimer of methanol. When Cu^- collides with Ar, it will remain the same and it will not dissociate. As a result in all different collision energies only m/z 63 (Cu^-) will be observed in the spectrum of the CID experiment. However, when $C_2H_7O_2^-$ collides with Ar, it will dissociate to CH_3O^- and CH_3OH in the proper collision energy and as a result m/z 31 (CH_3O^-) will be observed in addition to m/z 63 in the spectrum of the CID experiment.

2.4.3: Reacting metal anions with organic samples

In these experiments an ion with the desired m/z, more often the m/z of a metal anion, is selected in the first quadrupole and is allowed to travel through the instrument to reach the detector. Meanwhile, in the second hexapole or collision cell, one introduces the organic sample as a reactant gas (Figure 4).

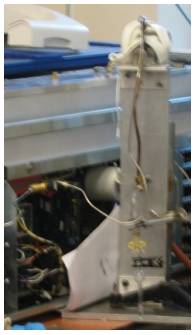

Figure 4: The designed device to introduce the organic sample into the collision cell

Products of the reaction of a metal anion with the organic sample that have a negative charge on them will be detected in the detector. An example of this type of experiment is one when the m/z 56 is selected in the first quadrupole and reacted with pentane gas in the second hexapole to investigate the reactions of Fe^- with pentane. As the collision energy is raised, the produced signals broaden and their intensity decreases because scattering of ions increases. With a greater collision energy, other reactions may be observed as more energy is provided for the system.

Chapter 3: Results and discussion of reactions of hydrocarbons

In this research, six metal anions of Fe^-, Co^-, Cu^-, Ag^-, Cs^- and K^- were allowed to react individually with seven organic samples of pentane, 1-pentene, 2-pentene, 1-pentyne, 1-butanol, 2-butanol and 2-methyl-2-propanol. The ionic products of the reactions were mass analyzed by the third quadrupole to produce the mass spectrum. A mass spectrum is a plot of m/z of signals versus the intensity of them. The instrument is set in the negative mode; thus, only negative, and not neutral, fragments are observed in the mass spectrum. Products of reactions in this thesis study produced low intensity signals in the mass spectrum due to the low reactivity of the starting materials.

At different energies in the collision cell, different fragments may be produced. Fragments that need less energy to be produced appear at lower collision energies, whereas fragments that need more energy to be produced appear at higher collision energies. However, increasing the collision energy causes broadening of signals as well as decreasing of the intensity of signals due to the scattering of ions which may cause some unwanted signal overlapping.

What follows are results of each set of reactions individually with their mass spectra as well as discussion on relative observations:

3.1: Reactions with pentane

3.1.1: Reactions of pentane with Fe^-

With the collision voltage of 0 eV, no reaction was observed. With the collision voltage of 5 eV, m/z 56 (Fe^-) and m/z 58 (FeH_2^-) were observed in the mass spectrum of the reaction of Fe^- with pentane (Figure 5).

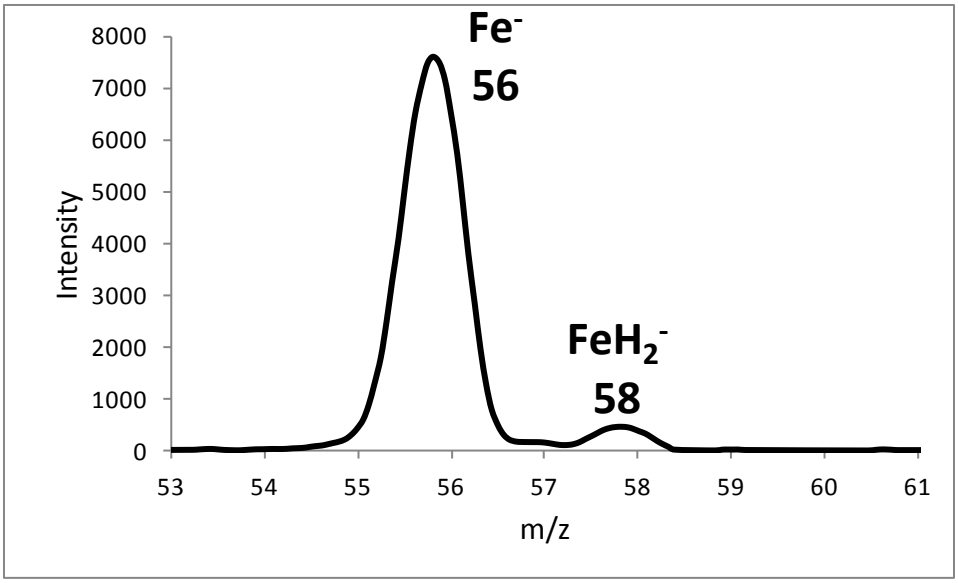

Figure 5: Mass spectrum of the reaction of pentane with Fe^- in voltages of (50-5-50) and the target gas pressure of 1.2 e-3 mbar

FeH_2^- is a product of the bisdehydrogenation reaction of pentane with Fe^- (reaction 20).

$$C_5H_{12} + Fe^- \rightarrow C_5H_{10} + FeH_2^- \quad (20)$$

To confirm that m/z 58 is not an artifact, the experiment was repeated with deuterated pentane. In deuterated pentane all hydrogens, with the atomic weight of 1 amu, were exchanged with deuterium, with the atomic weight of 2 amu. Thus, the m/z of related produced fragments will have a shift. In the mass spectrum of the reaction of pntane-d_{12} with Fe^- the signal of FeH_2^- shifted by 2 mass units (Figure 6).

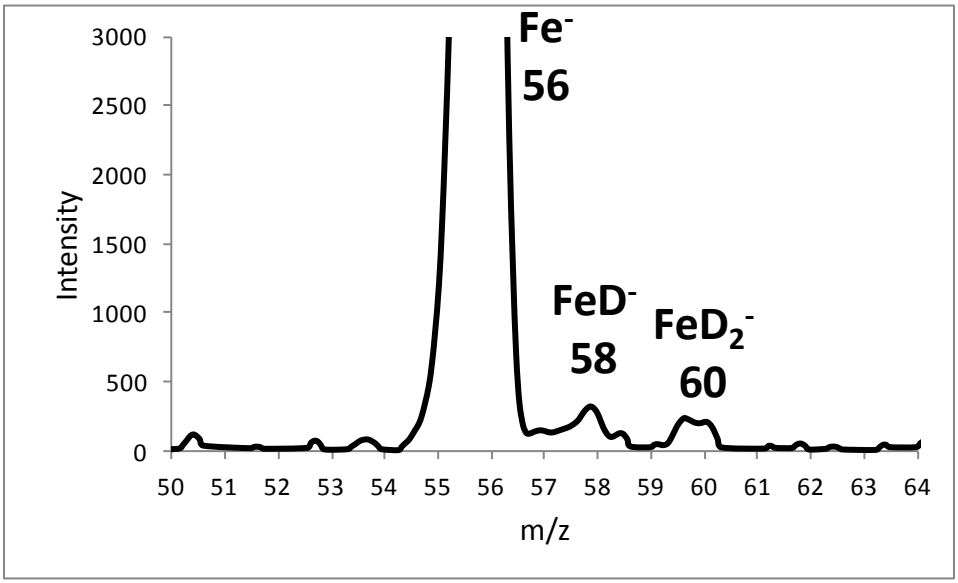

Figure 6: Mass spectrum of the reaction of pentane-d_{12} with Fe^- in voltages of (50-5-50) and the target gas pressure of 1.2 e-3 mbar

With the collision voltage of 10 eV, m/z 56 (Fe^-); m/z 57 (FeH^-) and m/z 58 (FeH_2^-) were observed (Figure 7).

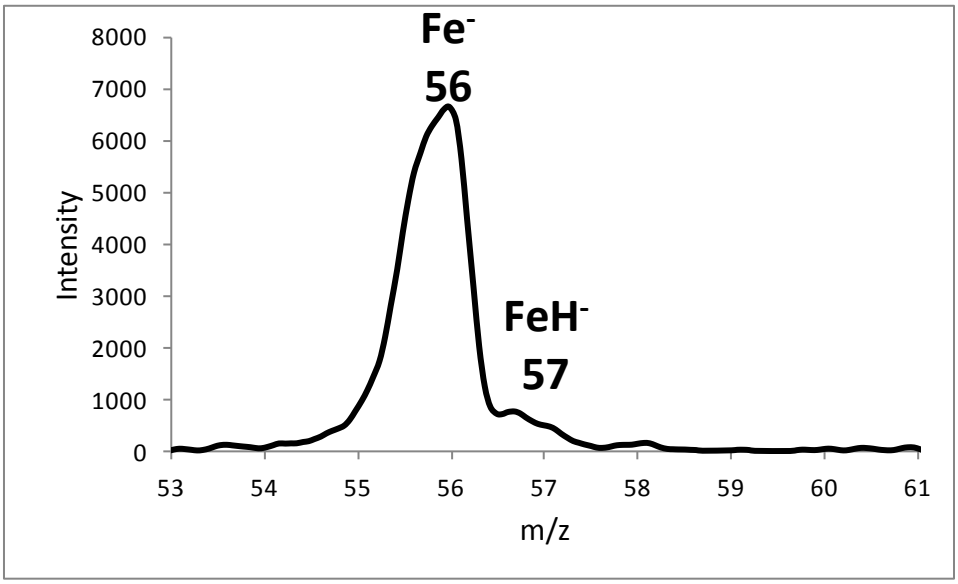

Figure 7: Mass spectrum of products of the reaction of pentane with Fe^- in voltages of (50-10-50) and the target gas pressure of 1.2 e-3 mbar

FeH^- is a product of the dehydrogenation reaction of pentane with Fe^- (reaction 21).

$$C_5H_{12} + Fe^- \rightarrow C_5H_{11} + FeH^- \quad (21)$$

In the reaction of Fe^- with deuterated pentane the signal of FeH^- shifted by 1 mass unit (Figure 6).

With the collision voltage of higher than 15 eV only m/z 56 (Fe^-) was observed.

3.1.2: Reactions of pentane with Co^-

At all collision energies, no reaction was observed. Thus, pentane shows no reaction with Co^-.

3.1.3: Reactions of pentane with Cu^-

With the collision voltage of 0 eV, no reaction was observed. With the collision voltage of 10 eV, m/z 65 (Cu^-); m/z 66 (CuH^-) and m/z 67 (CuH_2^-) were observed (Figure 8).

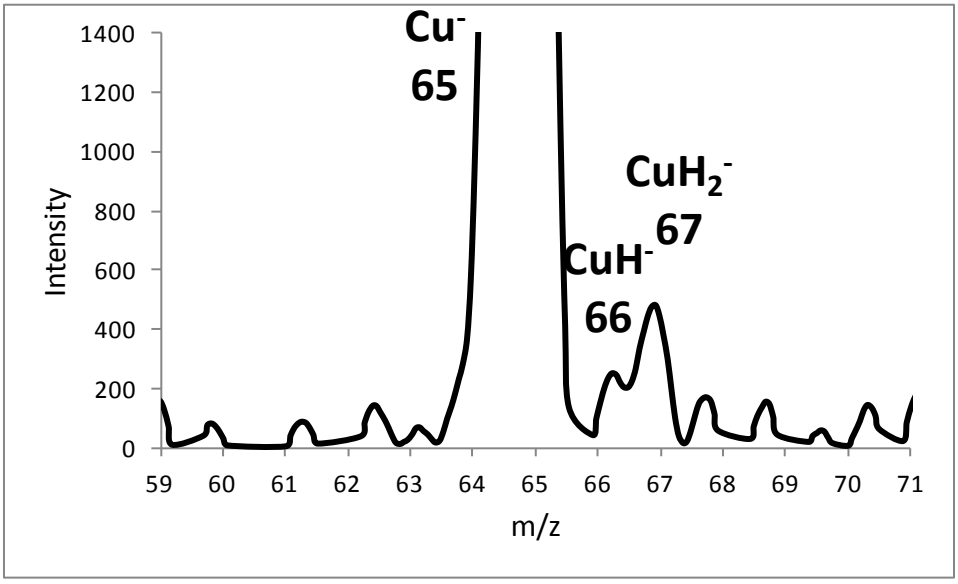

Figure 8: Mass spectrum of products of the reaction of pentane with $^{65}Cu^-$ in voltages of (50-10-50) and the target gas pressure of 1.2 e-3 mbar

CuH^- is a product of the dehydrogenation reaction of pentane with Cu^-. CuH_2^- is a product of the bisdehydrogenation reaction of pentane with Cu^- (reactions 22 and 23).

$$C_5H_{12} + Cu^- \rightarrow C_5H_{11} + CuH^- \quad (22)$$

$$C_5H_{12} + Cu^- \rightarrow C_5H_{10} + CuH_2^- \quad (23)$$

To confirm that m/z 66 and m/z 67 are not artifacts, the experiment was repeated with the deuterated pentane. With the collision voltage of 10 eV, the signal of CuH^- shifted by 1 mass unit and the signal of CuH_2^- shifted by 2 mass units in the mass spectrum of the reaction of pentane-d_{12} with Cu^- (Figure 9).

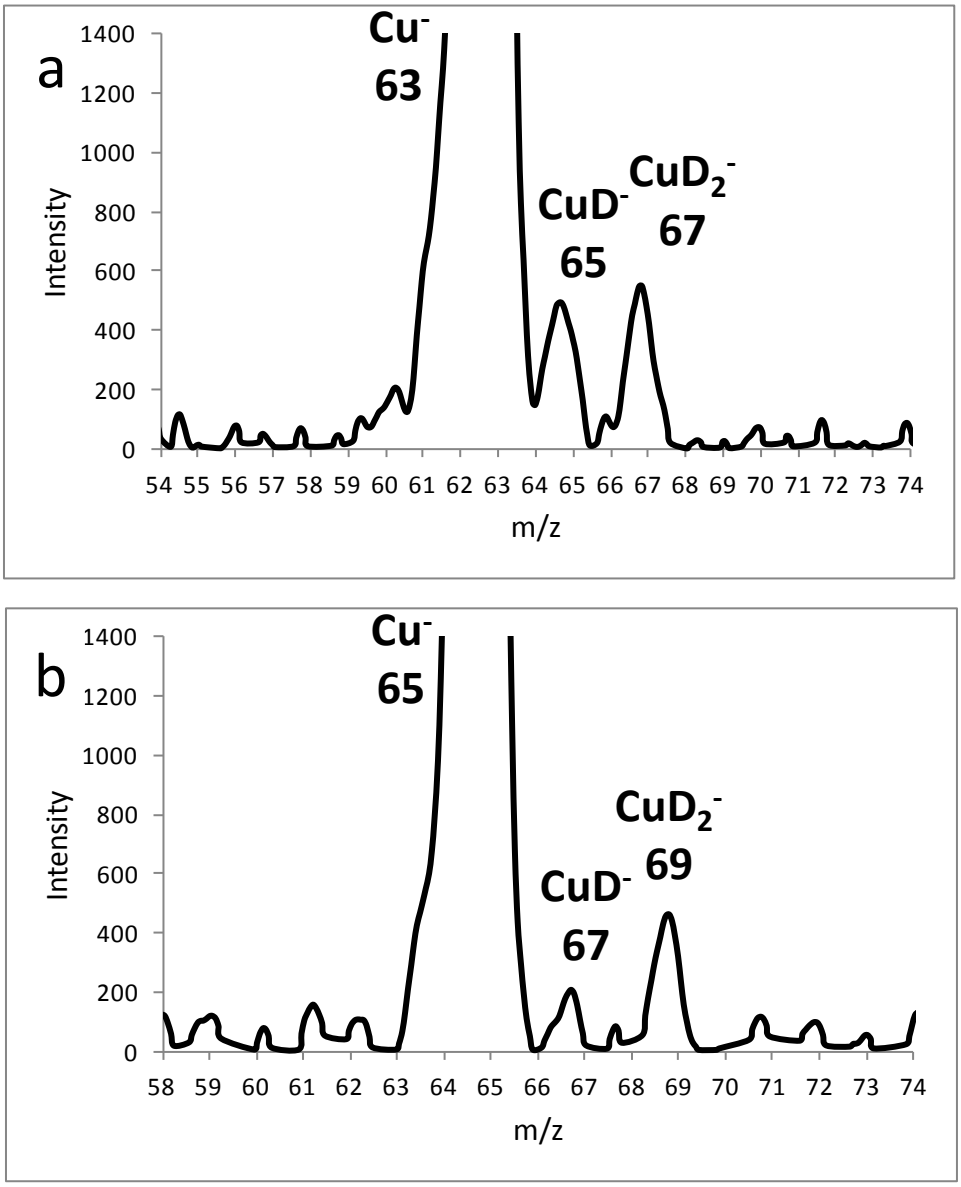

Figure 9: a) Mass spectrum of reaction of pentane-d_{12} with $^{63}Cu^-$ at voltages of (50-10-50) and the target gas pressure of 1.2 e-3 mbar; b) Mass spectrum of reaction of pentane-d_{12} with $^{65}Cu^-$ at voltages of (50-10-50) and the target gas pressure of 1.2 e-3 mbar

3.1.4: Reactions of pentane with Ag^-

At all collision energies, no reaction was observed. Thus, pentane shows no reaction with Ag^-.

3.1.5: Reactions of pentane with Cs^-

At all collision energies, no reaction was observed. Thus, pentane shows no reaction with Cs^-.

3.1.6: Reactions of pentane with K^-

At all collision energies, no reaction was observed. Thus, pentane shows no reaction with K^-.

3.2: Reactions with pentene

3.2.1: Reactions of pentene with Fe^-

With the collision voltage of 0 eV, no reaction was observed. With the collision voltage of 10 eV, m/z 56 (Fe^-); m/z of 57 (FeH^-) and m/z of 58 (FeH_2^-) were observed in the mass spectrum of the reaction of Fe^- with 1-pentene and 2-pentene (Figures 10).

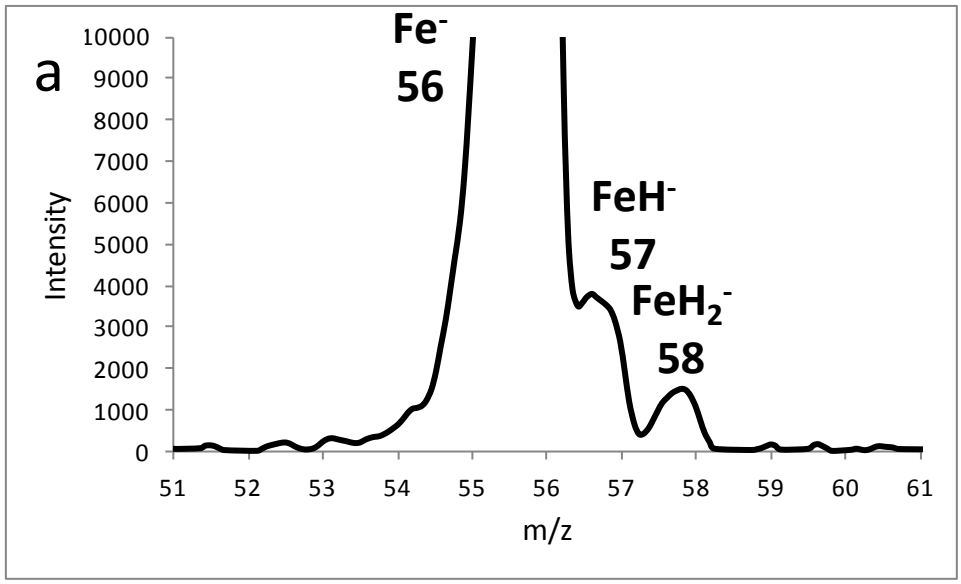

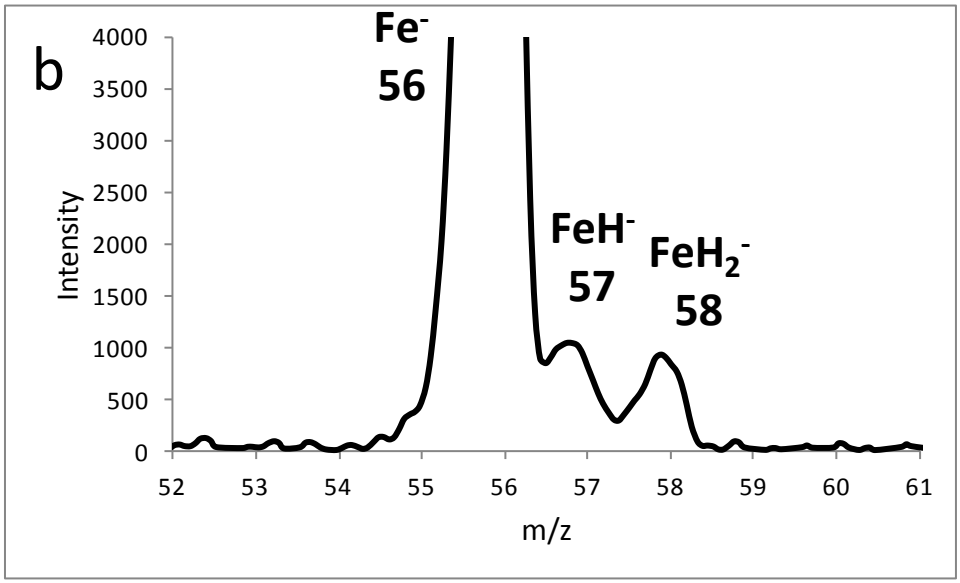

Figure 10: a) Mass spectrum of products of the reaction of 1-pentene with Fe^- in voltages of (50-10-50) and the target gas pressure of 1.2 e-3 mbar; b) Mass spectrum of products of the reaction of 2-pentene with Fe^- in voltages of (50-10-50) and the target gas pressure of 1.2 e-3 mbar

FeH^- is a product of the dehydrogenation reaction of pentane with Fe^-. FeH_2^- is a product of the bisdehydrogenation reaction of pentane with Fe^- (reactions 24 and 25).

$$C_5H_{10} + Fe^- \rightarrow C_5H_9^{\cdot} + FeH^{-\cdot} \qquad (24)$$

$C_5H_{10} + Fe^- \rightarrow C_5H_8^{\cdot} + FeH_2^{-\cdot}$ (25)

With the collision voltage of 40 eV, m/z 56 (Fe^-) and m/z 69 ($C_5H_9^-$) were observed in the mass spectrum of the reaction of Fe^- with pentene (Figures 11).

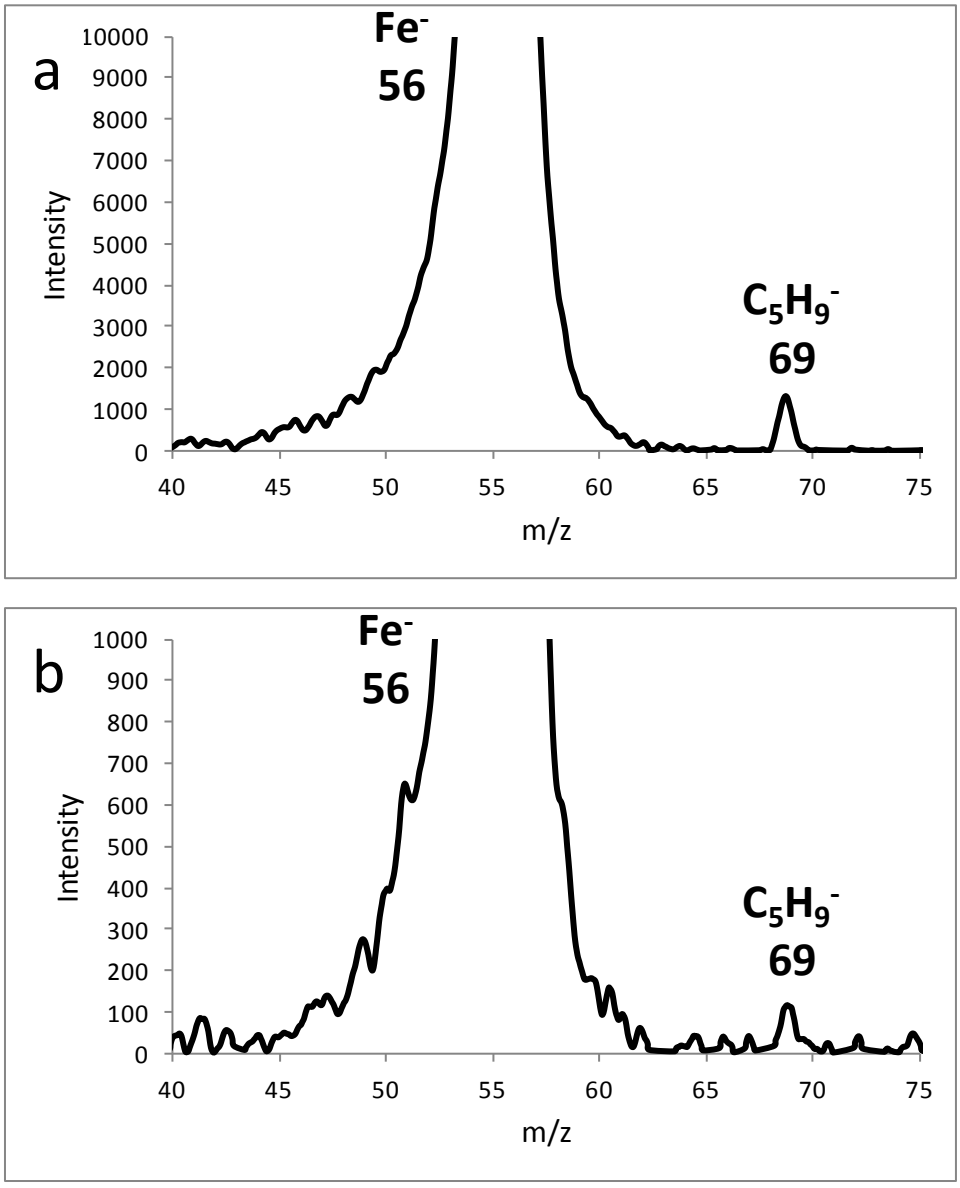

Figure 11: a) Mass spectrum of products of the reaction of 1-pentene with Fe^- in voltages of (50-40-50) and the target gas pressure of 1.2 e-3 mbar; b) Mass spectrum of products of the reaction of 2-pentene with Fe^- in voltages of (50-40-50) and the target gas pressure of 1.2 e-3 mbar

$C_5H_9^-$ is a product of the deprotonation reaction (reaction 26).

$$C_5H_{10} + Fe^- \rightarrow C_5H_9^- + FeH \quad (26)$$

3.2.2: Reactions of pentene with Co^-

At all collision energies, no reaction was observed. Thus, pentene shows no reaction with Co^-.

3.2.3: Reactions of pentene with Cu^-

With the collision voltage of 0 eV, no reaction was observed. With the collision voltage of 5 eV, m/z 65 (Cu^-) and m/z 67 (CuH_2^-) were observed in the mass spectrum of the reaction of pentene with Cu^- (Figure 12).

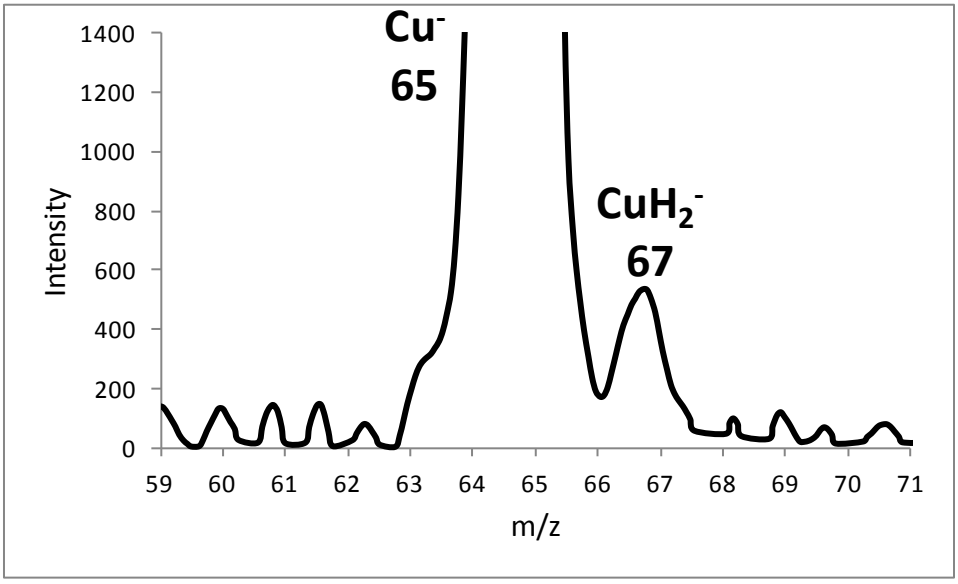

Figure 12: Mass spectrum of products of the reaction of 1-pentene with $^{65}Cu^-$ in voltages of (50-5-50) and the target gas pressure of 1.2 e-3 mbar

CuH_2^- is a product of the bisdehydrogenation reaction (reaction 27).

$$C_5H_{10} + Cu^- \rightarrow C_5H_8 + CuH_2^- \quad (27)$$

With the collision voltage of 10 eV, m/z 65 (Cu^-) and m/z 66 (CuH^-) were observed in the mass spectrum of the reaction of pentene with Cu^- (Figure 13).

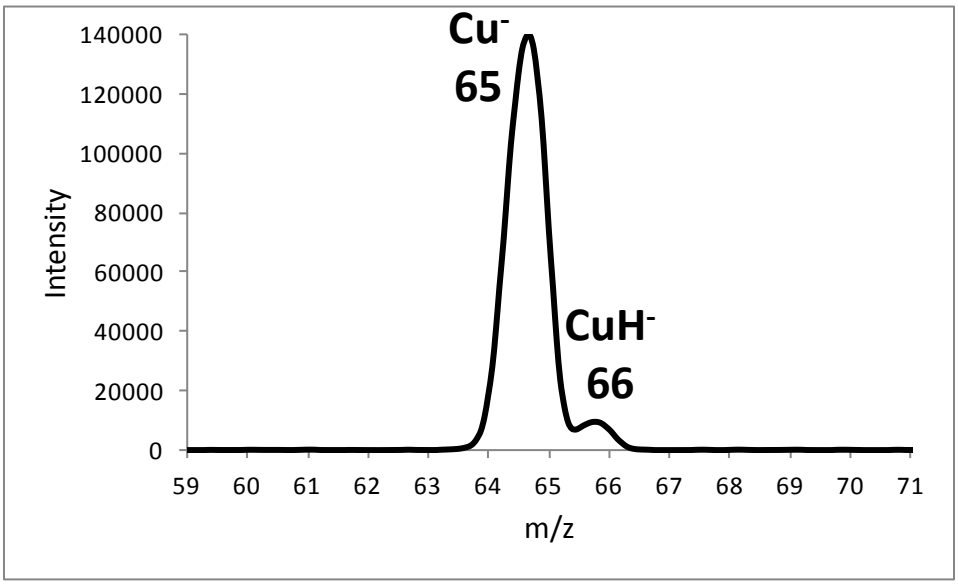

Figure 13: Mass spectrum of products of the reaction of 1-pentene with $^{65}Cu^-$ in voltages of (50-10-50) and the target gas pressure of 1.2 e-3 mbar

CuH^- is a product of the dehydrogenation reaction of Cu^- with pentene (reaction 28).

$$C_5H_{10} + Cu^- \rightarrow C_5H_9 + CuH^- \quad (28)$$

With the collision voltage of higher than 15 eV only m/z 65 (Cu^-) was observed.

3.2.4: Reactions of pentene with Ag^-

At all collision energies, no reaction was observed. Thus, pentene shows no reaction with Ag^-.

3.2.5: Reactions of pentene with Cs^-

With the collision voltage of 0 eV, no reaction was observed.

With the collision voltage of 10 eV, m/z 133 (Cs^-); m/z 27 ($C_2H_3^-$) and m/z 41 ($C_3H_5^-$) were observed in the mass spectrum of the reaction of 1-pentene with Cs^- (Figure 14).

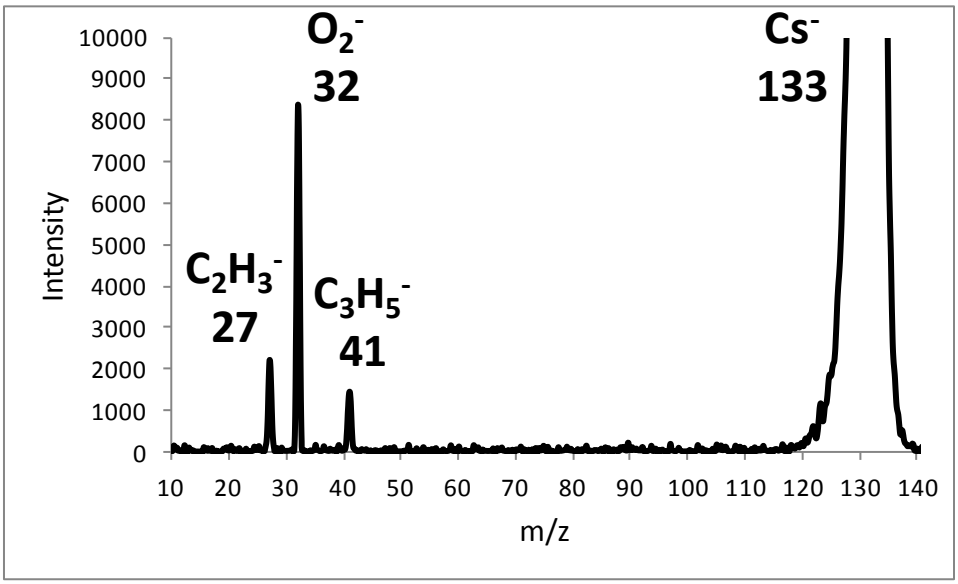

Figure 14: Mass spectrum of products of the reaction of 1-pentene with Cs^- in voltages of (50-10-50) and the target gas pressure of 1.2 e-3 mbar

$C_2H_3^-$ and $C_3H_5^-$ are products of spontaneous dissociation of deprotonated 1-pentene (reactions 29 and 30).

$C_5H_9^- \rightarrow C_3H_5^- + C_2H_4$ (29)

$C_5H_9^- \rightarrow C_2H_3^- + C_3H_6$ (30)

m/z 32 (O_2^-) is contamination of oxygen in the system.

With the collision voltage of 10 eV, m/z 133 (Cs^-); m/z 41 ($C_3H_5^-$) and m/z 55 ($C_4H_7^-$) were observed in the mass spectrum of the reaction of 2-pentene with Cs^- (Figure 15).

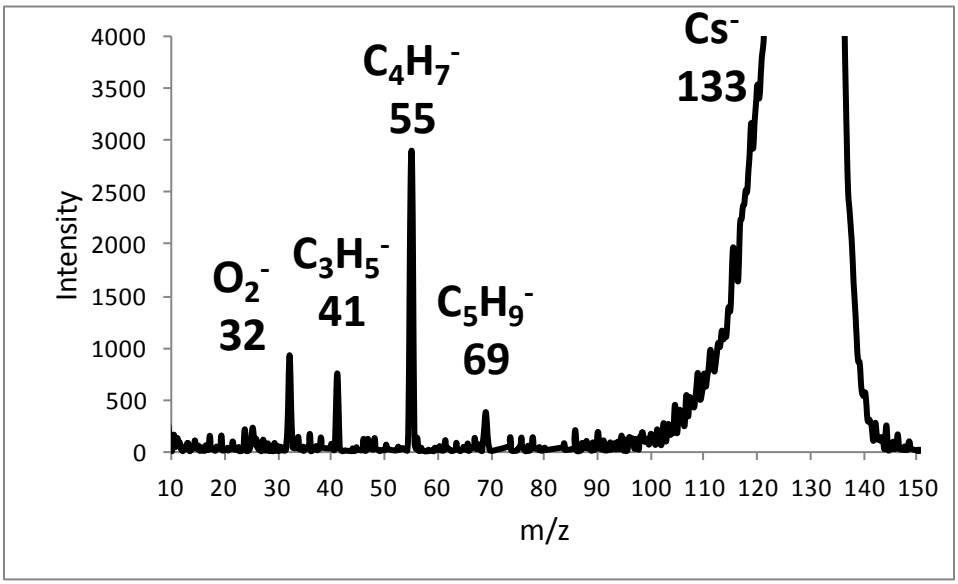

Figure 15: Mass spectrum of products of the reaction of 2-pentene with Cs^- in voltages of (50-10-50) and the target gas pressure of 1.2 e-3 mbar

$C_3H_5^-$ and $C_4H_7^-$ are products of spontaneous dissociation of deprotonated 2-pentene (reactions 31 and 32).

$C_5H_9^- \rightarrow C_3H_5^- + C_2H_4$ (31)

$C_5H_9^- \rightarrow C_4H_7^- + CH_2$ (32)

m/z 32 (O_2^-) is contamination of oxygen in the system.

3.2.6: Reactions of pentene with K^-

At all collision energies, no reaction was observed. Thus, pentene shows no reaction with K^-.

3.3: Reactions with 1-pentyne

3.3.1: Reactions of 1-pentyne with Fe^-

With the collision voltage of 0 eV, no reaction was observed. With the collision voltage of 10 eV, m/z 56 (Fe^-); m/z 57 (FeH^-); m/z of 58 (FeH_2^-) and m/z of 67 ($C_5H_7^-$) were observed in the mass spectrum of the reaction of 1-pentyne with Fe^- (Figure 16).

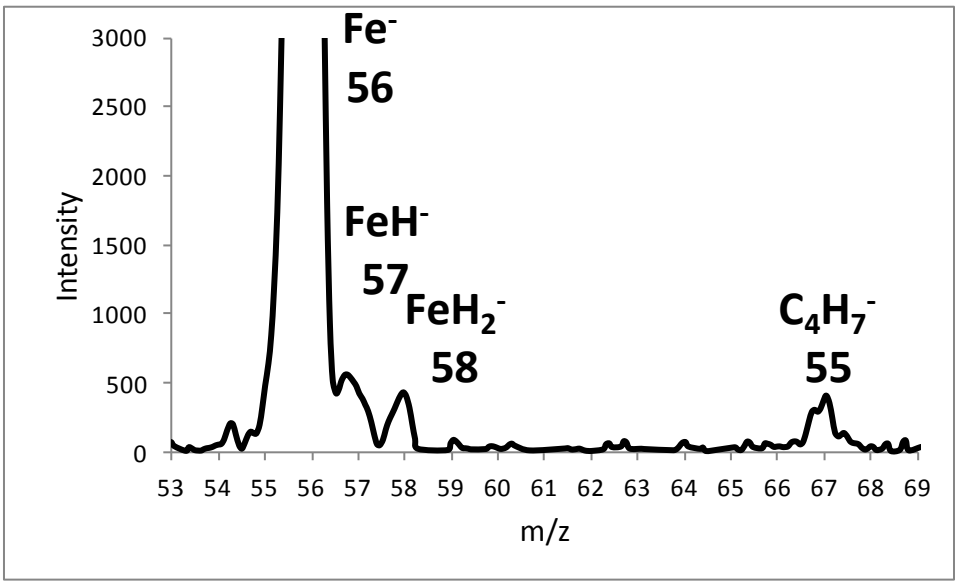

Figure 16: Mass spectrum of products of the reaction of 1-pentene with Fe^- in voltages of (50-10-50) and the target gas pressure of 1.2 e-3 mbar

FeH^- is a product of the dehydrogenation reaction. FeH_2^- is a product of the bisdehydrogenation reaction. $C_5H_7^-$ is a product of the deprotonation reaction (reactions 33 to 35).

$$C_5H_8 + Fe^- \rightarrow C_5H_7 + FeH^- \quad (33)$$

$$C_5H_8 + Fe^- \rightarrow C_5H_6 + FeH_2^- \quad (34)$$

$$C_5H_8 + Fe^- \rightarrow C_5H_7^- + FeH \quad (35)$$

3.3.2: Reactions of 1-pentyne with Co^-

With the collision voltage of 0eV, no reaction was observed. With the collision voltage of 5 eV, m/z 59 (Co^-); m/z 61 (CoH_2^-) and m/z 67 ($C_5H_7^-$) were observed in the mass spectrum of the reaction of 1-pentyne with Co^- (Figure 17).

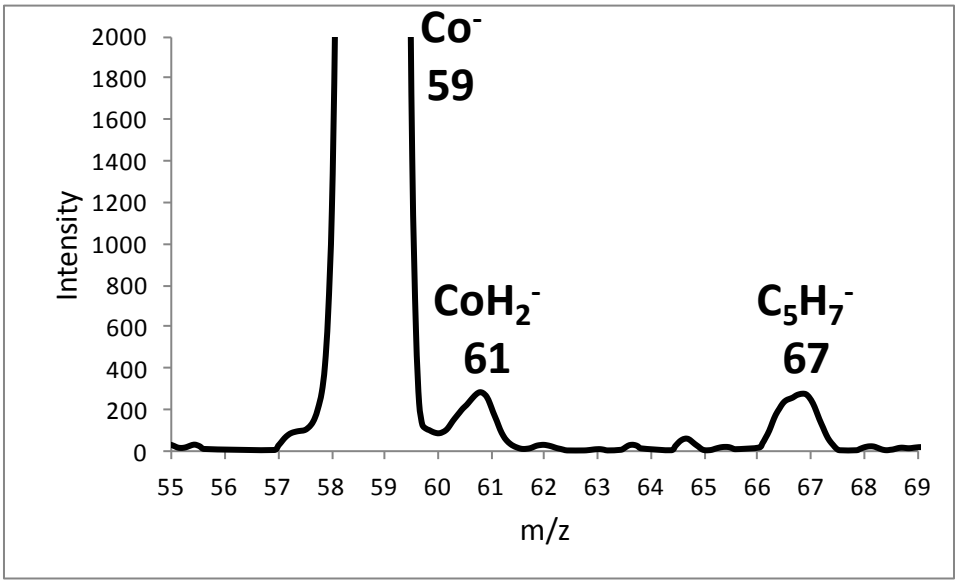

Figure 17: Mass spectrum of the reaction of 1-pentyne with Co^- in voltages of (50-5-50) and the target gas pressure of 1.2 e-3 mbar

Co^- and CH_3COO^- have the same molecular mass; thus, there is a chance of having CH_3COO^- contamination in the Co^- beam when m/z 59 is selected in the source. CH_3COO^- can be produced in the source by the decomposition of the solution of tricarbalilic acid in methanol. To confirm that m/z 61 is a result of reaction with Co^-, not with CH_3COO^- , a solution of acetic acid in methanol was injected into the source and the produced CH_3COO^- was reacted with 1-pentyne. No m/z 61 was observed (Figure 18).

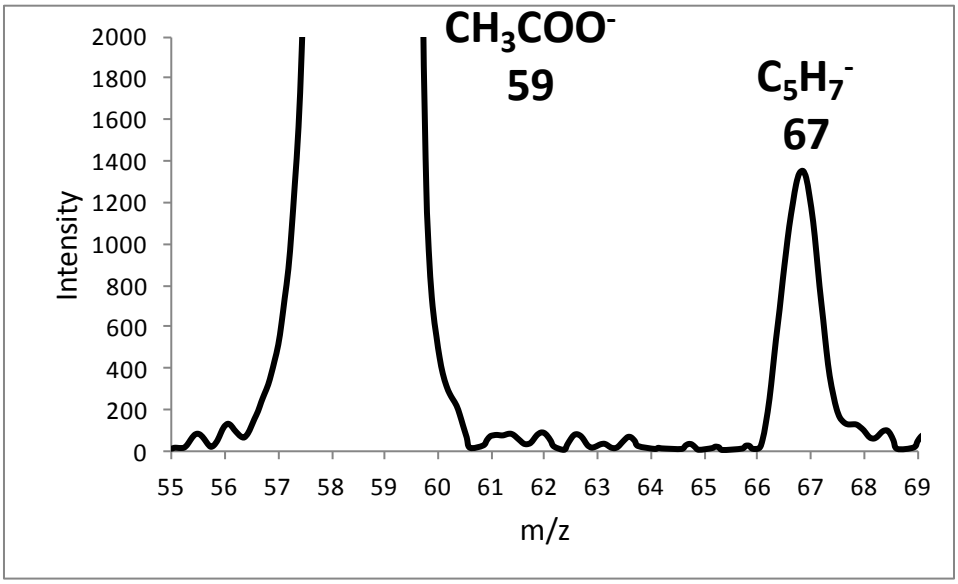

Figure 18: Mass spectrum of products of the reaction of 1-pentyne with CH3COO- in voltages of (50-5-50) and the target gas pressure of 2.3 e-3 mbar

CoH_2^- is a product of the bisdehydrogenation reaction of 1-pentyne with Co^-. $C_5H_7^-$ is a product of the deprotonation reaction of 1-pentyne with Co^- (reactions 36 and 37).

$$C_5H_8 + Co^- \rightarrow C_5H_6 + CoH_2^- \quad (36)$$

$$C_5H_8 + Co^- \rightarrow C_5H_7^- + CoH \quad (37)$$

3.3.3: Reactions of 1-pentyne with Cu^-

With the collision voltage of 0 eV, no reaction was observed. With the collision voltage of 5 eV, m/z 63 (Cu^-); m/z 65 (CuH_2^-) and m/z 67 ($C_5H_7^-$) were observed in the mass spectrum of the reaction of 1-pentyne with Cu^- (Figure 19).

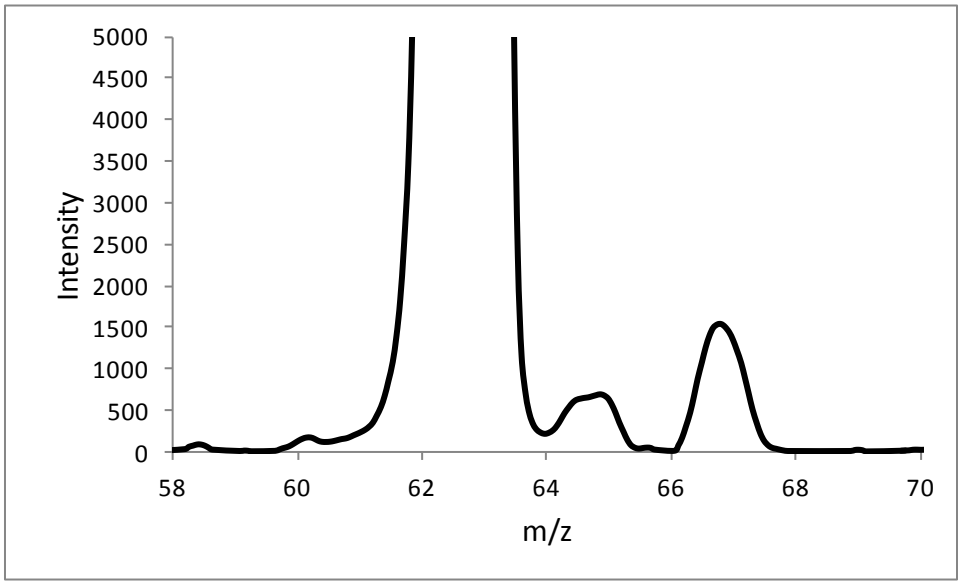

Figure 19: Mass spectrum of products of the reaction of 1-pentyne with $^{63}Cu^-$ in voltages of (50-5-50) and the target gas pressure of 1.2 e-3 mbar

CuH_2^- is a product of the bisdehydrogenation reaction and $C_5H_7^-$ is a product of the deprotonation reaction (eactions 38 and 39).

$$C_5H_8 + Cu^- \rightarrow C_5H_6 + CuH_2^- \quad (38)$$

$$C_5H_8 + Cu^- \rightarrow C_5H_7^- + CuH \quad (39)$$

With the collision voltage of 25 eV, m/z 63 (Cu^-); m/z 67 ($C_5H_7^-$); m/z 25 (C_2H^-) and m/z 39 ($C_3H_3^-$) were observed in the mass spectrum of the reaction of 1-pentyne with Cu^- (Figures 20).

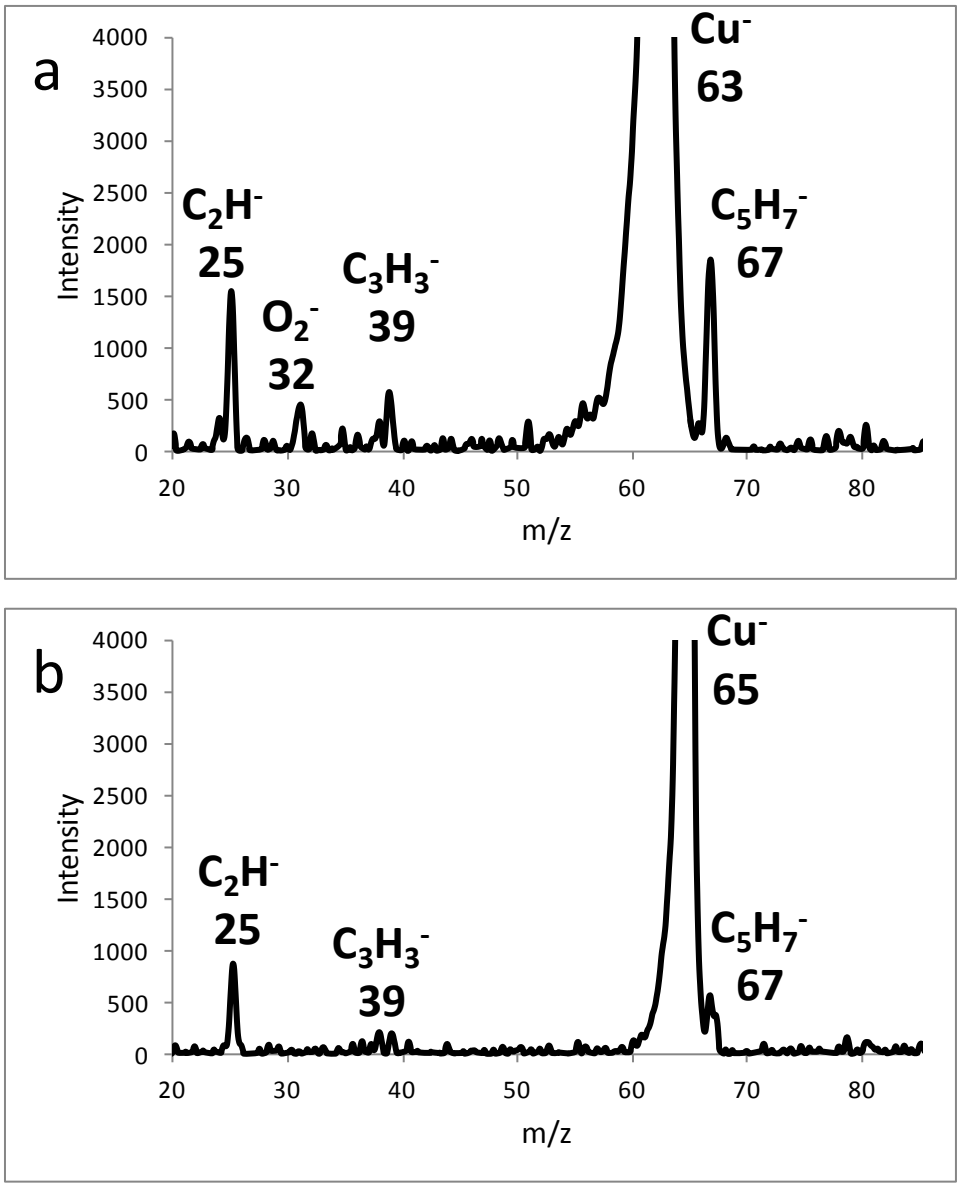

Figure 20: a) Mass spectrum of products of the reaction of 1-pentyne with $^{63}Cu^-$ in voltages of (50-25-50) and the target gas pressure of 1.2 e-3 mbar, b) Mass spectrum of products of the reaction of 1-pentyne with $^{65}Cu^-$ in voltages of (50-25-50) and the target gas pressure of 1.2 e-3 mbar

$C_5H_7^-$ is a product of the deprotonation reaction. C_2H^- and $C_3H_3^-$ are products of spontaneous dissociation of deprotonated 1-pentyne (reactions 40 and 41).

$$C_5H_7^- \rightarrow C_2H^- + C_3H_6 \quad (40)$$

$$C_5H_7^- \rightarrow C_3H_3^- + C_2H_4 \quad (41)$$

3.3.4: Reactions of 1-pentyne with Ag^-

With the collision voltage of 0 eV, no reaction was observed. With the collision voltage of 40 eV, m/z 107 (Ag^-); m/z 67 ($C_5H_7^-$); m/z 25 (C_2H^-) and m/z 39 ($C_3H_3^-$) were observed in the mass spectrum of the reaction of 1-pentyne with Ag^- (Figures 21).

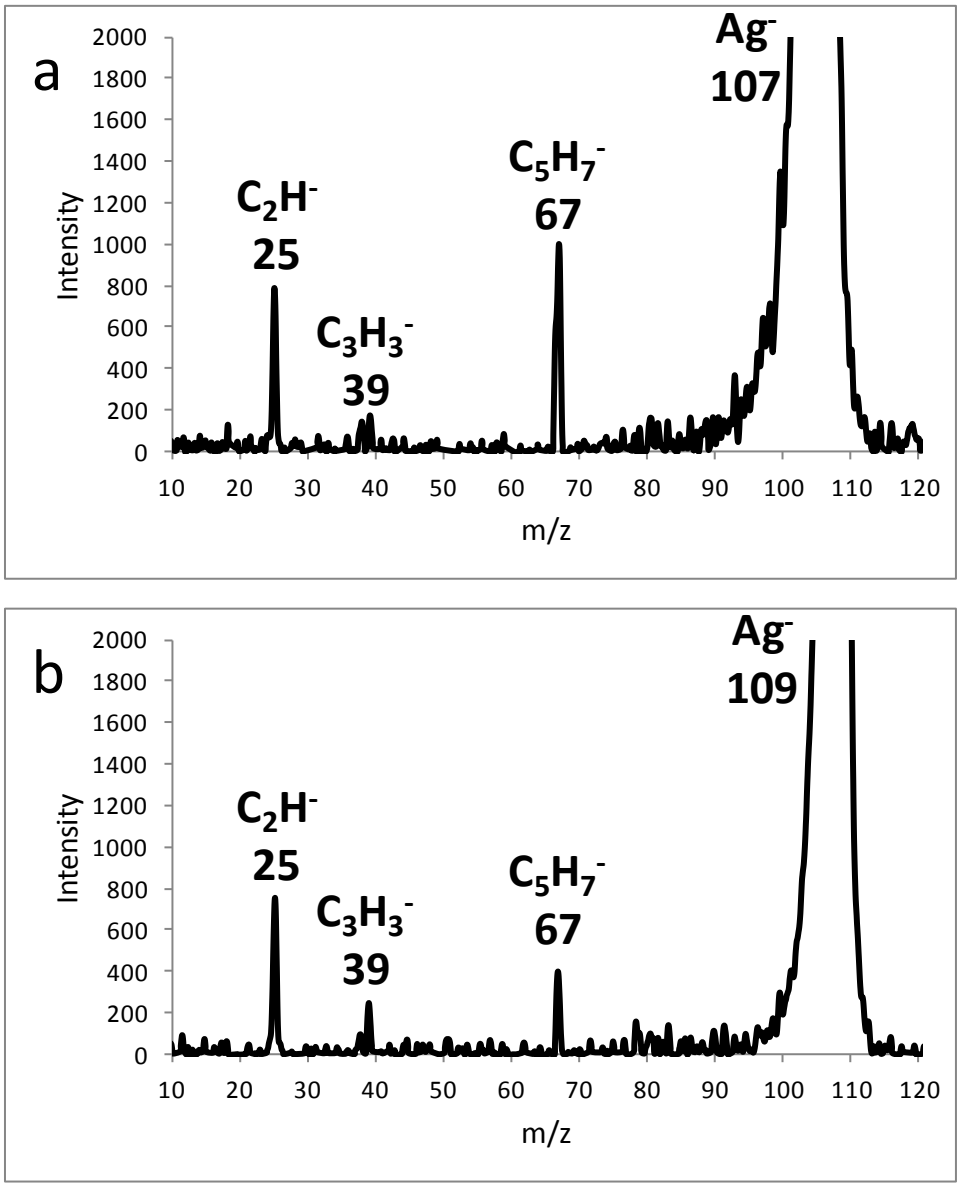

Figure 21: a) Mass spectrum of products of the reaction of 1-pentyne with $^{107}Ag^-$ in voltages of (50-40-50) and the target gas pressure of 1.2 e-3 mbar; b) Mass spectrum of products of the reaction of 1-pentyne with $^{109}Ag^-$ in voltages of (50-40-50) and the target gas pressure of 1.2 e-3 mbar

$C_5H_7^-$ is a product of the deprotonation reaction. C_2H^- and $C_3H_3^-$ are products of spontaneous dissociation of deprotonated 1-pentyne (reactions 42, 40 and 41).

$$C_5H_8 + Ag^- \rightarrow C_5H_7^- + AgH \quad (42)$$

$$C_5H_7^- \rightarrow C_2H^- + C_3H_6 \quad (40)$$

$$C_5H_7^- \rightarrow C_3H_3^- + C_2H_4 \quad (41)$$

3.3.5: Reactions of 1-pentyne with Cs^-

With the collision voltage of 0 eV, no reaction was observed. With the collision voltage of 40 eV, m/z (Cs^-); m/z 67 ($C_5H_7^-$); m/z 25 (C_2H^-) and m/z 39 ($C_3H_3^-$) were observed in the mass spectrum of the reaction of 1-pentyne with Cs^- (Figure 22).

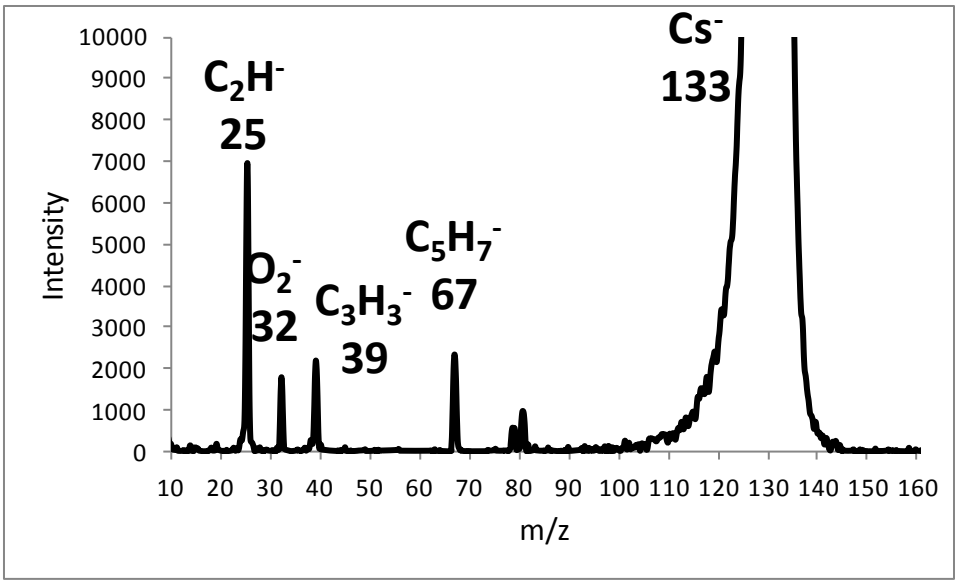

Figure 22: Mass spectrum of products of the reaction of 1-pentyne with Cs^- in voltages of (50-40-50) and the target gas pressure of 1.2 e-3 mbar

$C_5H_7^-$ is a product of the deprotonation reaction. C_2H^- and $C_3H_3^-$ are products of spontaneous dissociation of deprotonated 1-pentyne (reactions 43, 40 and 41).

$$C_5H_8 + Cs^- \rightarrow C_5H_7^- + CsH \quad (43)$$

$$C_5H_7^- \rightarrow C_2H^- + C_3H_6 \quad (40)$$

$$C_5H_7^- \rightarrow C_3H_3^- + C_2H_4 \quad (41)$$

3.3.6: Reactions of 1-pentyne with K^-

With the collision voltage of 0 eV, no reaction was observed. With the collision voltage of 40 eV, m/z 39 (K^-), m/z 67 ($C_5H_7^-$) and m/z 25 (C_2H^-) were observed in the mass spectrum of the reaction of 1-pentyne with K^- (Figure 23).

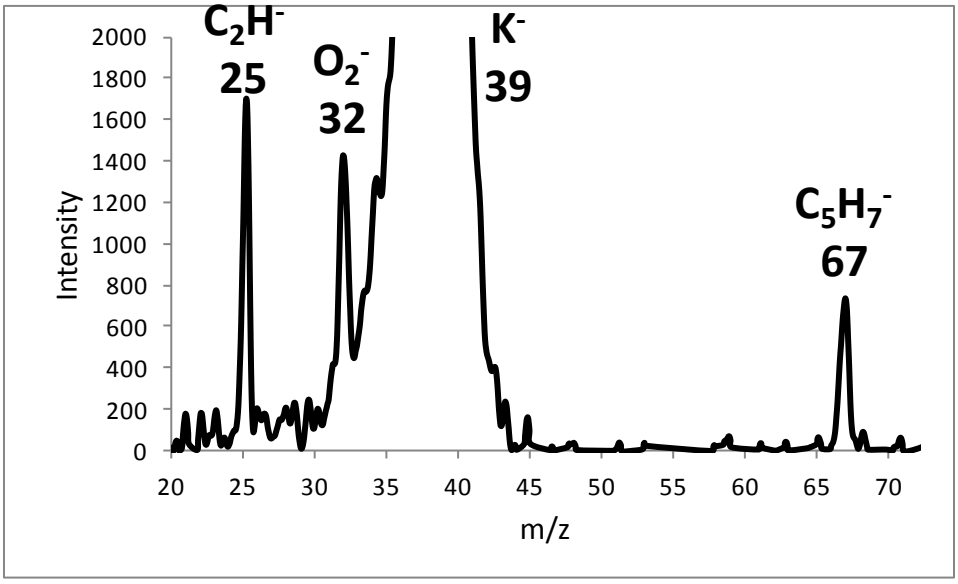

Figure 23: Mass spectrum of products of the reaction of 1-pentyne with K^- in voltages of (50-40-50) and the target gas pressure of 1.2 e-3 mbar

$C_5H_7^-$ is a product of the deprotonation reaction. C_2H^- is a product of spontaneous dissociation of deprotonated 1-pentyne (reaction 44, 40 and 41).

$$C_5H_8 + K^- \rightarrow C_5H_7^- + KH \quad (44)$$

$$C_5H_7^- \rightarrow C_2H^- + C_3H_6 \quad (40)$$

$$C_5H_7^- \rightarrow C_3H_3^- + C_2H_4 \quad (41)$$

It is generally understood that $C_3H_3^-$, a product of spontaneous dissociation of deprotonated 1-pentyne, is produced in this reaction. However, the signal of $C_3H_3^-$ cannot be observed separately because it overlaps with m/z of the potassium anion.

3.4: Summary of reactions of metal anions with hydrocarbons

3.4.1: Observed reactions

Hydrocarbons tested as organic samples or target gases in this thesis study show different types of reactions with metal anions such as:

1) Deprotonation reaction

A deprotonation reaction is the abstraction of a proton from the target gas by the metal anion. The products of this reaction are the neutral metal hydride, which is not observed in the spectrum, and the deprotonated target gas, which is observed in the spectrum. All metal anions show the deprotonation reaction with pentyne. Fe^- shows the deprotonation reaction with pentene (Table 2).

Table 2: The observation of the deprotonation reactions of metal anions with hydrocarbons; stars indicate the observed reactions

	Fe^-	Co^-	Cu^-	Ag^-	Cs^-	K^-
Pentane						
Pentene	★					
Pentyne	★	★	★	★	★	★

2) Dehydrogenation reaction

A dehydrogenation reaction is the abstraction of a hydrogen from the target gas by the metal anion. The products of this reaction are the metal hydride anion, which is observed in the spectrum, and the neutral dehydride radical, which is not observed in the spectrum. Fe^- shows the dehydrogenation reaction with all tested hydrocarbons. Cu^- shows the dehydrogenation reaction with pentane and pentene (Table 3).

Table 3: The observation of the dehydrogenation reactions of metal anions with hydrocarbons; stars indicate the observed reactions

	Fe^-	Co^-	Cu^-	Ag^-	Cs^-	K^-
Pentane	★		★			
Pentene	★		★			
Pentyne	★					

3) Bisdehydrogenation reaction

A bisdehydrogenation reaction is the abstraction of two hydrogens from the target gas by the metal anion. The products of this reaction are the metal dihydride anion, which is observed in the spectrum, and the bisdehydrated target gas, which is not observed in the spectrum. Fe^- and Cu^- show the bisdehydrogenation reaction with all tested hydrocarbons (Table 4).

Table 4: The observation of the bisdehydrogenation reactions of metal anions with hydrocarbons; stars indicate the observed reactions

	Fe^-	Co^-	Cu^-	Ag^-	Cs^-	K^-
Pentane	★		★			
Pentene	★		★			
Pentyne	★		★			

4) spontaneous dissociation of the deprotonated target gas

The deprotonated target gas can dissociate to smaller fragments when there is enough energy in the system. The metal anions have no role in this dissociation. Details of experiments that confirm this dissociation takes place spontaneously can be find in chapter 4.4.3 of this thesis study.

To find the driving force of these reactions and explain these results, the reactions can be discussed from different points of view, such as comparing the properties of the metal anions, the enthalpies of reactions, and the mechanism of reactions.

3.4.2: The comparison of properties of metals

The properties of metals, such as electronic configuration, electron affinity, hydrogen affinity and gas phase acidity, were studied in order to find a relationship between the properties of metal anions and their reactivity with regards to the dehydrogenation reaction (Table 5).[5,16]

Table 5: The table of the comparison of properties of metals

Metal	m/z	Electronic configuration	Electron affinity, eV	Hydrogen affinity, kJ/mol	Gas phase acidity, kJ/mol
Fe	56	[Ar] $3d^6$ $4s^2$	0.151	-22.05	1439
Co	59	[Ar] $3d^7$ $4s^2$	0.662	-168.59	1411
Cu	63, 65	[Ar] $3d^{10}$ $4s^1$	1.228	-188.06	1451
Ag	107, 109	[Kr] $4d^{10}$ $5s^1$	1.302	-133.02	1406
Cs	133	[Xe] $6s^1$	0.472	-198.10	1441
K	39	[Ar] $4s^1$	0.501	-203.62	1439

The electronic configuration shows that alkali metal anions do not have accessible d-orbitals in their outer valance shell and as a consequence cannot form intermediate complexes with organic compounds. The electron affinity of metal anions shows a different trend as their reactivity. The calculated hydrogen affinities of transition metal anions has the same trend as their reactivity. Fe^- and Cu^- have lower hydrogen affinity and show the dehydrogenation reaction. Fe^- has a high hydrogen affinity and shows a more intense products in a dehydrogenation reaction than other metal anions. The gas phase acidities of Fe^- and Cu^- are greater than the gas phase acidities of other metal anions. The gas phase acidity has the same trend as observations.

3.4.3: The enthalpies of reactions

A reaction can be observed when there is enough energy in the system to overcome the barrier of that reaction. Meanwhile, calculation of the enthalpies of reactions is more readily made than calculation of the barrier of reactions. All metal anions in the studied reactions are bare metal atomic anions without any ligand on them. In addition, all organic target gases are small linear organic neutral molecules with similar molecular weights. Moreover, all reactions in this thesis study were done in the gas phase with similar energies. Thus, the enthalpies of these reactions may be considered representative of the barriers of these reactions. The Marcus theory has a complete explanation for this assumption. Dr. Rudolph A. Marcus received the Nobel prize in 1992 for developing his theory about electron transfer reactions.[17] From working on hypotheses related to outer sphere electron transfer reactions, Dr. Marcus derived the following equation on the relationship between the barrier of a reaction, ΔE, and the enthalpy of that reaction, ΔG:

Equation 2: A simplified version of Marcus equation, ΔE is the barrier, ΔG is the enthalpy and λ is the reorganization energy

$$\Delta E = \frac{(\Delta G + \lambda)^2}{4\lambda}$$

According to Marcus's theory, in reactions where the structures of starting materials and products are similar, the reaction with a smaller enthalpy will have a smaller barrier (Figure 24).

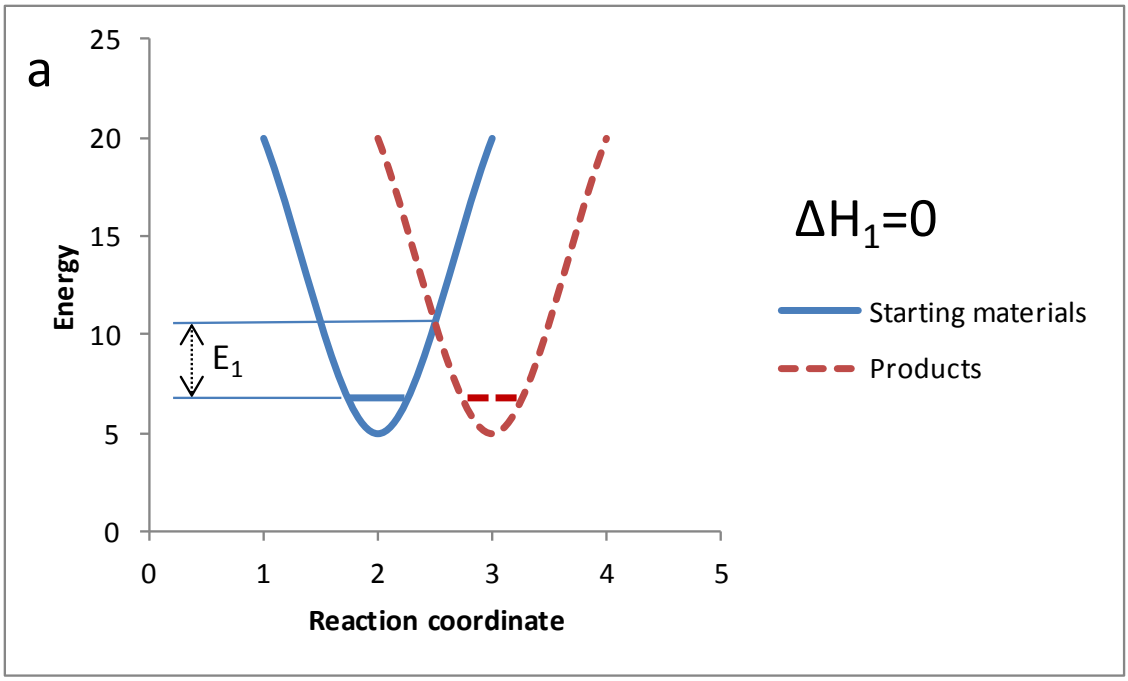
a
25
20
15
10
5
0
Energy
E1
0
1
2
3
4
5
Reaction coordinate
ΔH1=0
Starting materials
Products

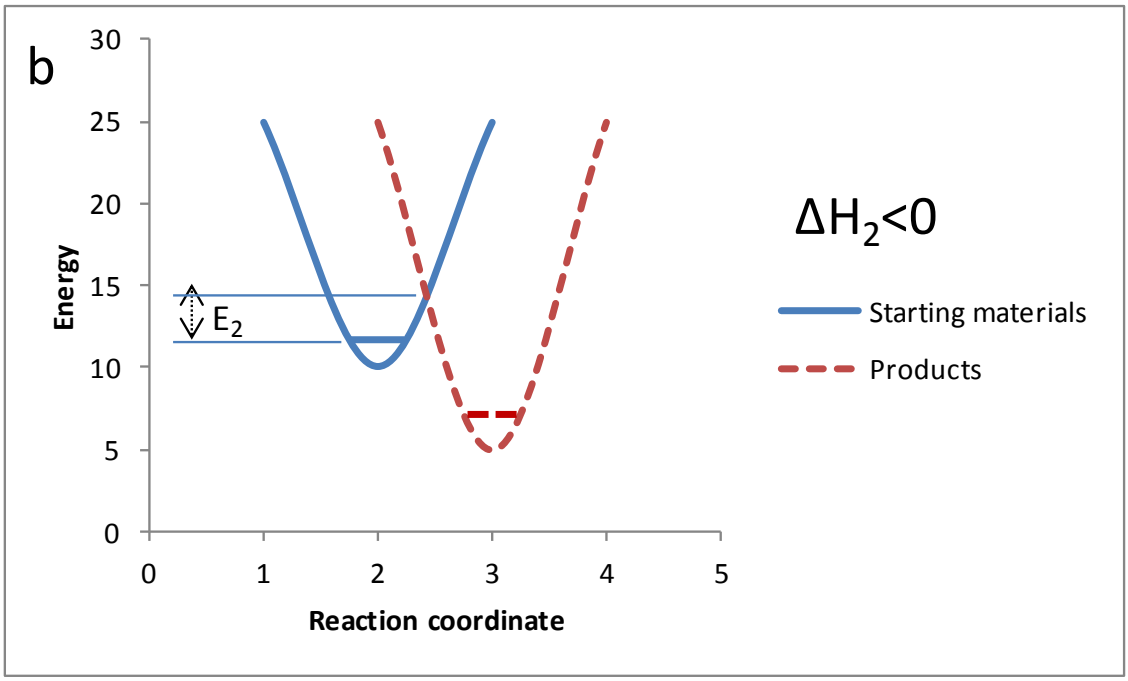
b
30
25
20
15
10
5
0
Energy
E2
0
1
2
3
4
5
Reaction coordinate
ΔH2<0
Starting materials
Products

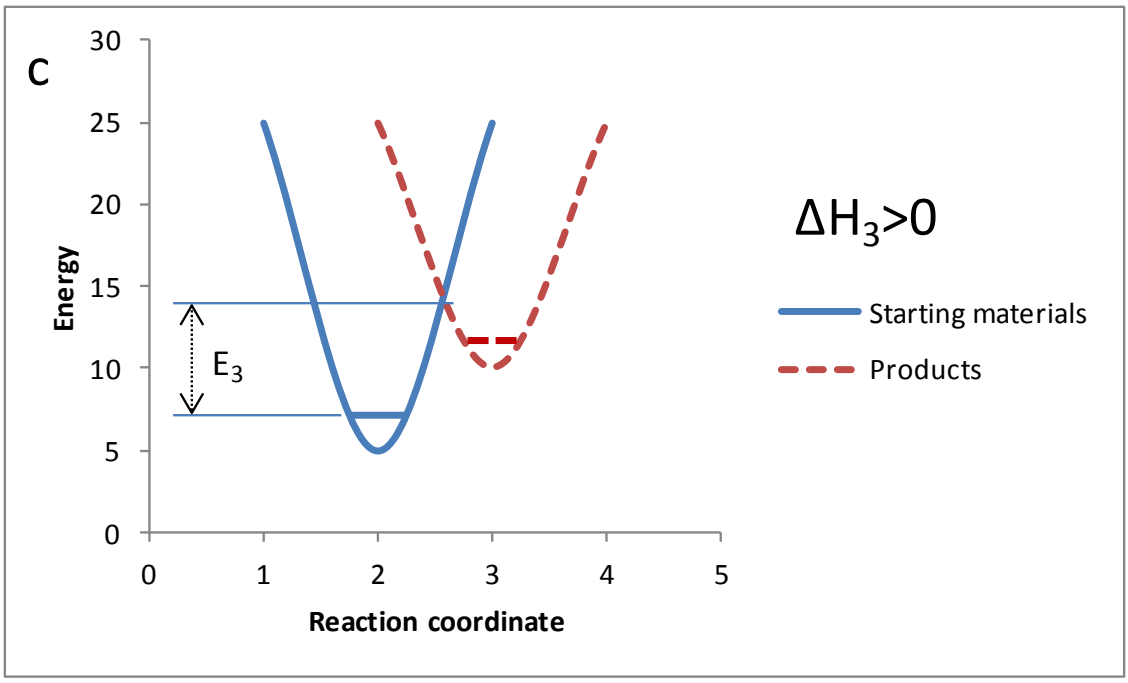

Figure 24: a) The relationship between the enthalpy, ΔH_1, and the barrier, E_1, of a thermoneutral reaction; b) The relationship between the enthalpy, ΔH_2, and the barrier, E_2, of an exothermic reaction; c) The relationship between the enthalpy, ΔH_3, and the barrier, E_3, of an endothermic reaction; According to the Marcus's theory this relationships shows that $E_2<E_1<E_3$ where $\Delta H_2<\Delta H_1<\Delta H_3$

Enthalpies of some observed and unobserved reactions were calculated and documented in Appendix 1 of this thesis. The enthalpy of a reaction is the sum of the heats of formation of products subtracted by the sum of heats of formation of starting materials. Enthalpies of unobserved reactions were calculated to compare with the observed similar reactions. Heats of formation of fragments were found in the NIST webbook[18] or the Gas-Phase Ion and Neutral Thermochemistry Book[19] and documented in the Appendix 4 and 5 of this thesis. Calculated enthalpies of reactions of hydrocarbons with metal anions are plotted for each tested metal anion in this thesis study (Figures 25 to 27).

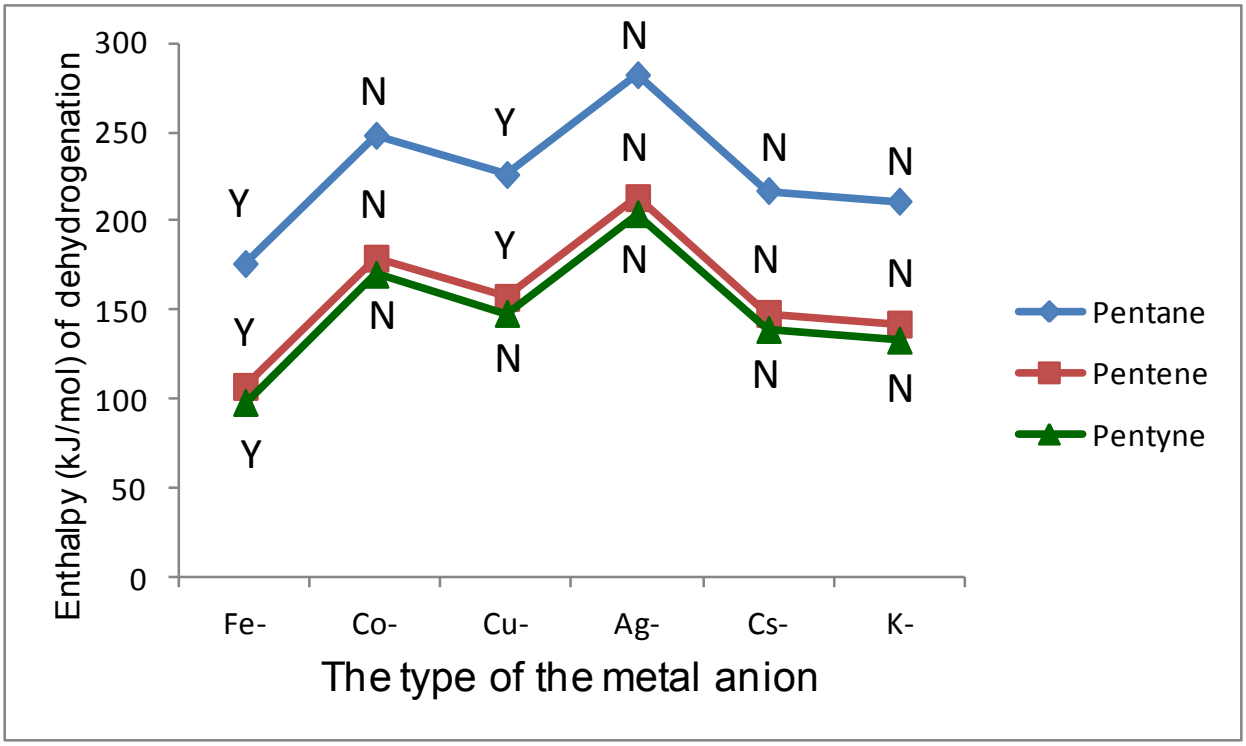

Figure 25: Enthalpies of the dehydrogenation reactions of metal anions with hydrocarbons, Y indicates observed reactions and N indicates unobserved reactions

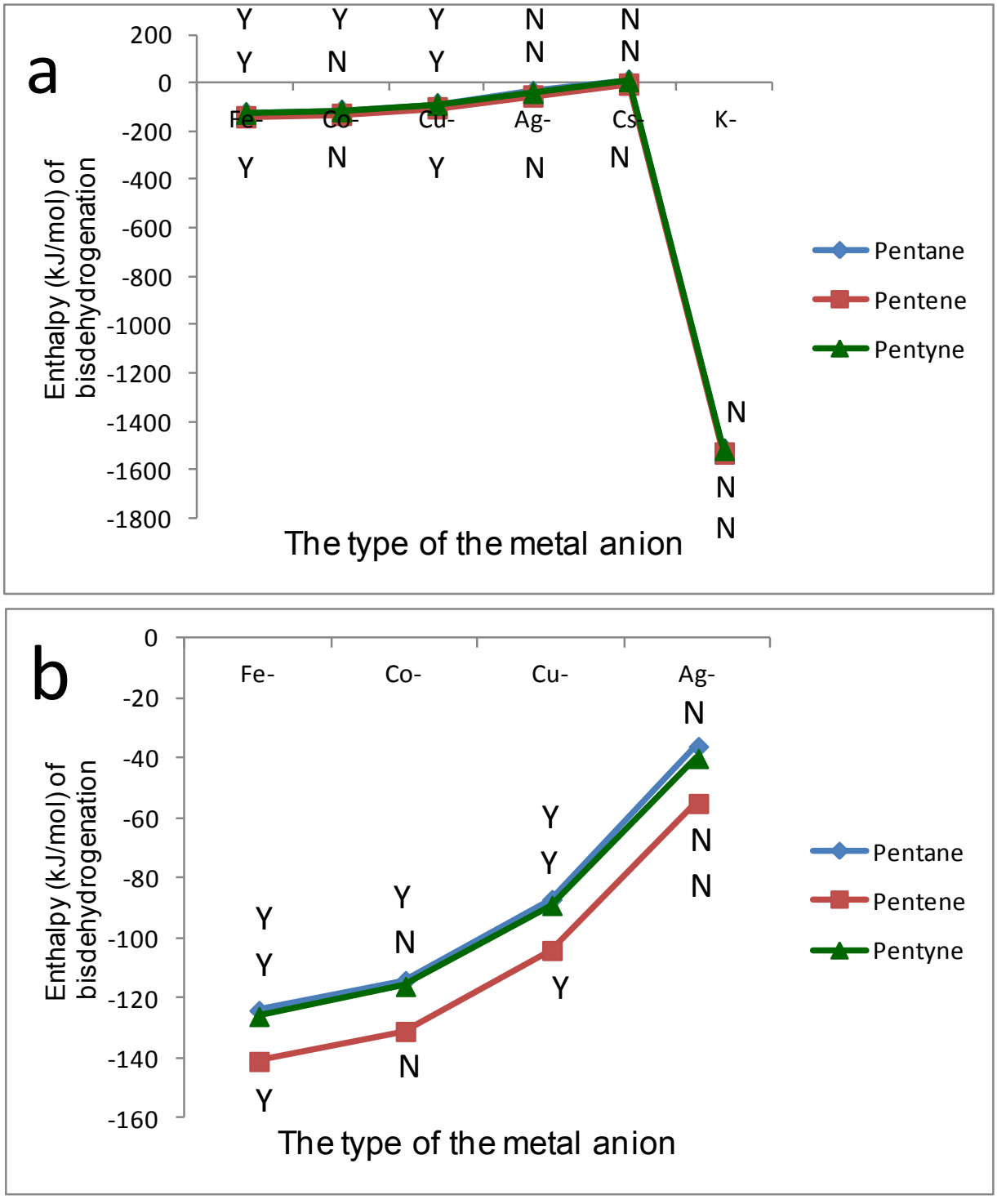

Figure 26: a) Enthalpies of the bisdehydrogenation reactions of metal anions with hydrocarbons; b) Extended Enthalpies of the bisdehydrogenation reactions of metal anions with hydrocarbons; Y indicates observed reactions and N indicates unobserved reactions

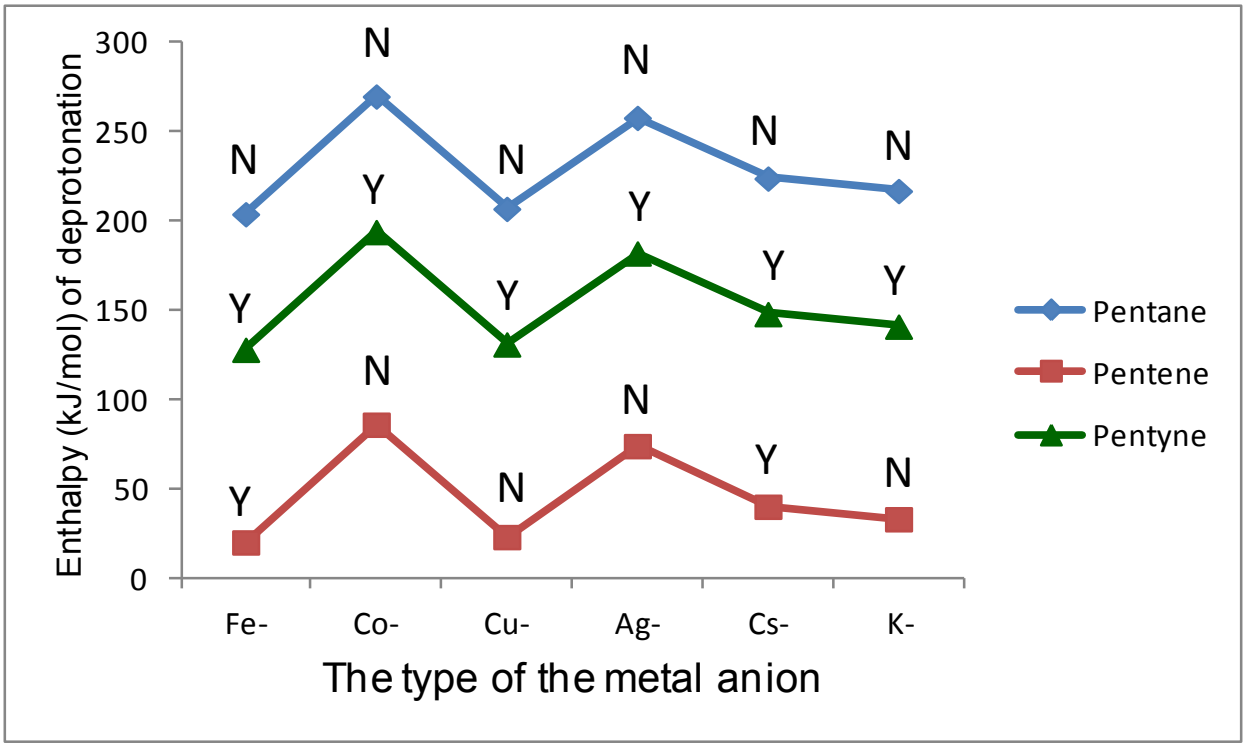

Figure 27: Enthalpies of the deprotonation reactions of metal anions with hydrocarbons; Y indicates observed reactions and N indicates unobserved reactions

Calculated enthalpies for reactions involving the iron anion or copper anion are typically lower than the calculated enthalpies for the cobalt anion or the silver anion, matching with the experimental results that show that the iron anion or copper anion show the dehydrogenation reaction whereas the cobalt anion or silver anion do not. Calculated enthalpies for 1-pentyne are lower than calculated enthalpies for pentene or pentane. Experiments show that 1-pentyne is more reactive than pentene and pentene is more reactive than pentane. This is expected since 1-pentyne and pentene have π orbitals and form a more stable intermediate complex by forming π back-bonding in the encounter complex. Calculated enthalpies for the bisdehydrogenation reactions are significantly lower than calculated enthalpies for the dehydrogenation reactions. Experiments show that metal dihydrides, products of the bisdehydrogenation reactions,

need less energy to be produced than metal hydrides, products of the dehydrogenation reactions. Below is a breakdown curve for the formation of FeH^- and FeH_2^- from the reaction of 2-pentene with Fe^-. A breakdown curve is a diagram of intensities of produced fragments in different voltages of the collision cell. This diagram shows that FeH_2^- starts to form at lower collision energies than FeH^- (Figure 28).

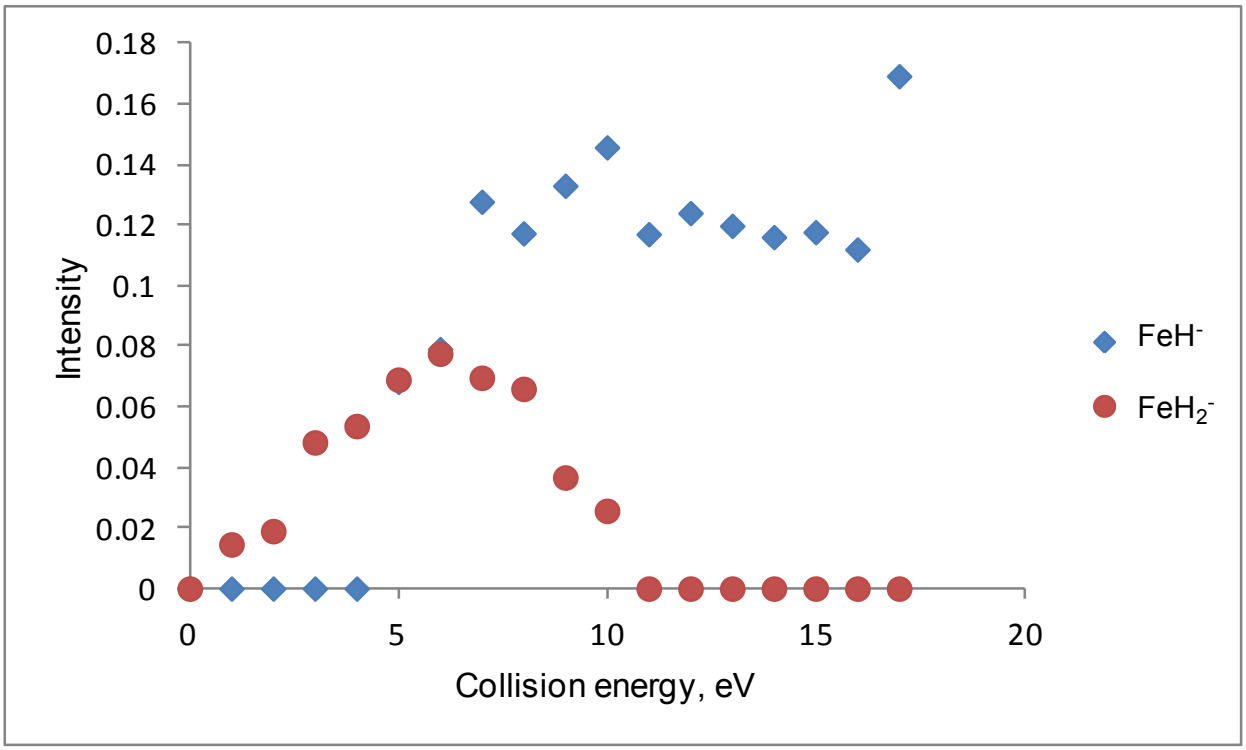

Figure 28: A break down curve of formation of FeH^- and FeH_2^- in the reaction of 2-pentene with Fe^- and shows that FeH_2^- needs less energy to be produced than FeH^-

Enthalpy values for the bisdehydrogenation reactions of alkali metal anions are unexpectedly low because cesium dihydride and potassium dihydride do not exist. The trend between calculated enthalpies matches with the trend between experimental data; however, calculated enthalpies are not a strong indicator to predict the

observation of a reaction. This could be due to the fact that the observation of a reaction depends directly on the barrier values of that reaction rather than enthalpy values. The mechanism of reaction may provide a better explanation for obtained results.

3.4.4: The mechanism of reactions

The deprotonation reaction of hydrocarbons follows the harpoon mechanism, a long range proton abstraction.[7] The deprotonation reaction is governed by the gas phase acidity of fragments. For example, all metal anions deprotonate 1-pentyne because it has a greater gas phase acidity than other metal anions. In a mass spectrometer, ions have high translational energy. For that reason, ions need less energy to show a deprotonation reaction than corresponding values in condensed phase .

The deprotonated hydrocarbon can dissociate spontaneously (reactions 40 and 41).

$C_5H_7^- \rightarrow C_2H^- + C_3H_6$ (40)

$C_5H_7^- \rightarrow C_3H_3^- + C_2H_4$ (41)

The driving force of this dissociation is the formation of stable products, such as propene and ethylene.

The research carried out by Dr. Mayer's group suggests that the dehydrogenation reaction of hydrocarbons follows a metal insertion mechanism. This may be similar to a novel oxidative addition-reductive elimination mechanism that has been previously suggested for reactions of metal-carbonyl anions with alcohols.[14] The first step in the reaction of metal anions with organic neutral target gases is the formation of the intermediate complex between the metal anion and the neutral target gas (Scheme 5).

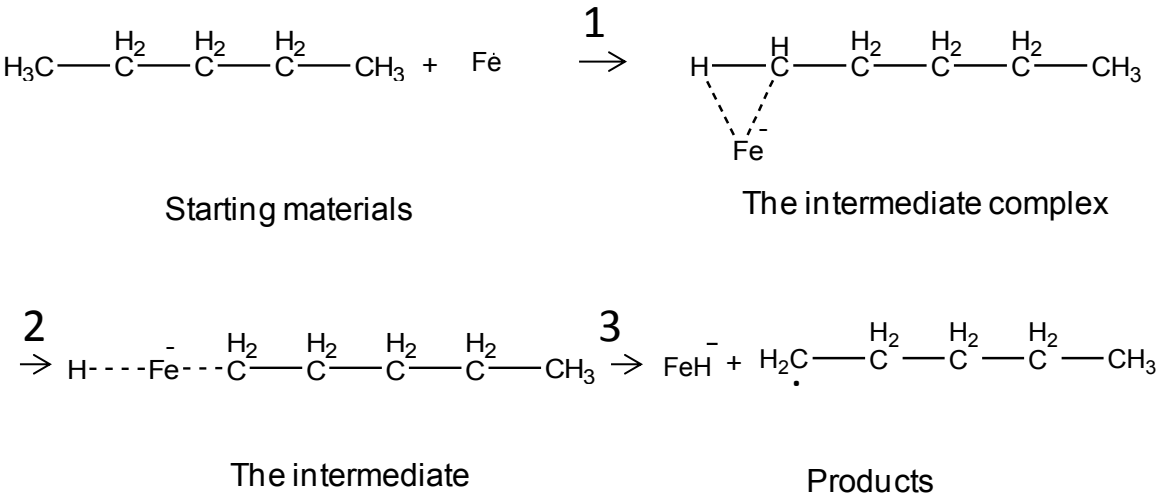

Scheme 5: The metal insertion mechanism for the dehydrogenation reaction of hydrocarbons with metal anions

The bond between 1-pentyne, with π orbitals, and the metal anions is stronger than the bond between pentane, with no π-orbitals, and the metal anions, due to the formation of π back-bonding in the intermediate complex. π back-bonding is formed between π-orbitals of 1-pentyne and empty orbitals of metal anions. Thus, 1-pentyne forms a more stable intermediate complex than pentane. As a result, 1-pentyne is more reactive than pentane. Alkali metal anions such as Cs^- and K^- have no accessible d-orbitals and are not able to form this intermediate complex.

The second step in the reaction of metal anions with organic neutral target gases is the insertion of the metal anion into the bond between the carbon and the functional group attached to it to form an intermediate. In this step, the negative charge of the metal anion in the intermediate complex is transferred to the empty anti-bonding orbital of the bond between carbon and the functional group, resulting in the breakage of this bond. When the functional group attached to the carbon atom is electronegative, the charge is more readily transferred to the empty anti-bonding orbital. The more electronegative the

functional group, the more exothermic the electron transfer step is. The electron transfer step is the rate-determining step of the mechanism. H has low electronegativity; thus, the electron transfer step, involving the movement of the negative charge from the metal to the C-H bond, is endothermic and the dehydrogenation reaction of hydrocarbons needs extra energy to take place.

The third step in the reaction of metal anions with organic neutral target gases is the dissociation of the intermediate to products that are observed in the mass spectrum. In the intermediate, the weaker bond, either the bond between the metal anion and hydrogen or the bond between the metal anion and carbon will break. The negative charge will remain on the more electronegative fragment.

The intermediate of the reaction of metal anion with the target gas can rearrange prior to the dissociation. The result of a β-H-shift, β-H-elimination, is the attachment of two hydrogens to the metal anion. The dissociation of this rearranged intermediate produces a metal dihydride anion. During this dissociation, the negative charge remains on the metal dihydride, indicating that metal dihydride is more electronegative than the other counterpart of this dissociation (Scheme 6).

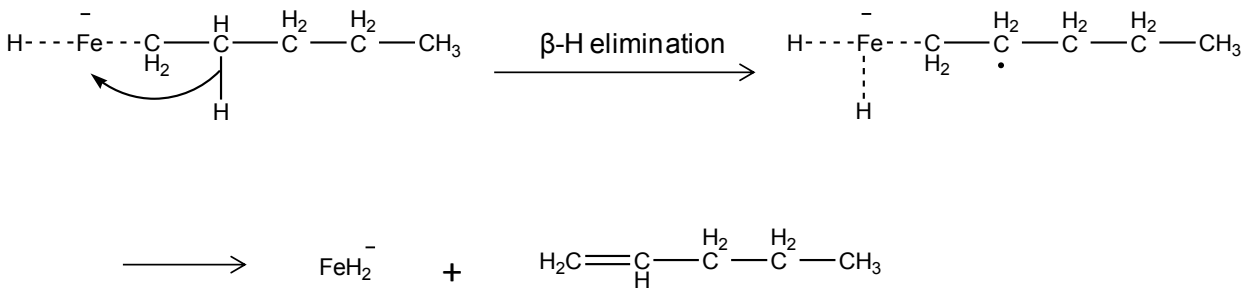

Scheme 6: The β-H elimination rearrangement of the intermediate leading to the formation of the metal dihydride anion

Chapter 4: Result and discussion of reactions of alcohols

4.1: Reactions with 1-butanol

4.1.1: Reactions of 1-butanol with Fe^-

With the collision voltage of 0 eV, no reaction was observed. With the collision voltage of 5 eV, m/z 56 (Fe^-); m/z 57 (FeH^-); m/z 58 (FeH_2^-); m/z 74 ($C_4H_{10}O^{\cdot-}$); m/z 73 ($C_4H_9O^-$); m/z 71 ($C_4H_7O^-$) and m/z 129 ($FeC_4H_9O^-$) were observed in the mass spectrum of the reaction of Fe^- with 1-butanol (Figure 29).

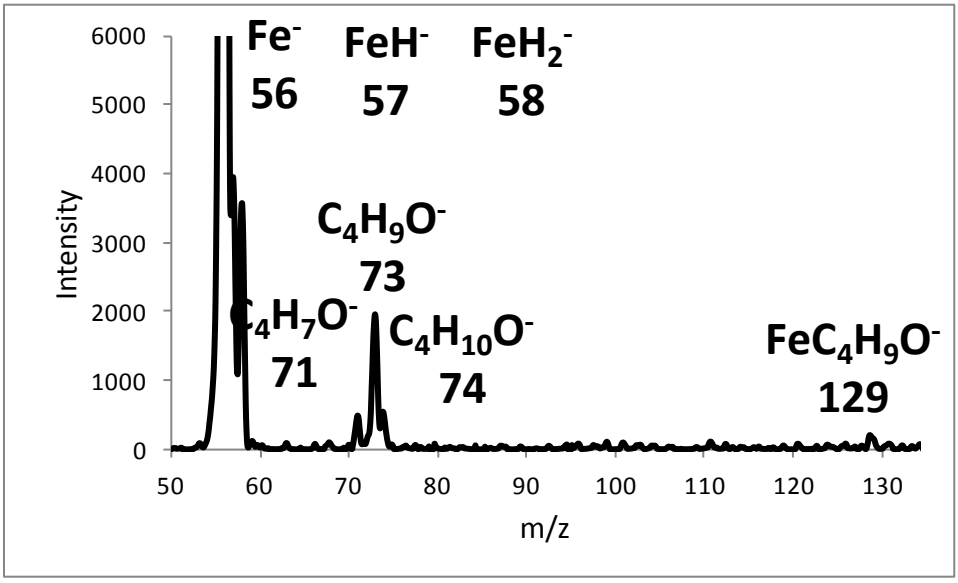

Figure 29: Mass spectrum of products of the reaction of 1-butanol with Fe^- in voltages of (50-5-50) and the target gas pressure of 1.2 e-3 mbar

FeH^- is a product of dehydrogenation; FeH_2^- is a product of bisdehydrogenation; $C_4H_{10}O^{\cdot -}$ is a product of electron transfer; $C_4H_9O^-$ is a product of deprotonation; $C_4H_7O^-$ is a product of dissociation of $C_4H_9O^-$; and $FeC_4H_9O^-$ is a product of complex formation of Fe^- with 1-butanol (reactions 45 to 50).

$$C_4H_{10}O + Fe^- \rightarrow C_4H_9O + FeH^- \quad (45)$$

$$C_4H_{10}O + Fe^- \rightarrow C_4H_8O + FeH_2^- \quad (46)$$

$$C_4H_{10}O + Fe^- \rightarrow C_4H_9O^- + FeH \quad (47)$$

$$C_4H_9O^- \rightarrow C_4H_7O^- + H_2 \quad (48)$$

$$C_4H_{10}O + Fe^- \rightarrow C_4H_{10}O^- + Fe \quad (49)$$

$$C_4H_{10}O + Fe^- \rightarrow FeC_4H_9O^- + H \quad (50)$$

To confirm that m/z 57, m/z 58 and m/z 129 are not artifacts, this experiment was repeated with a deuterated compound. In 1-butanol-d_{10}, all hydrogens, with the atomic weight of 1 amu, were exchanged with deuterium, with the atomic weight of 2 amu. Thus, the m/z of the corresponding fragments in the reaction will shift in the mass spectrum.

With the collision voltage of 5 eV, m/z 56 (Fe^-); m/z 58 (FeD^-); m/z 60 (FeD_2^-); m/z 82 ($C_4D_9O^-$) and m/z 138 ($FeC_4D_9O^-$) were observed in the mass spectrum of the reaction of Fe^- with 1-butanol-d_{10} (Figure 30).

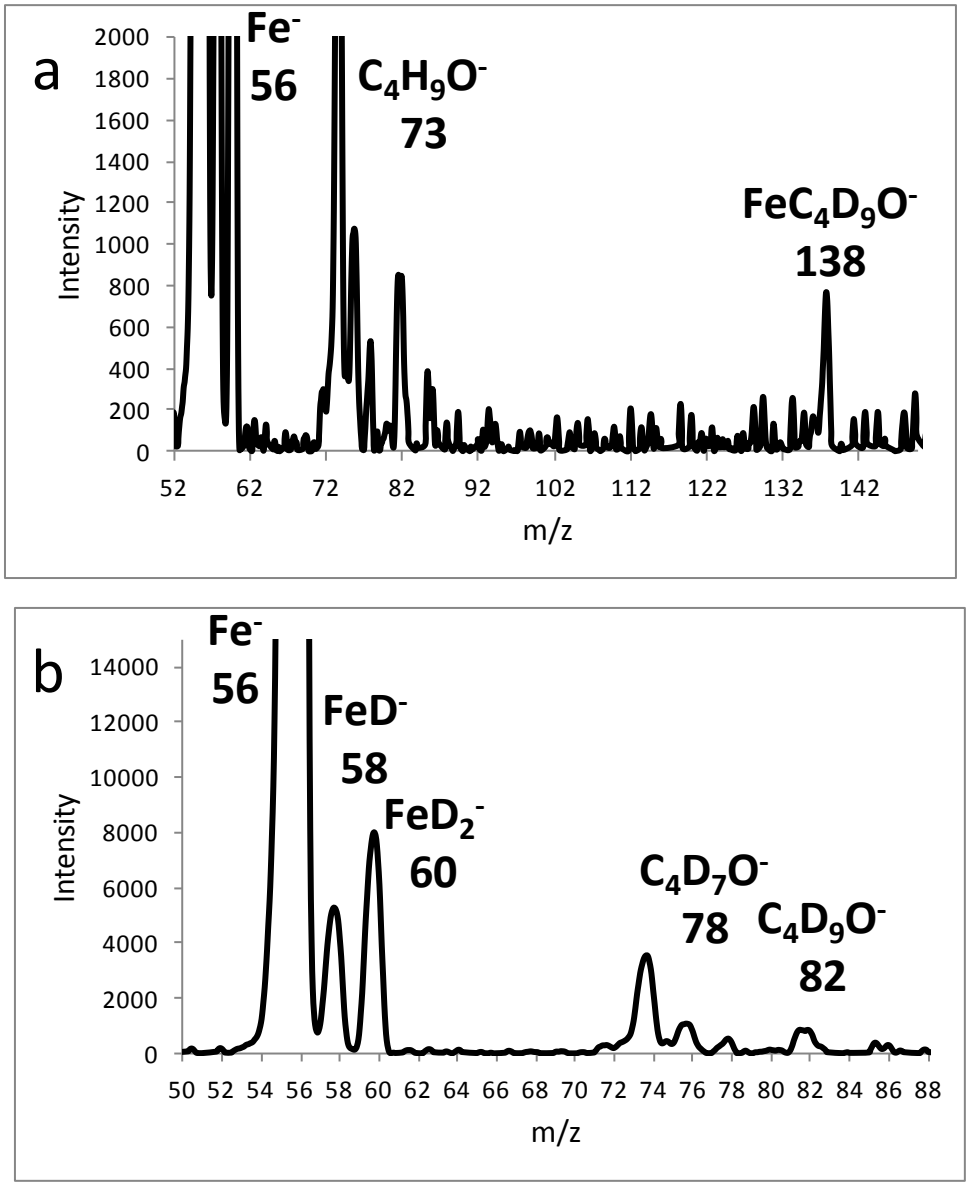

Figure 30: a) Mass spectrum of products of the reaction of 1-butanol-d_{10} with Fe^- in voltages of (50-5-50) and the target gas pressure of 1.2 e-3 mbar; b) The expanded spectrum shown in a, between 50 and 88 m/z

4.1.2: Reactions of 1-butanol with Co^-

With the collision voltage of 0 eV, m/z 59 (Co^-) and m/z 132 ($CoC_4H_9O^-$) were observed in the mass spectrum of the reaction of 1-butanol with Co^- (Figure 31).

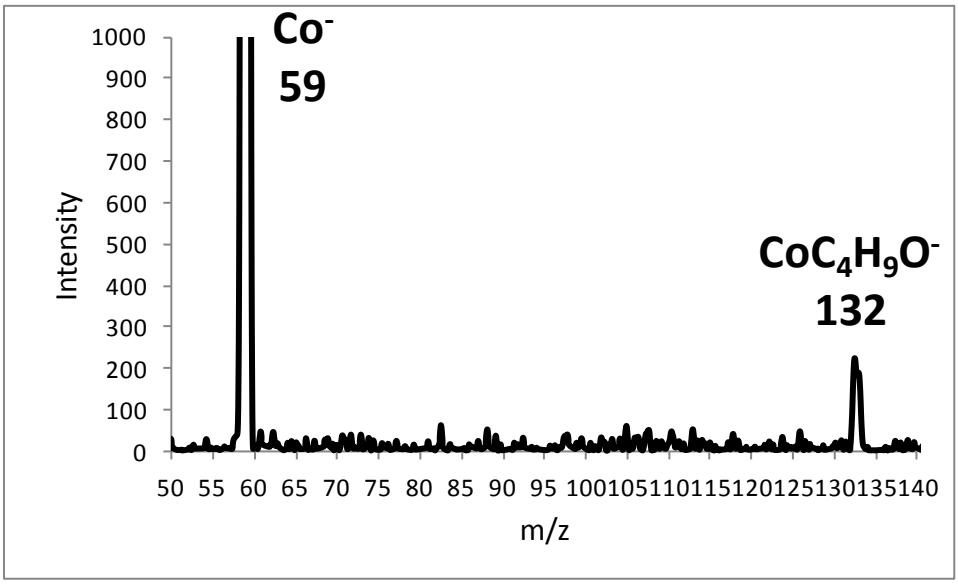

Figure 31: Mass spectrum of product of the reaction of 1-butanol with Co^- in voltages of (50-0-50) and the target gas pressure of 1.2 e-3 mbar

$CoC_4H_9O^-$ is a product of the complex formation reaction (reaction 51).

$$C_4H_{10}O + Co^- \rightarrow CoC_4H_9O^- + H \qquad (51)$$

4.1.3: Reactions of 1-butanol with Cu^-

With the collision voltage of 0 eV, no reaction was observed. With the collision voltage of 10 eV, m/z 65 (Cu^-); m/z 67 (CuH_2^-); m/z 82 ($CuOH^-$); m/z 81 (CuO^-); m/z 73 ($C_4H_9O^-$) and m/z 71 ($C_4H_7O^-$) were observed in the mass spectrum of the reaction of Cu^- with 1-butanol (Figure 32).

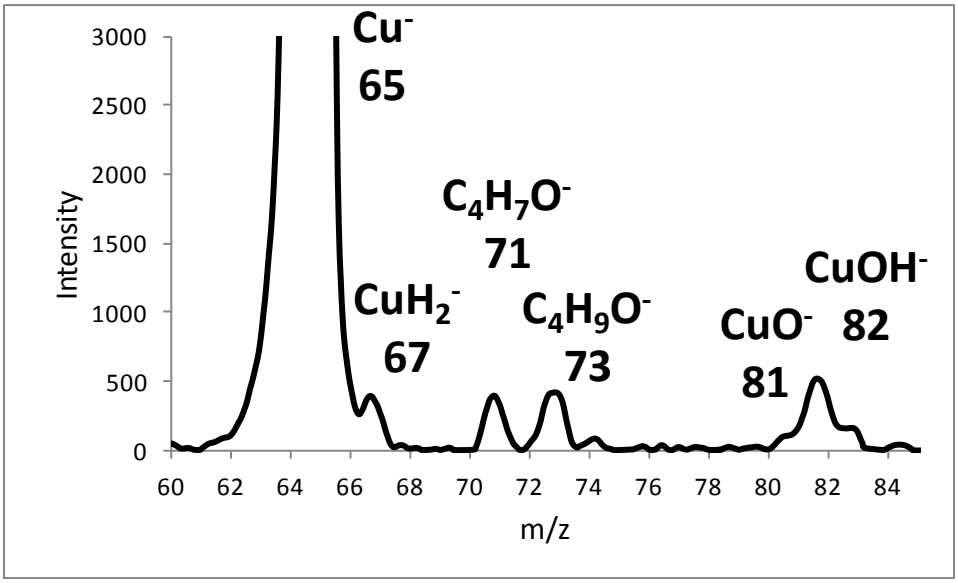

Figure 32: Mass spectrum of products of the reaction of 1-butanol with $^{65}Cu^-$ in voltages of (50-5-50) and the target gas pressure of 1.2 e-3

CuH_2^- is a product of bisdehydrogenation; $CuOH^-$ is a product of dehydroxylation; CuO^- is a product of O-atom abstraction; $C_4H_9O^-$ is a product of deprotonation and $C_4H_7O^-$ is a products of spontaneous dissociation of the deprotonated alcohol (reactions 52 to 56 and reaction 48).

$C_4H_{10}O + Cu^- \rightarrow C_4H_8O + CuH_2^-$ (52)

$C_4H_{10}O + Cu^- \rightarrow C_4H_9O^- + CuH$ (53)

$C_4H_9O^- \rightarrow C_4H_7O^- + H_2$ (48)

$C_4H_{10}O + Cu^- \rightarrow C_4H_9 + CuOH^-$ (54)

$C_4H_{10}O + Cu^- \rightarrow C_4H_{10} + CuO^-$ (55) [OR $CuOH^- \rightarrow CuO^- + H$ (56)]

To confirm this result, the experiment was repeated with a deuterated butanol. With the collision voltage of 10 eV, m/z 65 (Cu^-); m/z 69 (CuD_2^-); m/z 83 ($CuOD^-$); m/z 81 (CuO^-); m/z 73 ($C_4H_9O^-$) and m/z 71 ($C_4H_7O^-$) were observed in the mass spectrum of the reaction of Cu^- with 1-butanol-d_{10} (Figure 33).

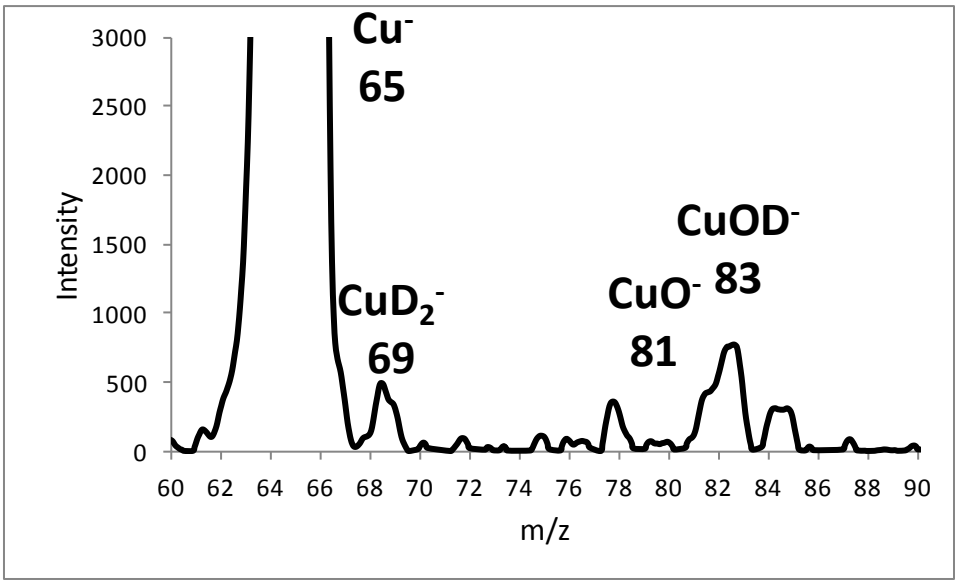

Figure 33: Mass spectrum of products of the reaction of 1-butanol-d_{10} with $^{65}Cu^-$ in voltages of (50-5-50) and the gas pressure of 1.2 e-3 mbar

4.1.4: Reactions of 1-butanol with Ag^-

With the collision voltage of 0 eV, no reaction was observed. With the collision voltage of 10 eV, m/z 107 (Ag^-); m/z 124 ($AgOH^-$) and m/z 123 (AgO^-) were observed in the mass spectrum of the reaction of Ag^- with 1-butanol (Figure 34).

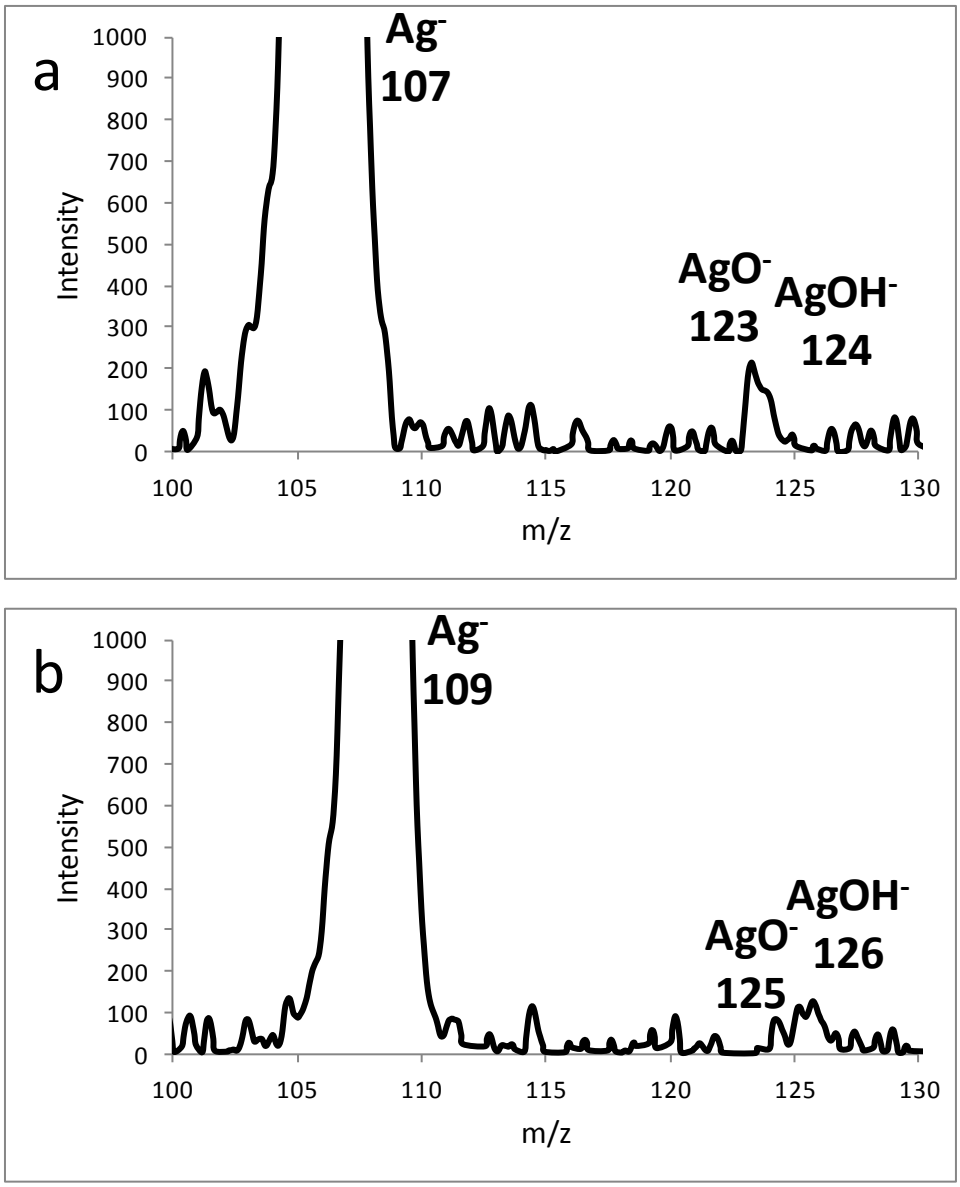

Figure 34: a) Mass spectrum of products of the reaction of 1-butanol with $^{107}Ag^-$ in voltages of (50-10-50) and the target gas pressure of 1.2 e-3 mbar; b) Mass spectrum of products of the reaction of 1-butanol with $^{109}Ag^-$ in voltages of (50-10-50) and the target gas pressure of 1.2 e-3 mbar

With the collision voltage of 20 eV, m/z 107 (Ag^-); m/z 73 ($C_4H_9O^-$) and m/z 71 ($C_4H_7O^-$) were observed in the mass spectrum of the reaction of Ag^- with 1-butanol (Figure 35).

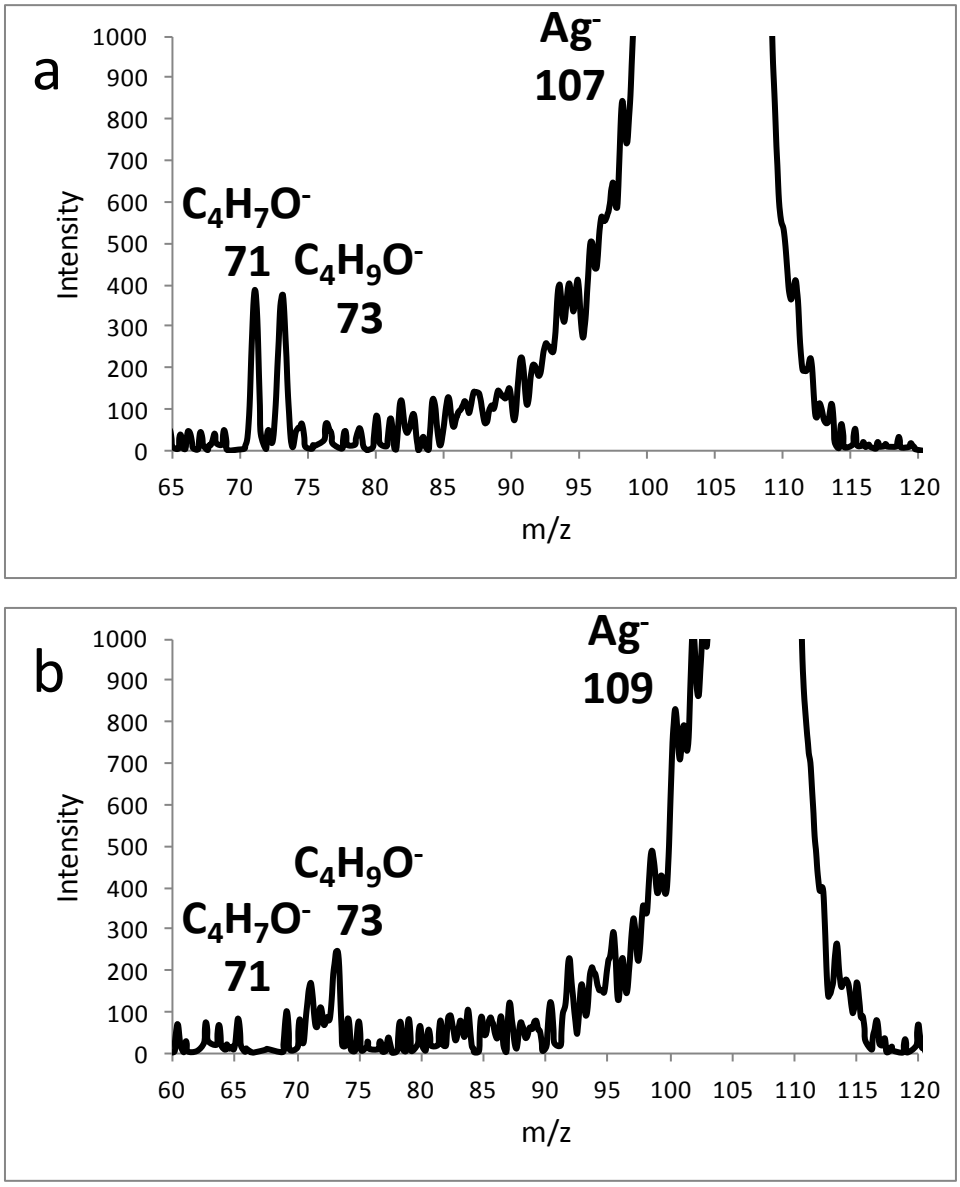

Figure 35: a) Mass spectrum of products of the reaction of 1-butanol with $^{107}Ag^-$ in voltages of (50-20-50) and the target gas pressure of 1.2 e-3 mbar; b) Mass spectrum of products of the reaction of 1-butanol with $^{109}Ag^-$ in voltages of (50-20-50) and the target gas pressure of 1.2 e-3 mbar

$AgOH^-$ is a product of dehydroxylation; AgO^- is a product of O-atom abstraction; $C_4H_9O^-$ is a product of deprotonation; and $C_4H_7O^-$ is a product of spontaneous dissociation of the deprotonated fragment (reactions 57 to 60 and reaction 48).

$$C_4H_{10}O + Ag^- \rightarrow C_4H_9O^- + AgH \quad (57)$$

$$C_4H_9O^- \rightarrow C_4H_7O^- + H_2 \quad (48)$$

$$C_4H_{10}O + Ag^- \rightarrow C_4H_9 + AgOH^- \quad (58)$$

$$C_4H_{10}O + Ag^- \rightarrow C_4H_{10} + AgO^- \quad (59) \quad [OR \quad AgOH^- \rightarrow AgO^- + H \quad (60)\ ]$$

4.1.5: Reactions of 1-butanol with Cs^-

With the collision voltage of 0 eV, no reaction was observed. With the collision voltage of 20 eV, m/z 133 (Cs^-); m/z 73 ($C_4H_9O^-$); m/z 71 ($C_4H_7O^-$); m/z 57 (R^-); m/z 17 (OH^-) and m/z 147 (ROH2-1$^-$) were observed in the mass spectrum of the reaction of 1-butanol with Cs^- (Figure 36).

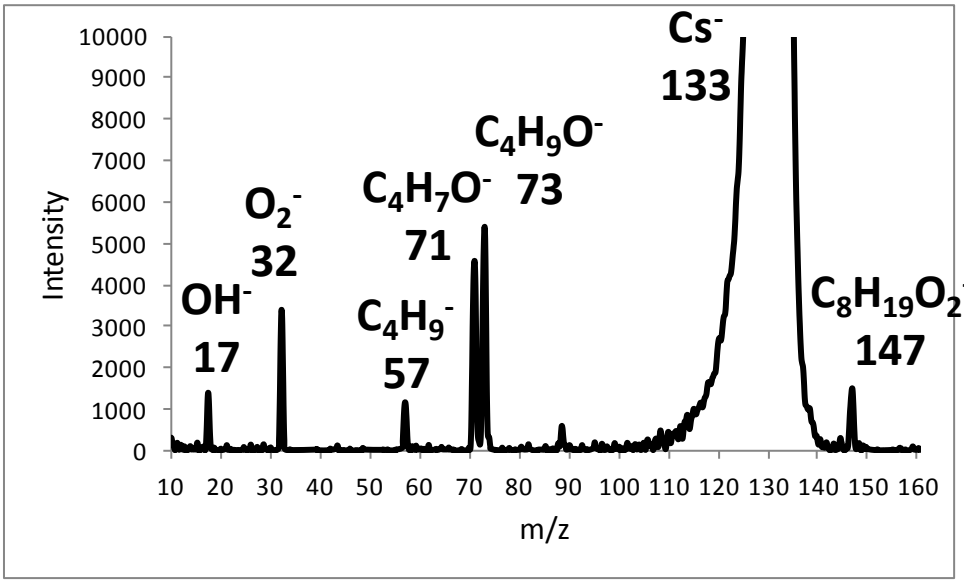

Figure 36: Mass spectrum of products of the reaction of 1-butanol with Cs^- in voltages of (50-20-50) and the target gas pressure of 1.2 e-3 mbar

$C_4H_9O^-$ is a product of deprotonation; $C_4H_7O^-$, $C_4H_9^-$ and OH^- are products of spontaneous dissociation of the deprotonated fragment and $C_8H_{19}O^-$ is a product of dimerization. m/z 32 (O_2^-) is a contamination of oxygen in the system (reactions 61 to 64 and reaction 48).

$$C_4H_{10}O + Cs^- \rightarrow C_4H_9O^- + CsH \quad (61)$$

$$C_4H_9O^- \rightarrow C_4H_7O^- + H_2 \quad (48)$$

$$C_4H_9O^- \rightarrow C_4H_9^- + O \quad (62)$$

$$C_4H_9O^- \rightarrow C_4H_8 + OH^- \quad (63)$$

$$C_4H_9O^- + C_4H_{10}O \rightarrow C_8H_{19}O^- \quad (64)$$

4.1.6: Reactions of 1-butanol with K^-

With the collision voltage of 0 eV, no reaction was observed. With the collision voltage of 20 eV, m/z 39 (K^-); m/z 73 ($C_4H_9O^-$) and m/z 17 (OH^-) were observed in the mass spectrum of the reaction of 1-butanol with K^- (Figure 37).

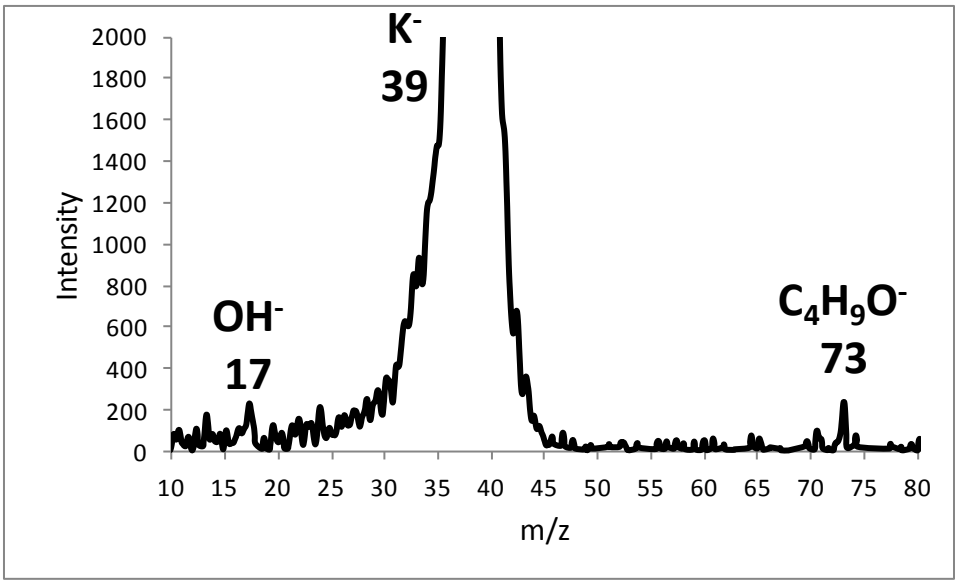

Figure 37: Mass spectrum of products of the reaction of 1-butanol with K^- in voltages of (50-20-50) and the target gas pressure of 1.2 e-3 mbar

$C_4H_9O^-$ is a product of deprotonation and OH^- is a product of spontaneous dissociation of the deprotonated fragment (reactions 65 and 63).

$$C_4H_{10}O + K^- \rightarrow C_4H_9O^- + KH \quad (65)$$

$$C_4H_9O^- \rightarrow C_4H_8 + OH^- \quad (63)$$

4.2: Reactions of 2-butanol with metal anions

4.2.1: Reactions of 2-butanol with Fe^-

With the collision voltage of 0 eV, no reaction was observed. With the collision voltage of 5 eV, m/z 56 (Fe^-); m/z 57 (FeH^-); m/z 58 (FeH_2^-); m/z 74 ($C_4H_{10}O^{\cdot-}$); m/z 73 ($C_4H_9O^-$); m/z 71 ($C_4H_7O^-$) and m/z 129 ($FeC_4H_9O^-$) were observed in the mass spectrum of the reaction of Fe^- with 2-butanol (Figure 38).

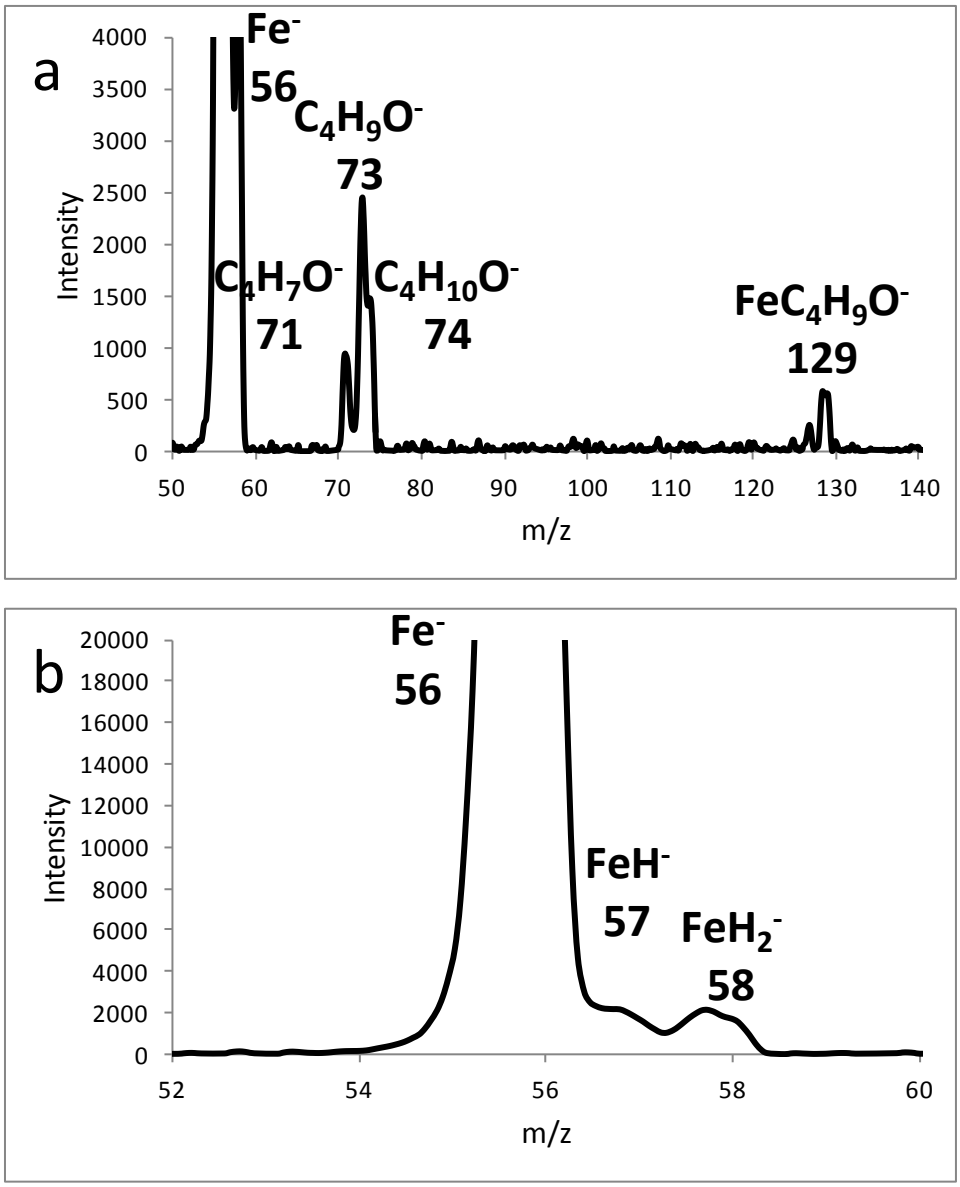

Figure 38: a) Mass spectrum of products of the reaction of 2-butanol with Fe^- in voltages of (50-5-50) and the target gas pressure of 1.2 e-3 mbar; b) The expanded mass spectrum shown in a, between 52 and 60 m/z

FeH^- is a product of dehydrogenation; FeH_2^- is a product of bisdehydrogenation; $C_4H_{10}O^-$ is a product of electron transfer; $C_4H_9O^-$ is a product of deprotonation; $C_4H_7O^-$

is a product of dissociation of $C_4H_9O^-$; and $FeC_4H_9O^-$ is a product of complex formation reaction of Fe^- with 2-butanol (reactions 66 to 71).

$$C_4H_{10}O + Fe^- \rightarrow C_4H_9O + FeH^- \quad (66)$$

$$C_4H_{10}O + Fe^- \rightarrow C_4H_8O + FeH_2^- \quad (67)$$

$$C_4H_{10}O + Fe^- \rightarrow C_4H_9O^- + FeH \quad (68)$$

$$C_4H_9O^- \rightarrow C_4H_7O^- + H_2 \quad (69)$$

$$C_4H_{10}O + Fe^- \rightarrow C_4H_{10}O^- + Fe \quad (70)$$

$$C_4H_{10}O + Fe^- \rightarrow FeC_4H_9O^- + H \quad (71)$$

With the collision voltage of 20 eV, m/z 56 (Fe^-); m/z 73 ($C_4H_9O^-$); m/z 71 ($C_4H_7O^-$); m/z 17 (OH^-) and m/z 147 ($C_8H_{19}O^-$) were observed in the mass spectrum of the reaction of 2-butanol with Fe^- (Figure 39).

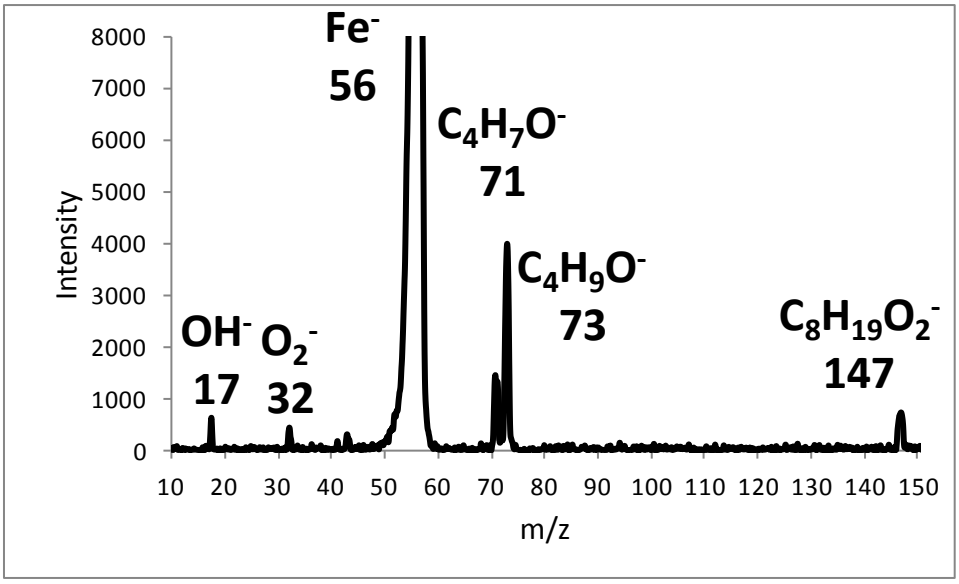

Figure 39: Mass spectrum of products of the reaction of 2-butanol with Fe^- in voltages of (50-20-50) and the target gas pressure of 1.2 e-3 mbar

$C_4H_9O^-$ is a product of deprotonation; $C_4H_7O^-$ and OH^- are products of spontaneous dissociation of the deprotonated fragment; and ($C_8H_{19}O^-$) is a product of dimerization in the reaction of Fe^- with 2-butanol (reactions 68, 69, 72 and 73).

$$C_4H_{10}O + Fe^- \rightarrow C_4H_9O^- + FeH \quad (68)$$

$$C_4H_9O^- \rightarrow C_4H_7O^- + H_2 \quad (69)$$

$$C_4H_9O^- \rightarrow C_4H_8 + OH^- \quad (72)$$

$$C_4H_9O^- + C_4H_{10}O \rightarrow C_8H_{19}O^- \quad (73)$$

4.2.2: Reactions of 2-butanol with Co^-

With the collision voltage of 0 eV, m/z 59 (Co^-) and m/z 132 ($CoC_4H_9O^-$) were observed in the mass spectrum of the reaction of 2-butanol with Co^- (Figure 40).

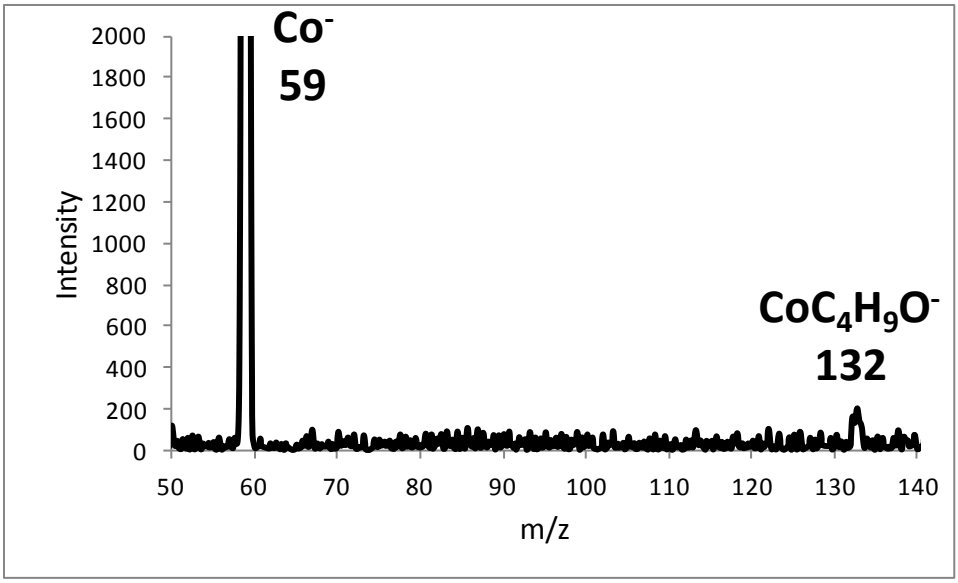

Figure 40: Mass spectrum of product of the reaction of 1-butanol with Co^- in voltages of (50-0-50) and the target gas pressure of 1.2 e-3 mbar

$CoC_4H_9O^-$ is a product of complex formation reaction of Co^- with 2-butanol (reaction 74).

$$C_4H_{10}O + Co^- \rightarrow CoC_4H_9O^- + H \quad (74)$$

With the collision voltage of 15 eV, m/z 59 (Co); m/z 73 ($C_4H_9O^-$) and m/z 71 ($C_4H_7O^-$) were observed in the mass spectrum of the reaction of 2-butanol with Co^- (Figure 41).

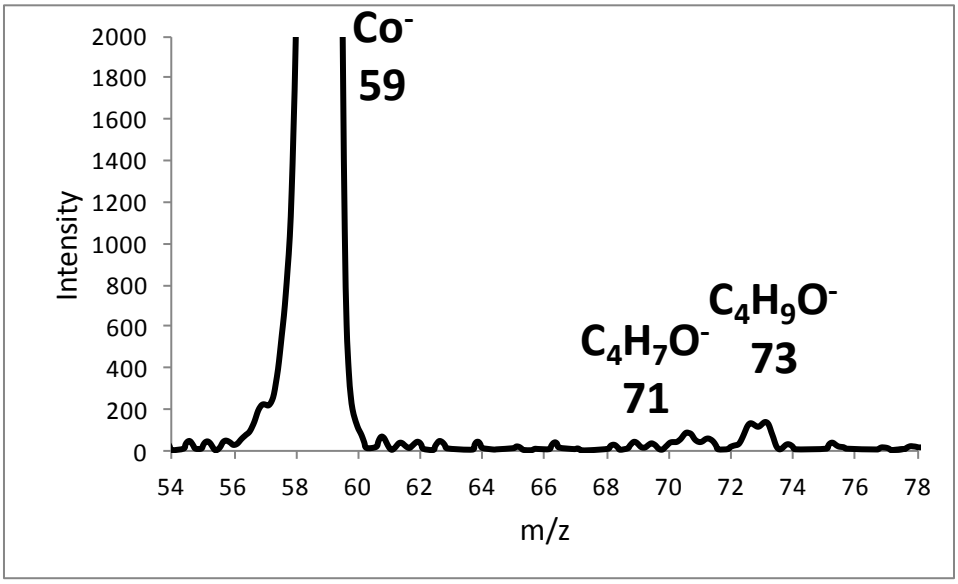

Figure 41: Mass spectrum of product of the reaction of 2-butanol with Co^- in voltages of (50-15-50) and the target gas pressure of 1.2 e-3 mbar

$C_4H_9O^-$ is a product of deprotonation and $C_4H_7O^-$ is a product of spontaneous dissociation of the deprotonated fragment (reactions 75 and 69).

$$C_4H_{10}O + Co^- \rightarrow C_4H_9O^- + CoH \quad (75)$$

$$C_4H_9O^- \rightarrow C_4H_7O^- + H_2 \quad (69)$$

4.2.3: Reactions of 2-butanol with Cu^-

With the collision voltage of 0 eV, no reaction was observed. With the collision voltage of 5 eV, m/z 65 (Cu^-); m/z 67 (CuH_2^-); m/z 82 ($CuOH^-$); m/z 81 (CuO^-); m/z 73 ($C_4H_9O^-$)

and m/z 71 ($C_4H_7O^-$) were observed in the mass spectrum of the reaction of Cu^- with 2-butanol (Figure 42).

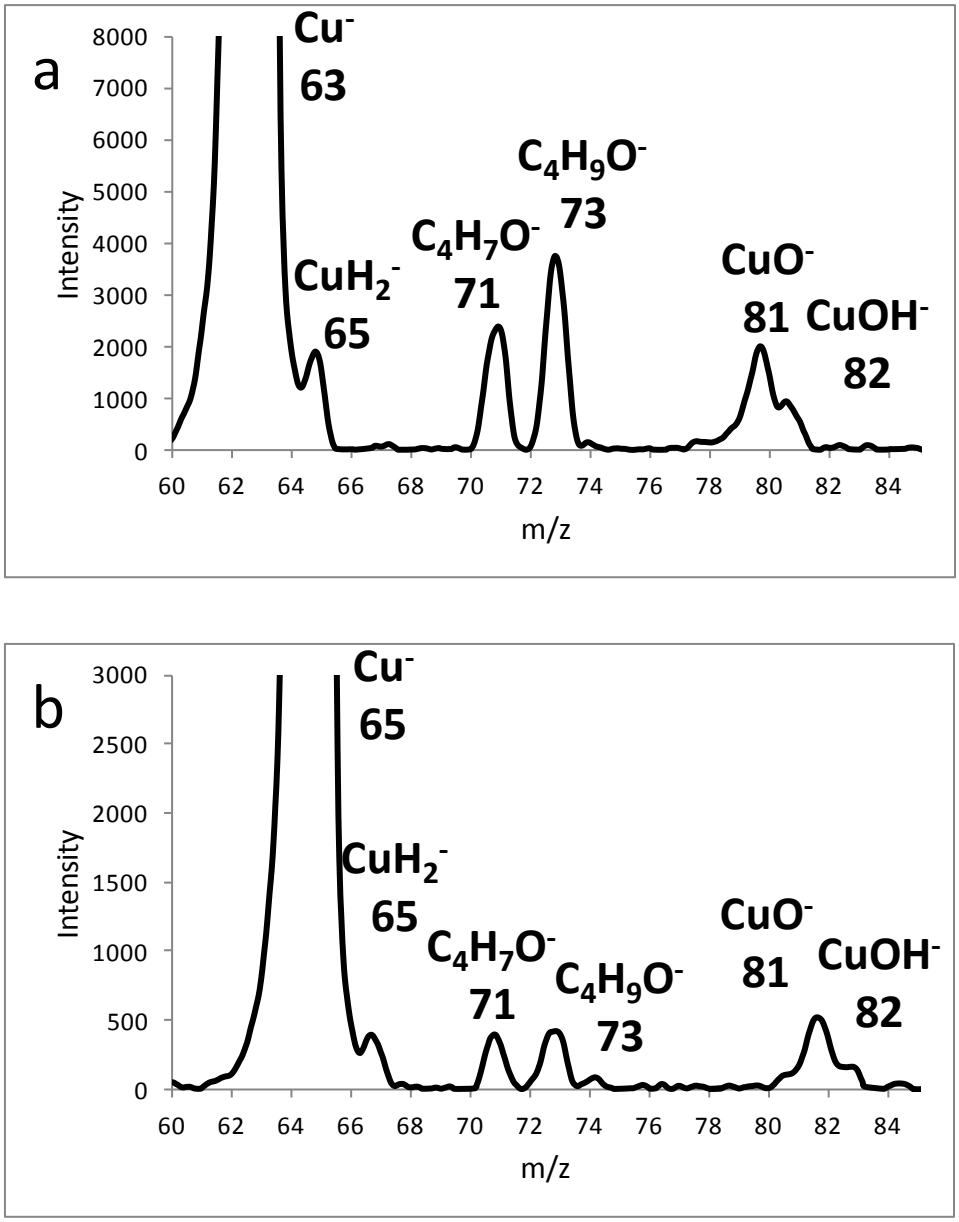

Figure 42: a) Mass spectrum of products of the reaction of 2-butanol with $^{63}Cu^-$ in voltages of (50-5-50) and the target gas pressure of 1.2 e-3 mbar; b) Mass spectrum of products of the reaction of 2-butanol with $^{65}Cu^-$ in voltages of (50-5-50) and the target gas pressure of 1.2 e-3 mbar

CuH_2^- is a product of bisdehydrogenation; $CuOH^-$ is a product of dehydroxylation; CuO^- is a product of O-atom abstraction; $C_4H_9O^-$ is a product of deprotonation; and $C_4H_7O^-$ is a product of spontaneous dissociation of the deprotonated alcohol (reactions 76 to 79 and reactions 69 and 56).

$C_4H_{10}O + Cu^- \rightarrow C_4H_8O + CuH_2^-$ (76)

$C_4H_{10}O + Cu^- \rightarrow C_4H_9O^- + CuH$ (77)

$C_4H_9O^- \rightarrow C_4H_7O^- + H_2$ (69)

$C_4H_{10}O + Cu^- \rightarrow C_4H_9 + CuOH^-$ (78)

$C_4H_{10}O + Cu^- \rightarrow C_4H_{10} + CuO^-$ (79) [OR $CuOH^- \rightarrow CuO^- + H$ (56)]

With the collision voltage of 15 eV, m/z 65 (Cu^-); m/z 81 (CuO^-); m/z 73 ($C_4H_9O^-$); m/z 71 ($C_4H_7O^-$); m/z 57 ($C_4H_9^-$); m/z 17 (OH^-) and m/z 147 ($C_8H_{19}O^-$) were observed in the mass spectrum of the reaction of Cu^- with 2-butanol (Figure 43).

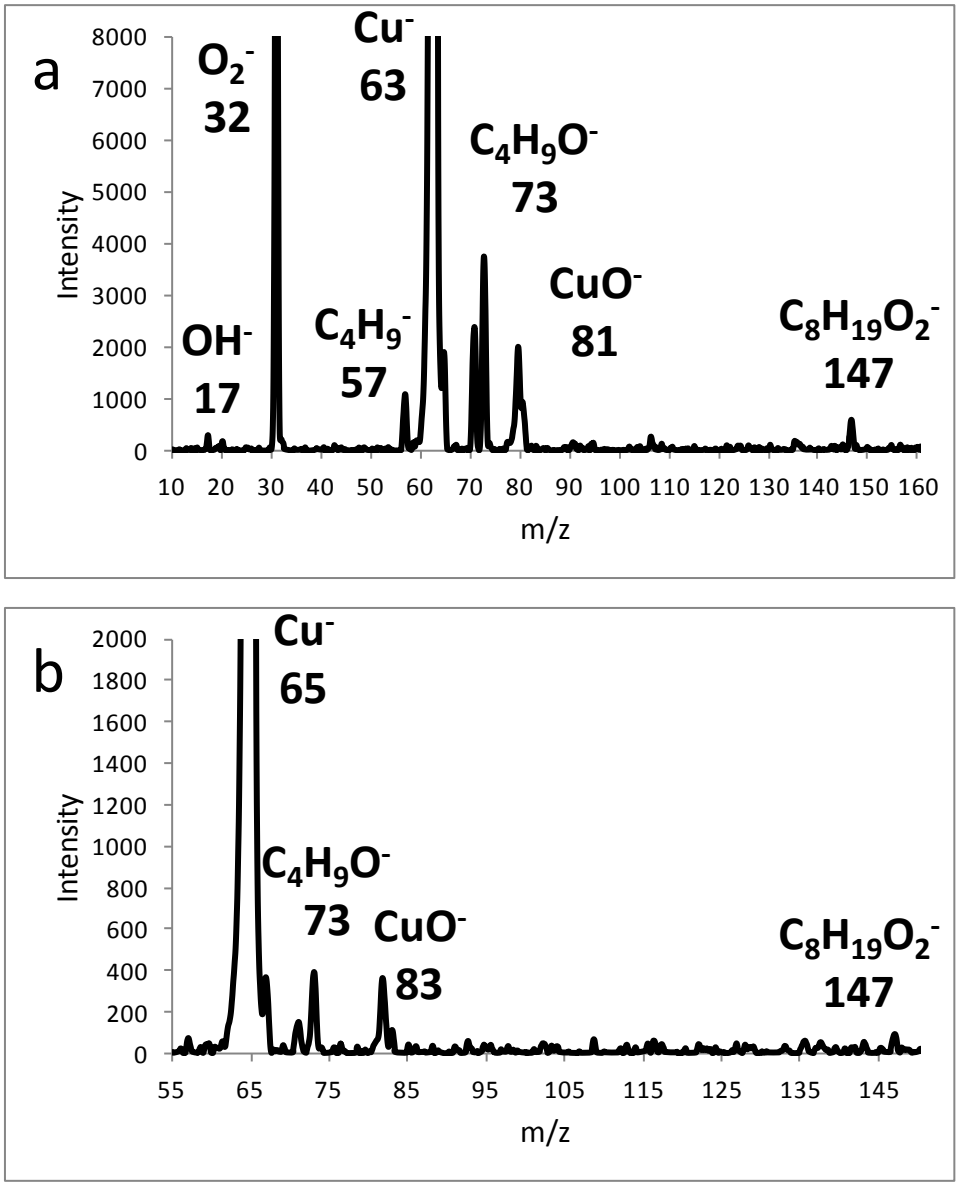

Figure 43: a) Mass spectrum of products of the reaction of 2-butanol with $^{63}Cu^-$ in voltages of (50-15-50) and the target gas pressure of 1.2 e-3 mbar; b) Mass spectrum of products of the reaction of 2-butanol with $^{65}cu^-$ in voltages of (50-15-50) and the target gas pressure of 1.2 e-3 mbar

CuO^- is a product of O-atom abstraction; $C_4H_9O^-$ is a product of deprotonation; $C_4H_7O^-$, $C_4H_9^-$ and OH^- are products of spontaneous dissociation of the deprotonated fragment; and ($C_8H_{19}O^-$) is a product of dimerization (reactions 77, 69, 80, 72 and 73).

$$C_4H_{10}O + Cu^- \rightarrow C_4H_9O^- + CuH \quad (77)$$

$$C_4H_9O^- \rightarrow C_4H_7O^- + H_2 \quad (69)$$

$$C_4H_9O^- \rightarrow C_4H_9^- + O \quad (80)$$

$$C_4H_9O^- \rightarrow C_4H_8 + OH^- \quad (72)$$

$$C_4H_9O^- + C_4H_{10}O \rightarrow C_8H_{19}O^- \quad (73)$$

4.2.4: Reactions of 2-butanol with Ag^-

With the collision voltage of 0 eV, no reaction was observed. With the collision voltage of 10 eV, m/z 107 (Ag^-), m/z 124 ($AgOH^-$) and m/z 123 (AgO^-) were observed in the mass spectrum of the reaction of Ag^- with 2-butanol (Figure 44).

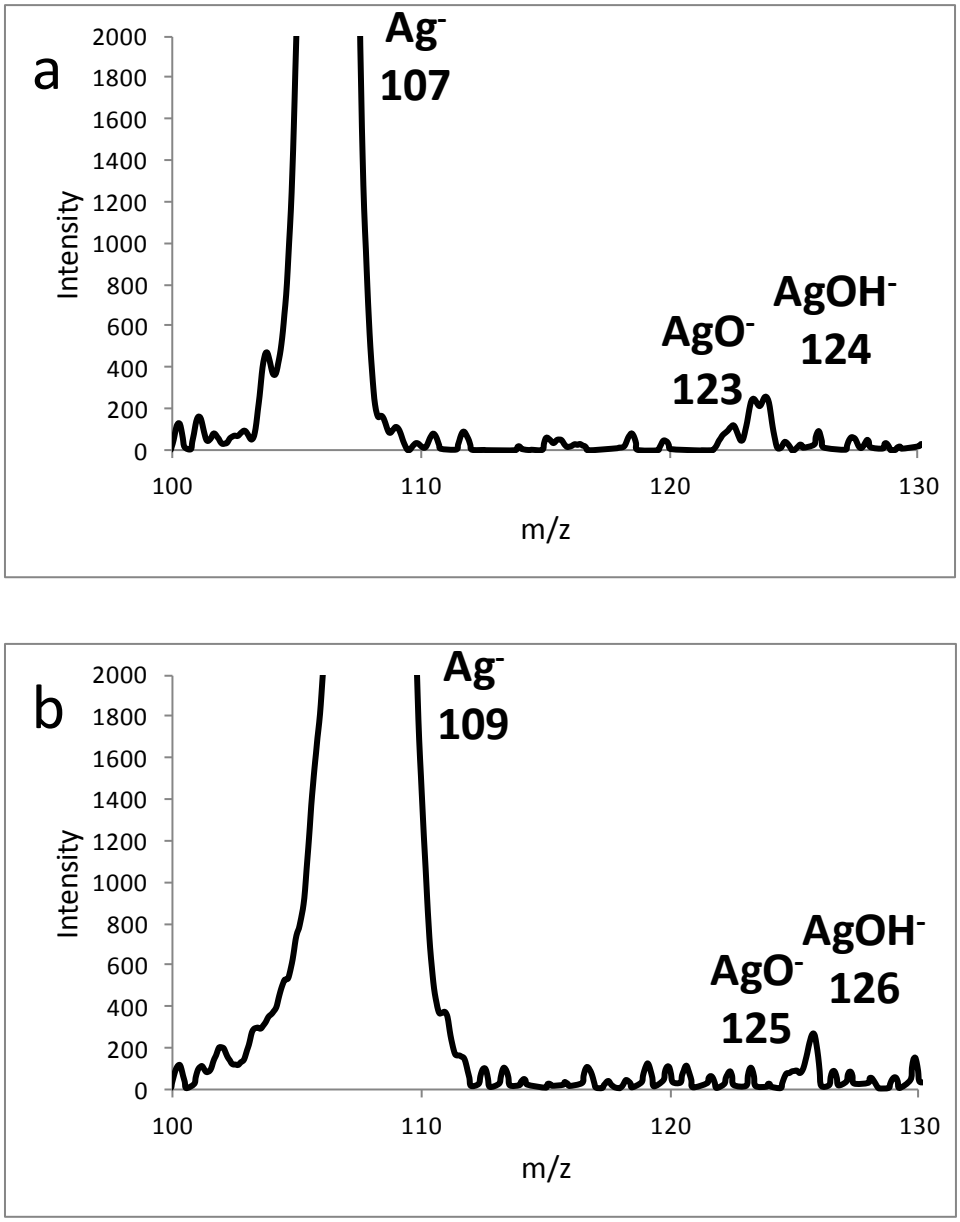

Figure 44: a) Mass spectrum of products of the reaction of 2-butanol with $^{107}Ag^-$ in voltages of (50-10-50) and the target gas pressure of 1.2 e-3 mbar; b) Mass spectrum of products of the reaction of 2-butanol with $^{109}Ag^-$ in voltages of (50-10-50) and the target gas pressure of 1.2 e-3 mbar

$AgOH^-$ is a product of dehydroxylation and AgO^- is a product of O-atom abstraction (reactions 81, 82 and 60).

$C_4H_{10}O + Ag^- \rightarrow C_4H_9 + AgOH^-$ (81)

$C_4H_{10}O + Ag^- \rightarrow C_4H_{10} + AgO^-$ (82) [OR $AgOH^- \rightarrow AgO^- + H$ (60)]

With the collision voltage of 20 eV, m/z 107 (Ag^-); m/z 73 ($C_4H_9O^-$); m/z 71 ($C_4H_7O^-$); m/z 57 ($C_4H_9^-$) and m/z 17 (OH^-) were observed in the mass spectrum of the reaction of Ag^- with 2-butanol (Figure 45).

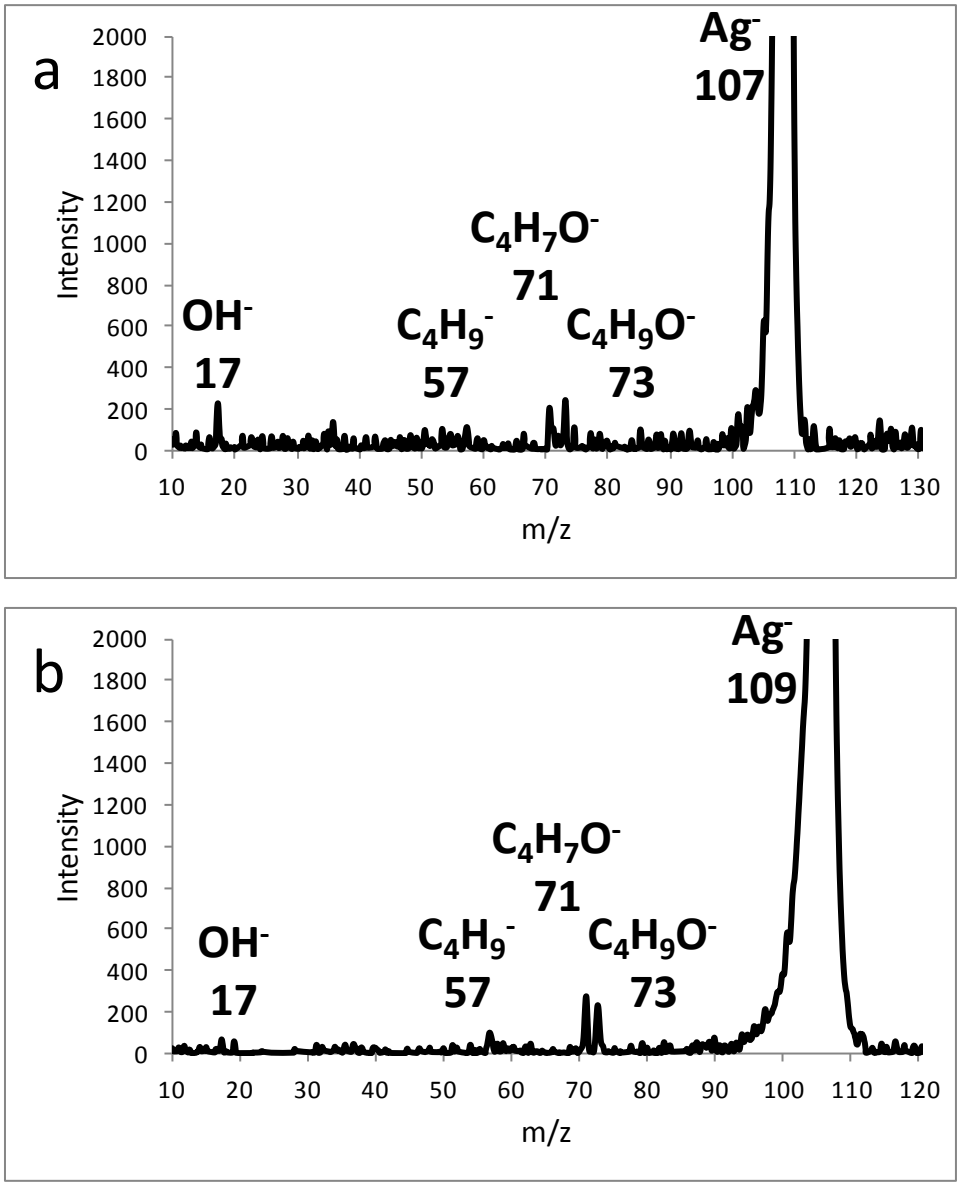

Figure 45: a) Mass spectrum of products of the reaction of 2-butanol with $^{107}Ag^-$ in voltages of (50-20-50) and the target gas pressure of 1.2 e-3 mbar; b) Mass spectrum of products of the reaction of 2-butanol with $^{109}Ag^-$ in voltages of (50-20-50) and the target gas pressure of 1.2 e-3 mbar

$C_4H_9O^-$ is a product of deprotonation and $C_4H_7O^-$, $C_4H_9^-$ and OH^- are products of spontaneous dissociation of the deprotonated fragment (reactions 83, 69, 80 and 72).

$C_4H_{10}O + Ag^- \rightarrow C_4H_9O^- + AgH$ (83)

$C_4H_9O^- \rightarrow C_4H_7O^- + H_2$ (69)

$C_4H_9O^- \rightarrow C_4H_9^- + O$ (80)

$C_4H_9O^- \rightarrow C_4H_8 + OH^-$ (72)

4.2.5: Reactions of 2-butanol with Cs^-

With the collision voltage of 0 eV, no reaction was observed. With the collision voltage of 40 eV, m/z 133 (Cs^-); m/z 73 ($C_4H_9O^-$); m/z 71 ($C_4H_7O^-$); m/z 57 ($C_4H_9^-$); m/z 17 (OH^-) and m/z 147 ($C_8H_{19}O^-$) were observed in the mass spectrum of the reaction of 2-butanol with Cs^- (Figure 46).

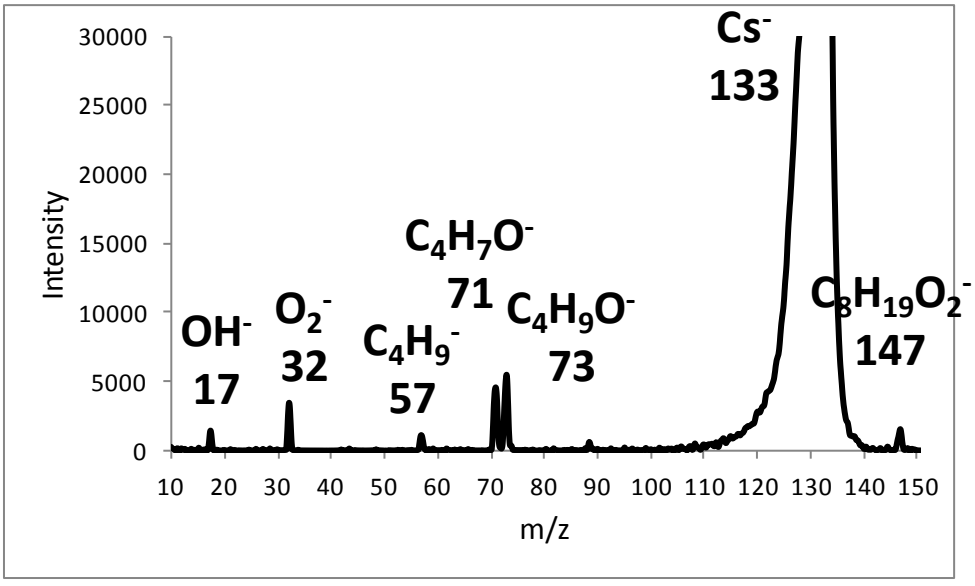

Figure 46: Mass spectrum of products of the reaction of 2-butanol with Cs^- in voltages of (50-40-50) and the target gas pressure of 1.2 e-3 mbar

$C_4H_9O^-$ is a product of deprotonation; $C_4H_7O^-$, $C_4H_9^-$ and OH^- are products of spontaneous dissociation of the deprotonated fragment; and $C_8H_{19}O^-$ is a product of dimerization. m/z 32 (O_2^-) is a contamination of oxygen in the system. (reactions 84, 69, 80, 72 and 73).

$$C_4H_{10}O + Cs^- \rightarrow C_4H_9O^- + CsH \quad (84)$$

$$C_4H_9O^- \rightarrow C_4H_7O^- + H_2 \quad (69)$$

$$C_4H_9O^- \rightarrow C_4H_9^- + O \quad (80)$$

$$C_4H_9O^- \rightarrow C_4H_8 + OH^- \quad (72)$$

$$C_4H_9O^- + C_4H_{10}O \rightarrow C_8H_{19}O^- \quad (73)$$

4.2.6: Reactions of 2-butanol with K^-

With the collision voltage of 0 eV, no reaction was observed. With the collision voltage of 20 eV, m/z 39 (K^-); m/z 73 ($C_4H_9O^-$); m/z 71 ($C_4H_7O^-$); m/z 57 ($C_4H_9^-$) and m/z 17 (OH^-) were observed in the mass spectrum of the reaction of 2-butanol with K^- (Figure 47).

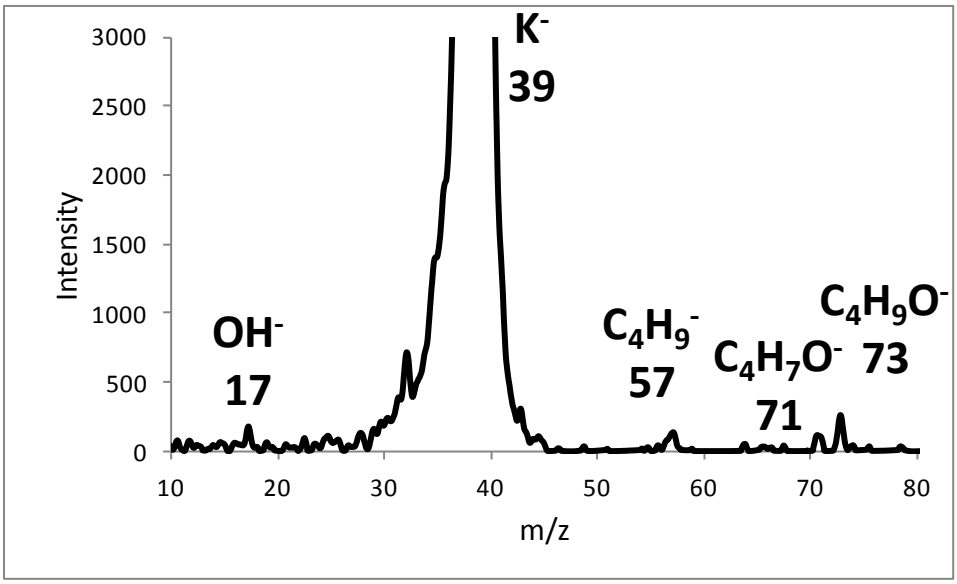

Figure 47: Mass spectrum of products of the reaction of 2-butanol with K^- in voltages of (50-20-50) and the target gas pressure of 1.2 e-3 mbar

$C_4H_9O^-$ is a product of deprotonation and $C_4H_7O^-$, $C_4H_9^-$ and OH^- are products of spontaneous dissociation of the deprotonated fragment (reactions 85, 69, 80 and 72).

$C_4H_{10}O + K^- \rightarrow C_4H_9O^- + KH$ (85)

$C_4H_9O^- \rightarrow C_4H_7O^- + H_2$ (69)

$C_4H_9O^- \rightarrow C_4H_9^- + O$ (80)

$C_4H_9O^- \rightarrow C_4H_8 + OH^-$ (72)

4.3: Reactions of 2-methyl-2-propanol

4.3.1: Reactions of 2-methyl-2-propanol with Fe^-

With the collision voltage of 0 eV, no reaction was observed. With the collision voltage of 5 eV, m/z 56 (Fe^-); m/z 57 (FeH^-) and m/z 73 ($C_4H_9O^-$) were observed in the mass spectrum of the reaction of Fe^- with 2-methyl-2-propanol (Figure 48).

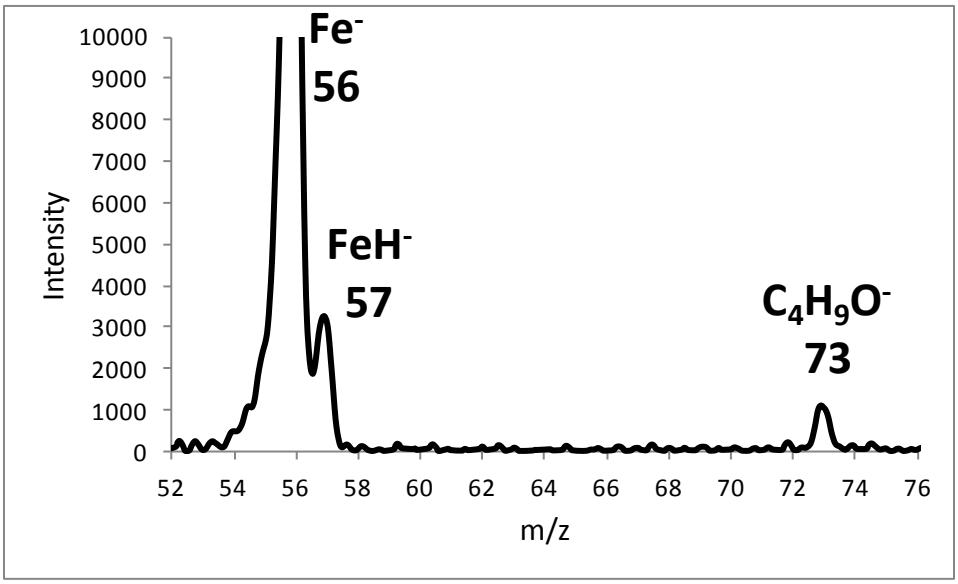

Figure 48: Mass spectrum of products of the reaction of 2-methyl-2-propanol with Fe^- in voltages of (50-5-50) and the target gas pressure of 1.2 e-3 mbar

FeH^- is a product of dehydrogenation and $C_4H_9O^-$ is a product of deprotonation (reactions 86 and 87).

$$C_4H_{10}O + Fe^- \rightarrow C_4H_9O + FeH^- \quad (86)$$

$$C_4H_{10}O + Fe^- \rightarrow C_4H_9O^- + FeH \quad (87)$$

4.3.2: Reactions of 2-methyl-2-propanol with Co^-

With the collision voltage of 0 eV, m/z 59 (Co^-) and m/z 132 ($CoC_4H_9O^-$) were observed in the mass spectrum of the reaction of 2-methyl-2-propanol with Co^- (Figure 49).

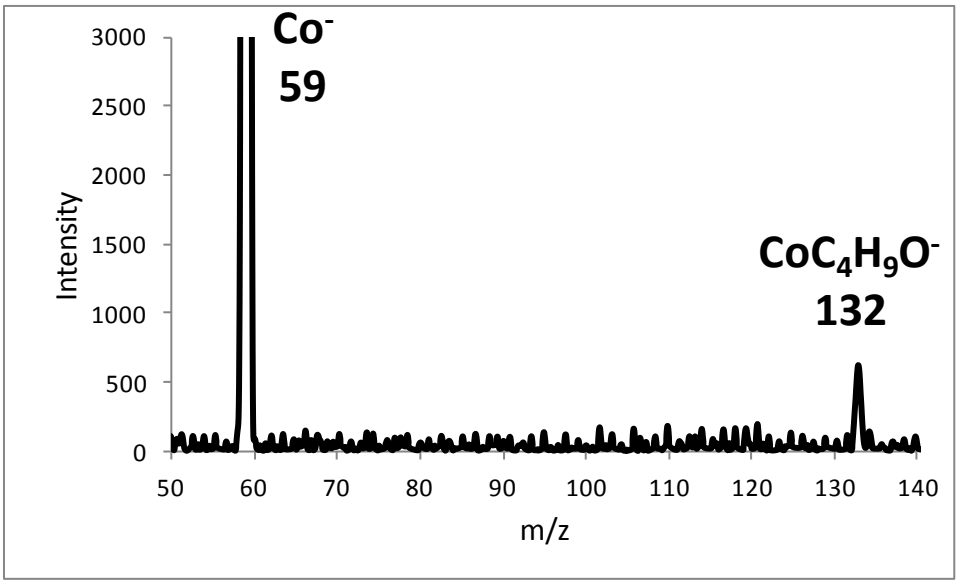

Figure 49: Mass spectrum of products of the reaction of 2-methyl-2-propanol with Co^- in voltages of (50-0-50) and the target gas pressure of 1.2 e-3 mbar

$CoC_4H_9O^-$ is a product of complex formation reaction of Co^- with 2-methyl-2-propanol (reaction 88).

$$C_4H_{10}O + Co^- \rightarrow CoC_4H_{10}O^- \quad (88)$$

With the collision voltage of 15 eV, m/z 59 (Co^-) and m/z 73 ($C_4H_9O^-$) were observed in the mass spectrum of the reaction of 2-methyl-2-propanol with Co^- (Figure 50).

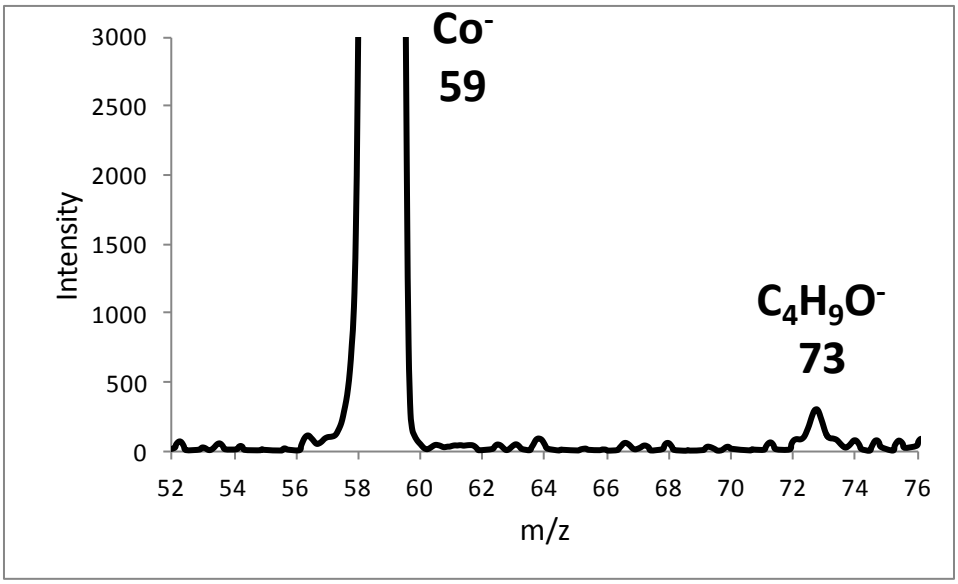

Figure 50: Mass spectrum of products of the reaction of 2methyl-2-propanol with Co^- in voltages of (50-15-50) and the target gas pressure of 1.2 e-3 mbar

$C_4H_9O^-$ is a product of deprotonation (reaction 89).

$$C_4H_{10}O + Co^- \rightarrow C_4H_9O^- + CoH \qquad (89)$$

4.3.3: Reactions of 2-methyl-2-propanol with Cu^-

With the collision voltage of 0 eV, no reaction was observed. With the collision voltage of 10 eV, m/z 65 (Cu^-), m/z 82 ($CuOH^-$); m/z 81 (CuO^-); m/z 57 ($C_4H_9^-$) and m/z 73 ($C_4H_9O^-$) were observed in the mass spectrum of the reaction of Cu^- with 2-methyl-2-propanol (Figure 51).

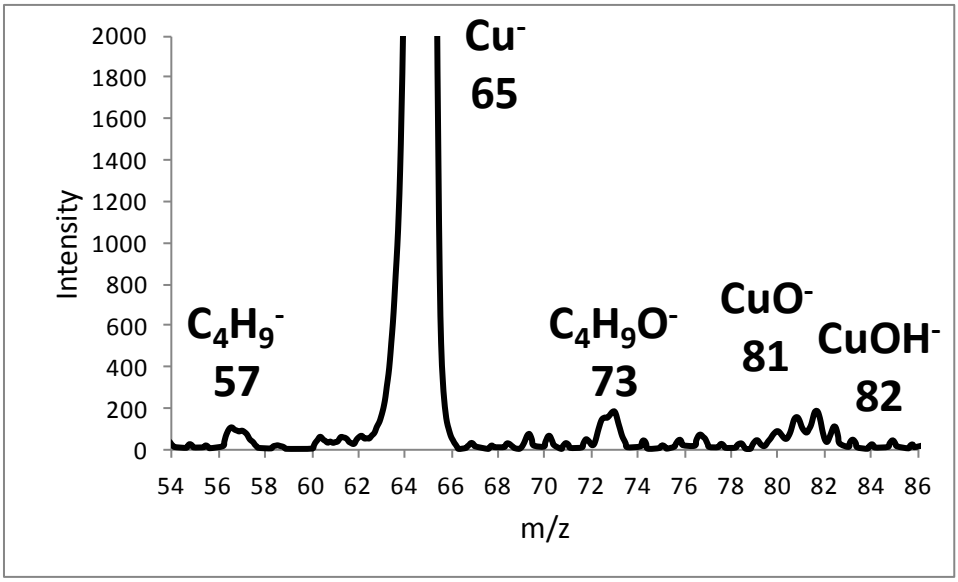

Figure 51: Mass spectrum of products of the reaction of 2-methyl-2-propanol with Cu^- in voltages of (50-10-50) and the target gas pressure of 1.2 e-3 mbar

$CuOH^-$ is a product of dehydroxylation; CuO^- is a product of O-atom abstraction; and $C_4H_9O^-$ is a product of deprotonation (reactions 90 to 93 and reaction 56).

$C_4H_{10}O + Cu^- \rightarrow C_4H_9O^- + CuH$ (90)

$C_4H_9O^- \rightarrow C_4H_9^- + O$ (91)

$C_4H_{10}O + Cu^- \rightarrow C_4H_9 + CuOH^-$ (92)

$C_4H_{10}O + Cu^- \rightarrow C_4H_{10} + CuO^-$ (93) [OR $CuOH^- \rightarrow CuO^- + H$ (56)]

4.3.4: Reactions of 2-methyl-2-propanol with Ag^-

With the collision voltage of 0 eV, no reaction was observed. With the collision voltage of 10 eV, m/z 107 (Ag^-); m/z 124 ($AgOH^-$); m/z 57 ($C_4H_9^-$) and m/z 73 ($C_4H_9O^-$) were observed in the mass spectrum of the reaction of Ag^- with 2-methyl-2-propanol (Figure 52).

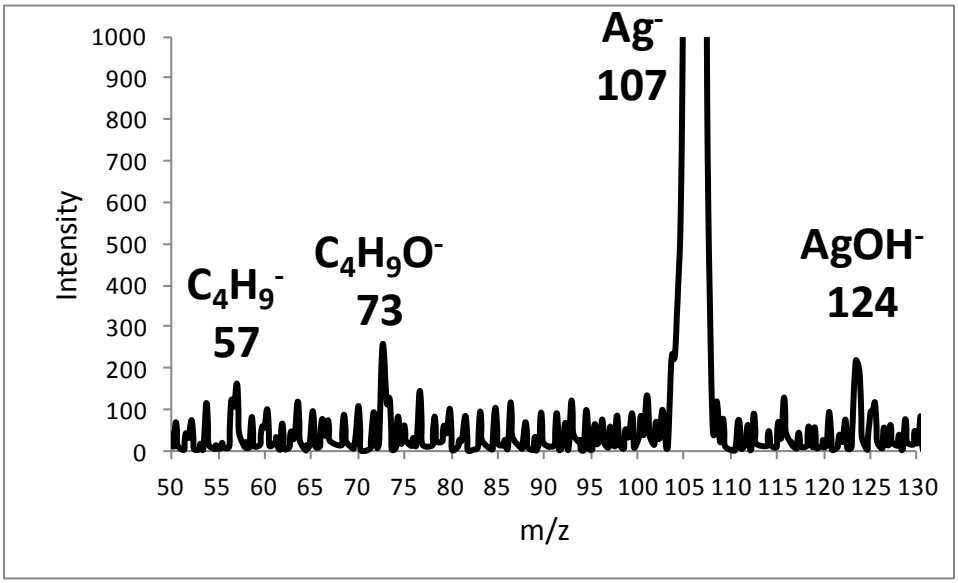

Figure 52: Mass spectrum of products of the reaction of 2-methyl-2-propanol with Ag^- in voltages of (50-10-50) and the target gas pressure of 1.2 e-3 mbar

$AgOH^-$ is a product of dehydroxylation and $C_4H_9O^-$ is a product of deprotonation (reactions 94, 91 and 95).

$$C_4H_{10}O + Ag^- \rightarrow C_4H_9O^- + AgH \quad (94)$$

$$C_4H_9O^- \rightarrow C_4H_9^- + O \quad (91)$$

$$C_4H_{10}O + Ag^- \rightarrow C_4H_9 + AgOH^- \quad (95)$$

4.3.5: Reactions of 2-methyl-2-propanol with Cs^-

With the collision voltage of 0 eV, no reaction was observed. With the collision voltage of 40 eV, m/z 133 (Cs^-); m/z 73 ($C_4H_9O^-$); m/z 57 ($C_4H_9^-$); m/z 17 (OH^-) and m/z 147 ($C_8H_{19}O^-$) were observed in the mass spectrum of the reaction of 2-methyl-2-propanol with Cs^- (Figure 53).

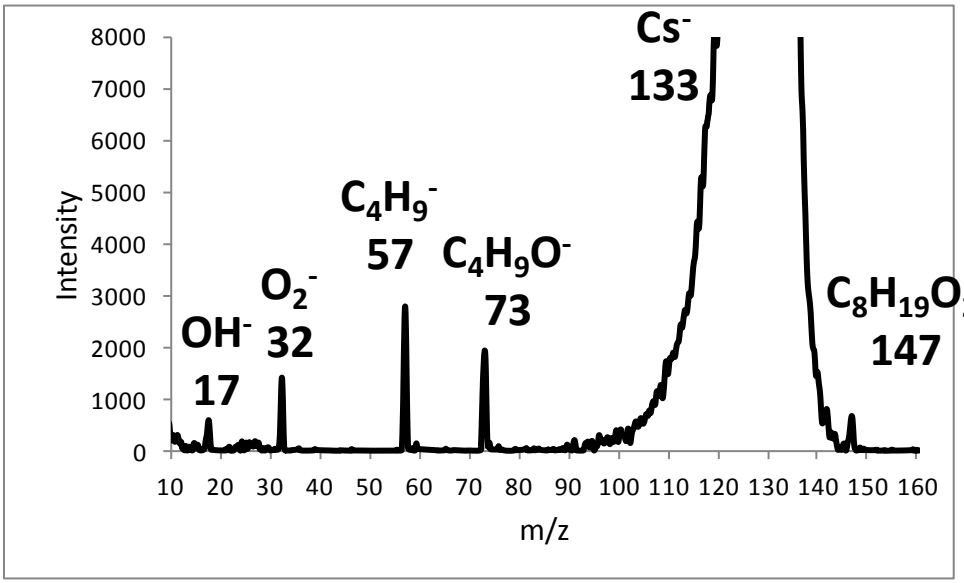

Figure 53: Mass spectrum of products of the reaction of 2-methyl-2-propanol with Cs^- in voltages of (50-40-50) and the target gas pressure of 1.2 e-3 mbar

$C_4H_9O^-$ is a product of deprotonation; $C_4H_9^-$ and OH^- are products of spontaneous dissociation of the deprotonated fragment; and $C_8H_{19}O^-$ is a product of dimerization. m/z 32 (O_2^-) is a contamination of oxygen in the system. (reactions 96 to 98 and reaction 91).

$$C_4H_{10}O + Cs^- \rightarrow C_4H_9O^- + CsH \quad (96)$$

$$C_4H_9O^- \rightarrow C_4H_9^- + O \quad (91)$$

$$C_4H_9O^- \rightarrow C_4H_8 + OH^- \quad (97)$$

$$C_4H_9O^- + C_4H_{10}O \rightarrow C_8H_{19}O^- \quad (98)$$

4.3.6: Reactions of 2-methyl-2-propanol with K^-

With the collision voltage of 0 eV, no reaction was observed. With the collision voltage of 40 eV, m/z 39 (K^-); m/z 73 ($C_4H_9O^-$) and m/z 57 ($C_4H_9^-$) were observed in the mass spectrum of the reaction of 2-methyl-2-propanol with K^- (Figure 54).

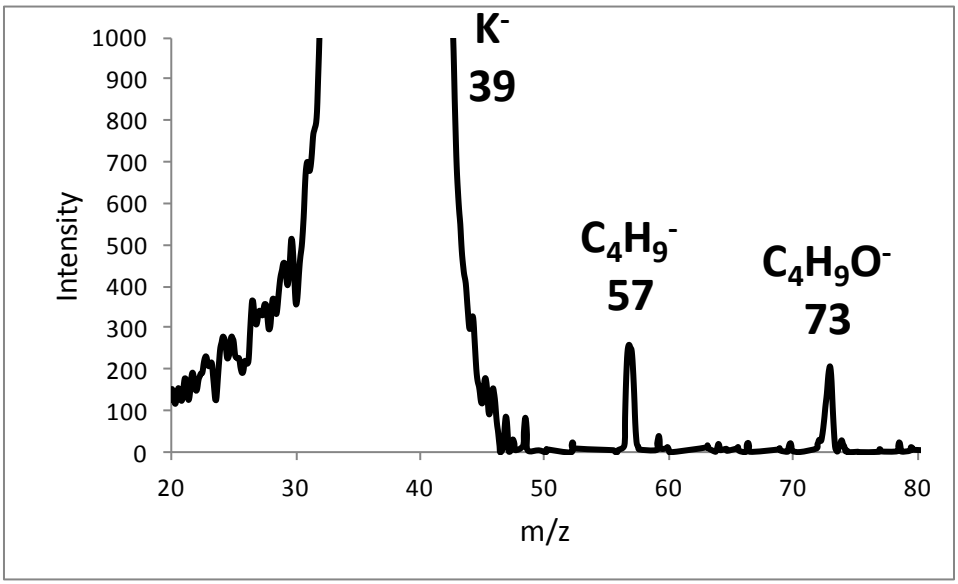

Figure 54: Mass spectrum of products of the reaction of 2-methyl-2-propanol with K^- in voltages of (50-40-50) and the target gas pressure of 1.2 e-3 mbar

$C_4H_9O^-$ is a product of deprotonation, $C_4H_9^-$ is a products of spontaneous dissociation of the deprotonated fragment (reactions 99 and 91).

$$C_4H_{10}O + K^- \rightarrow C_4H_9O^- + KH \quad (99)$$

$$C_4H_9O^- \rightarrow C_4H_9^- + O \quad (91)$$

4.4: Summary of reactions of alcohols with metal anions

4.4.1: Observed reactions

Alcohols are more reactive than hydrocarbons with regards to the reactions with the metal anions. Alcohols contain an electronegative atom, oxygen. In addition to all the reactions of the hydrocarbons, alcohols show the dehydroxylation reaction with metal anions too.

Alcohols show the following types of reactions with the metal anions:

1) Deprotonation reaction

A deprotonation reaction is the abstraction of a proton from the target gas by the metal anion. The products of this reaction are the neutral metal hydride, which is not observed in the spectrum, and the deprotonated target gas, which is observed in the spectrum. All metal anions show the deprotonation reaction with all tested alcohols (Table 6).

Table 6: The observation of the deprotonation reactions of metal anions with alcohols; stars indicate the observed reactions

	Fe^-	Co^-	Cu^-	Ag^-	Cs^-	K^-
1-butanol	★	★	★	★	★	★
2-butanol	★	★	★	★	★	★
2-methyl-2-propanol	★	★	★	★	★	★

2) Spontaneous dissociation of the deprotonated alcohol

The deprotonated target gas can dissociate to smaller fragments when there is enough energy in the system.

3) Dimer formation

The deprotonated target gas can collide with the neutral target gas to form a dimer.

4) Dehydrogenation reactions

A dehydrogenation reaction is the abstraction of a hydrogen from the target gas by the metal anion. The products of this reaction are the metal hydride anion, which is observed in the spectrum, and the neutral dehydride radical, which is not observed in the spectrum. Fe^- shows the dehydrogenation reaction with tested alcohols (Table 7).

Table 7: The observation of the dehydrogenation reactions of metal anions with alcohols; stars indicate the observed reactions

	Fe^-	Co^-	Cu^-	Ag^-	Cs^-	K^-
1-butanol	★					
2-butanol	★					
2-methyl-2-propanol	★					

5) Bisdehydrogenation reactions

A bisdehydrogenation reaction is the abstraction of two hydrogens from the target gas by the metal anion. The products of this reaction are the metal dihydride anion, which is observed in the spectrum, and the bisdehydrated target gas, which is not observed in the spectrum. Fe^- and Cu^- show the bisdehydrogenation reaction only with tested primary and secondary alcohols (Table 8).

Table 8: The observation of the bisdehydrogenation reactions of metal anions with alcohols; stars indicate the observed reactions

	Fe^-	Co^-	Cu^-	Ag^-	Cs^-	K^-
1-butanol	☆		☆			
2-butanol	☆		☆			
2-methyl-2-propanol						

6) Dehydroxylation reaction

A dehydroxylation reaction is the abstraction of a hydroxyl group from the target gas by the metal anion. The products of this reaction are the metal hydroxide anion, which is observed in the spectrum, and the dehydroxylated alcohol, which is not observed in the spectrum. Fe^-, Cu^- and Ag^- show the dehydroxylation reaction (Table 9).

Table 9: The observation of the dehydroxylation reactions of metal anions with alcohols; stars indicate the observed reactions

	Fe^-	Co^-	Cu^-	Ag^-	Cs^-	K^-
1-butanol	★		★	★		
2-butanol	★		★	★		
2-methyl-2-propanol	★		★	★		

7) Complex formation

A complex formation reaction is the attachment of the metal anion to the organic neutral target gas followed by the loss of a hydrogen atom to form an organometalic anion fragment. The product of this reaction is $MC_4H_9O^-$, where M is the metal. Fe^-, Co^- and Ag^- show the complex formation reaction (Table 10).

Table 10: The observation of the complex formation reactions of metal anions with alcohols; stars indicate the observed reactions

	Fe^-	Co^-	Cu^-	Ag^-	Cs^-	K^-
1-butanol	★	★		★		
2-butanol	★	★		★		
2-methyl-2-propanol	★	★		★		

8) Electron transfer

An electron transfer reaction is the transfer of electron from the metal anion to the target gas. The products of this reaction is the alcohol anion, which is observed in the spectrum, and the neutral metal, which is not observed in the spectrum. Fe^- is the only metal anion to show the electron transfer reaction with alcohols (Table 11).

Table 11: The observation of the electron transfer reactions of metal anions with alcohols; stars indicate the observed reactions

	Fe^-	Co^-	Cu^-	Ag^-	Cs^-	K^-
1-butanol	★					
2-butanol	★					
2-methyl-2-propanol	★					

4.4.2The enthalpies of reactions

Enthalpies of some observed and unobserved reactions were calculated and documented in Appendix 1 of this thesis. The enthalpy of a reaction is the sum of the heats of formation of products subtracted by the sum of heats of formation of starting materials. Enthalpies of unobserved reactions were calculated to compare with the similar observed same reaction. Heats of formation of fragments were found in the NIST

webbook[18] or the Gas-Phase Ion and Neutral Thermochemistry Book[19] and documented in the Appendix 4 and 5 of this thesis. Calculated enthalpies of reactions of alcohols with metal anions are plotted for each tested metal anion in this thesis study (Figures 55 to 57).

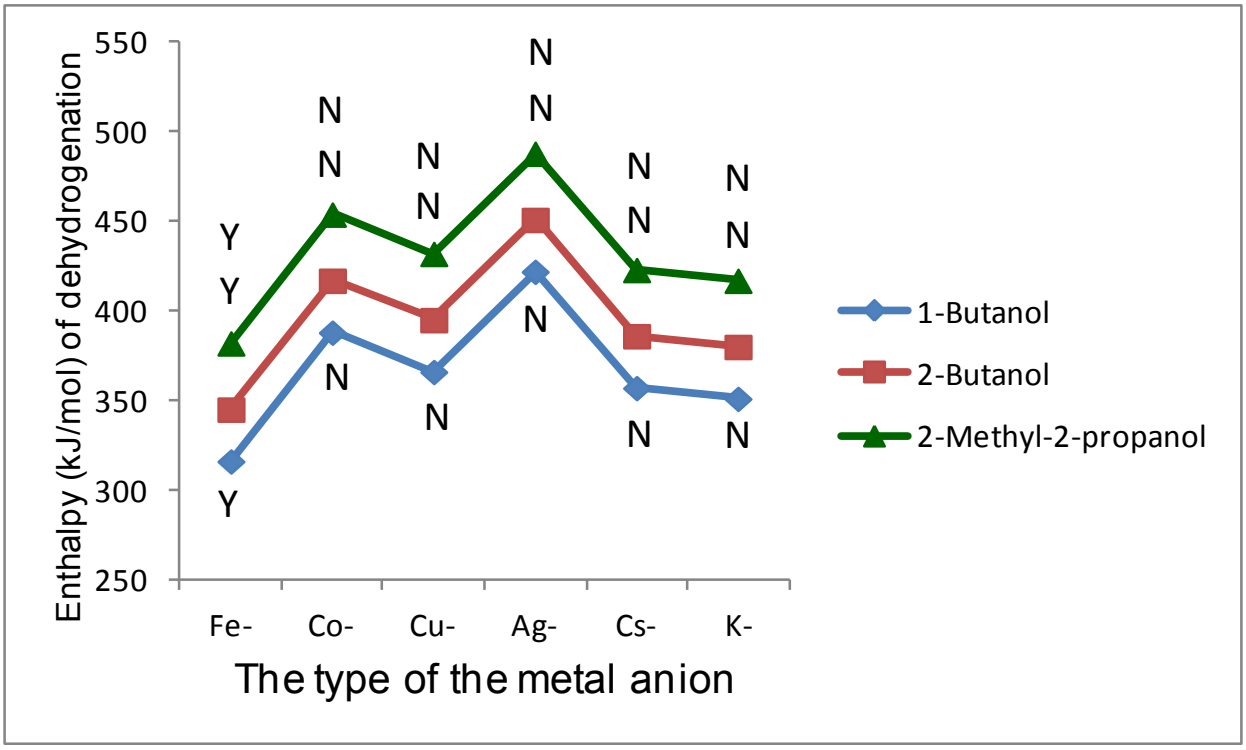

Figure 55: Enthalpies of the dehydrogenation reactions of metal anions with alcohols; Y indicates observed reactions and N indicates unobserved reactions

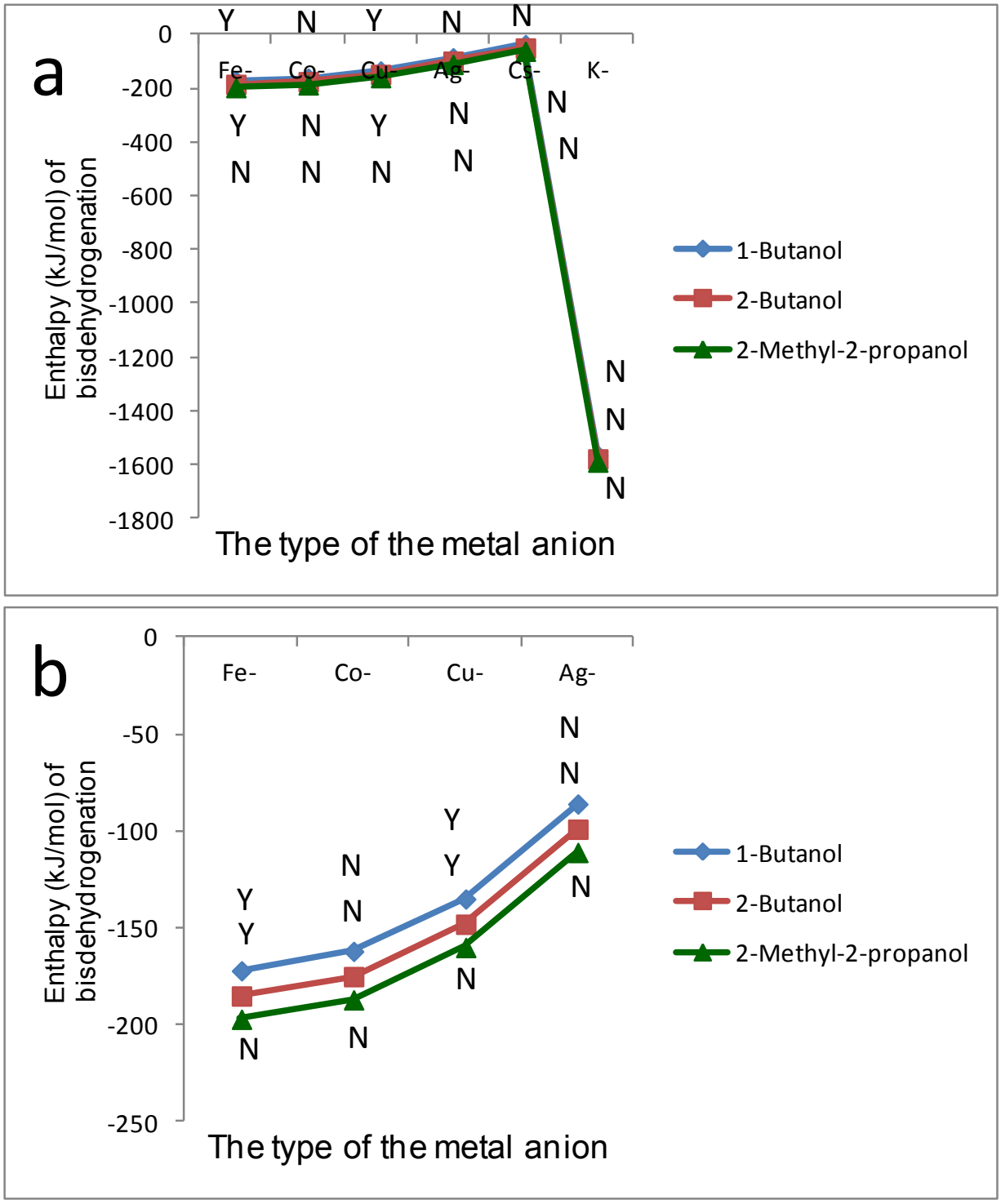

Figure 56: a) Enthalpies of the bisdehydrogenation reactions of metal anions with alcohols; b) Expanded Enthalpies of the bisdehydrogenation reactions of metal anions with alcohols; Y indicates observed reactions and N indicates unobserved reactions

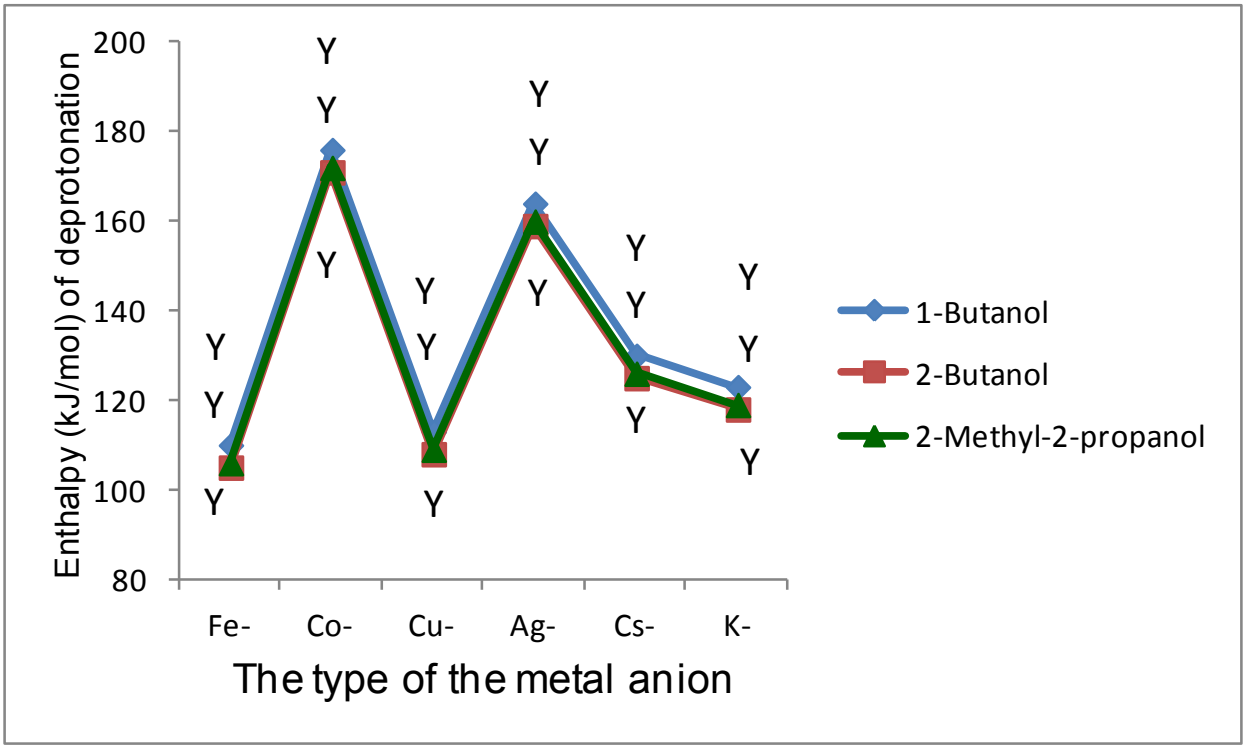

Figure 57: Enthalpies of the deprotonation reactions of metal anions with alcohols; Y indicates observed reactions and N indicates unobserved reactions

Calculated enthalpies for alcohols has the same trend as that for hydrocarbons. Calculated enthalpies for dehydrogenation reactions of Fe^- with alcohols are lower than calculated enthalpies for other metal anions. Fe^- is the only metal anion that shows the dehydrogenation reaction with alcohols.

Unlike hydrocarbons, calculated enthalpies for the bisdehydrogenation reactions of metal anions with primary, secondary and tertiary alcohols are similar. Thus, it is probable that the structures of intermediate complexes of these reactions are similar. The reactions that have a lower calculated enthalpy were observed. However, the enthalpy data cannot be used to predict the observation. This could be due to the fact that in a reaction, barrier values govern the observation rather than enthalpy values.

Also, it seems there is no direct relationship between the enthalpy values and barrier values of these reactions. The mechanism of reactions produces a better explanation for these observations.

4.4.3: The mechanism of reactions

The deprotonation reaction of metal anions with alcohols follows the harpoon mechanism, a long range proton abstraction.[7] The gas phase acidity of fragments governs the observation of the deprotonation reaction. Alcohols have a greater gas phase acidity than hydrocarbons and they are more reactive with regard to the deprotonation reaction.

The deprotonated target gas can dissociate to smaller fragments, without the help of the metal anion, when enough energy is provided. The spontaneous dissociation of the deprotonated alcohol is a sequential reaction in the reactions of the metal anions with alcohols as indicated below:

$C_4H_9O^- \rightarrow C_4H_7O^- + H_2$ (48)

$C_4H_9O^- \rightarrow C_4H_9^- + O$ (62)

$C_4H_9O^- \rightarrow C_4H_8 + OH^-$ (63).

To confirm that the metal anion has no role in the production of these fragments, the dissociation of the deprotonated alcohol was tested. 1 g potassium was added to 20 ml 2-butanol to facilitate the production of $C_4H_9O^-$ anion in this solution. This solution was injected into the ESI source. The produced $C_4H_9O^-$ anion was selected in the first quadrupole. Then the dissociation pattern of $C_4H_9O^-$ fragment, in the absence of a metal anion, was investigated through a CID experiment (Figure 58).

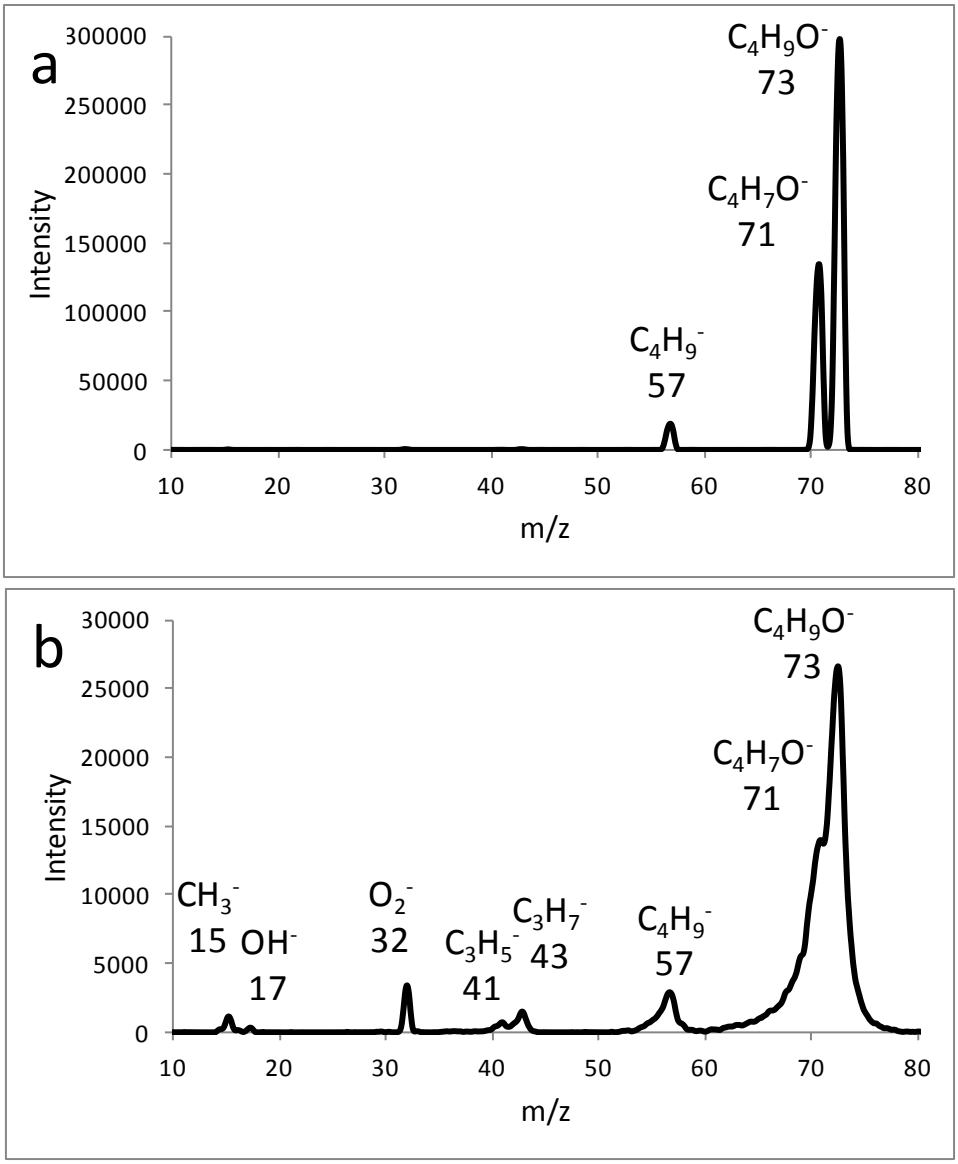

Figure 58: a) Mass spectrum of the CID experiment of $C_4H_9O^-$ with Ar in voltages of (50-5-50); b) Mass spectrum of the CID experiment of $C_4H_9O^-$ with Ar in voltages of (50-60-50)

The same pattern of this dissociation was observed in the mass spectrum of the reaction of 2-butanol with Cs^-, confirming that metal anions have no role in this dissociation.

The driving force for the spontaneous dissociation of an organic ion is the formation of stable organic neutral products such as C_4H_8 and H_2.

In the dissociation of $C_4H_9O^-$ to $C_4H_7O^-$, a double bond is formed between the carbon atom that is attached to the hydroxyl group and the adjacent carbon to this carbon. When an alcohol has no hydrogen in any of these carbons, the double bond cannot be formed. Thus, tertiary alcohols or 2,2-dimethyl propanol do not show the formation of a $C_4H_7O^-$ fragment (Scheme 7).

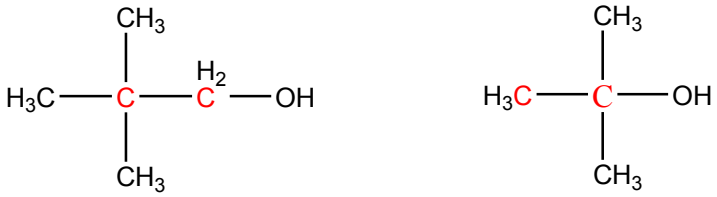

Scheme 7: 2,2-dimethyl propanol and 2-methyl-2-propanol cannot form a double bond between the carbon atom that is attached to the hydroxyl group and the adjacent carbon, thus, their deprotonated anion, $C_4H_9O^-$, does not dissociate to $C_4H_7O^-$

The deprotonated fragment may collide with the neutral organic target gas to form a dimer. Dimer formation is the result of a three body collision when $C_4H_9O^-$ collides with $C_4H_{10}O$ to form an excited complex which will be relaxed by the buffer gas down to a sufficient energy to produce a dimer (reaction 100).

$$[\ C_4H_9O^- \ + \ C_4H_{10}O\ ]^* \ + \ N_2 \ \rightarrow \ C_8H_{19}O_2^- \ + \ N_2^* \qquad (100)$$

In the reaction 84, * indicates the exited state of the fragment.

Raising of the pressure of the target gas raises the probability of the three body collision. Thus, the greater intensity of production of a dimer anion fragment is observed with the higher pressure of the organic neutral target gas.

The mechanism of the metal anion insertion reactions of alcohol is the same as that of hydrocarbon that was discussed earlier. The metal anion can insert into either the O-H bond or the C-O bond of alcohols to form the respective intermediate complex. Oxygen is more electronegative than hydrogen; consequently, the electron transfer step of the

mechanism for alcohols is less endothermic than it is for hydrocarbons. The insertion of metal anions into a O-H bond or a C-O bond is more favorable than insertion of metal anions into a C-H bond, which indicates that alcohols are more reactive than hydrocarbons.

A complex formation reaction takes place when the metal-H bond in the intermediate formed by the metal insertion into the O-H bond breaks and the negative charge remains on the metal-containing fragment.

A dehydrogenation reaction takes place when the metal-O bond in the intermediate formed by the metal insertion into the O-H bond breaks and the negative charge remains on the metal-containing fragment.

A bisdehydrogenation reaction takes place when the intermediate formed by metal insertion into the O-H bond undergoes a β-H shifts rearrangement. The metal-O bond breaks and the negative charge remains on the metal-containing fragment. 2-methyl-2-propanol, which is a tertiary alcohol, shows no bisdehydrogenation reaction as it has no α-H atom to the oxygen in the alcohol. (Scheme 8).

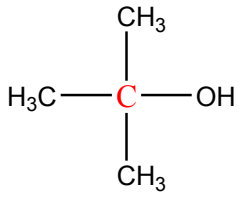

Scheme 8: 2-methyl-2-propanol has no α-H atom to the oxygen, thus, does not show a bisdehydrogenation reaction

During these dissociations, the metal-containing anion, metal dihydride anion, does not lose its negative charge indicating that the metal-containing fragment is more electronegative than the other produced fragment in this dissociation.

In the observed reactions of metal-carbonyl anions with alcohols, the intermediate loses two hydrogen atoms instead of a metal dihydride anion.[14] The reason for this could be that the metal-O bond in the intermediate is stabilized by resonance over O=C-M-O (Scheme 9).

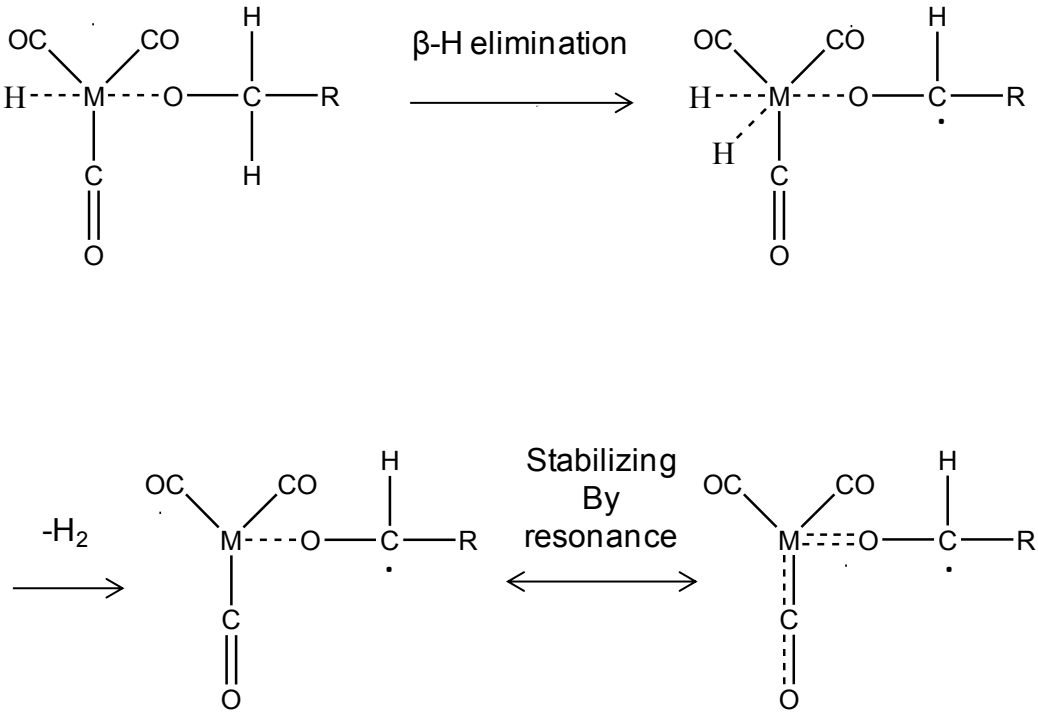

Scheme 9: The intermediate in the reaction of metal-carbonyl anions with alcohols loses dihydrogen instead of metal-carbonyl dihydride anion, probably due to the resonance stabilization of the metal-O bond over O=C-M-O

The dehydroxylation reaction and the O-atom abstraction reaction result from metal anion insertion into a C-O bond of alcohols. A dehydroxylation reaction takes place when the metal anion inserts into the C-O bond and the metal-C bond breaks, leaving the negative charge on the metal-containing fragment. A O-atom abstraction reaction takes place when the intermediate formed by metal insertion into the C-O bond undergoes a hydrogen shift from the hydroxyl group to the carbon. The metal-C bond breaks and the negative charge remains on the metal-containing fragment. Another path to form a metal oxide anion might be the dissociation of the metal hydroxide anion to the metal oxide anion.

Electron transfer is the transference of an electron from the metal anion to the organic neutral target gas. Fe^- is the only metal anion that shows an electron transfer reaction. The observation of an electron transfer reaction is governed by the electron affinity of fragments. The fact that alcohols are able to abstract an electron from Fe^- shows that alcohols have a higher electron affinity than iron. Meanwhile, no electron transfer reaction was observed in the reaction of alcohols with other metal anions. Thus, the electron affinity of alcohols is lower than the electron affinity of other metal anions. According to the electron affinity values of metals, we can deduce that the electron affinity of alcohols should be between 0.151 eV and 0.472 eV (Table 1).

Chapter 5: Conclusion

In this thesis study the generation of metal anions and their reactions with organic samples such as hydrocarbons and alcohols was investigated. All experiments were done in the negative mode of an electrospray ionization triple quadrupole mass spectrometer instrument (ESI-TQ-MS). To explain the result, properties of metal anions such as electronic configuration, electron affinity, hydrogen affinity and gas phase acidity as well as enthalpies of reactions and the possible mechanism, were explored. Metals are the active core of many catalysts. The investigation of properties of metals in the gas phase helps to improve understanding of the mechanism of catalytic reactions involving these types of catalysts. Metals are the most electropositive elements of the periodic table. Therefore, there are numerous studies about metal cations in the gas phase, due to the ease of their production, but not about metal anions. Recently, in Dr. Mayer's research laboratory, a new, simple and efficient method to generate atomic metal anions such as Fe^-, Co^-, Cu^-, Ag^-, Cs^- and K^- in an ESI source has been developed.

The activation of a C-H bond is of interest to the petroleum industry in regards to the production of more valuable starting materials from abundant sources of hydrocarbons. This thesis study investigated the reactions of produced metal anions with hydrocarbons such as pentane, 1-pentene, 2-pentene and 1-pentyne as well as alcohols such as 1-butanol, 2-butanol and 2-methyl-2-propanol in the second quadrupole of an ESI-TQ-MS. Moreover, in addition to the linear hydrocarbons with five carbons, certain other hydrocarbons and alcohols, such as heptane and pentanol, were also reacted with metal anions and similar results were observed. Metal anions show various reactions of

dehydrogenation, bisdehydrogenation, deprotonation, dehydroxylation, electron transfer and complex formation. the observation of studied reactions is summarized in table 12.

Table 12: The summary of observed reactions of metal anions with hydrocarbons and alcohols; stars indicate the observed reactions

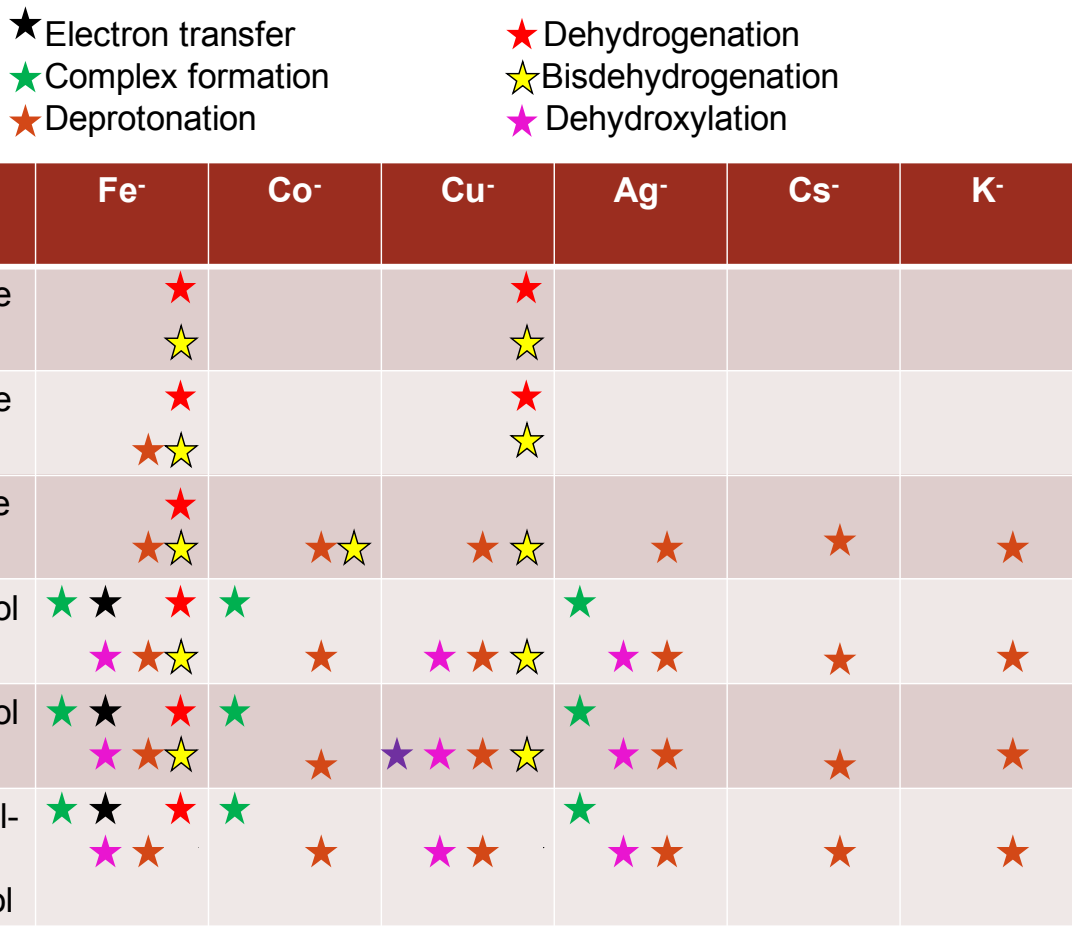

All metal anions show the deprotonation reaction. The deprotonation reaction follows the harpoon mechanism and depends on the gas phase acidity of fragments. The deprotonated fragment of the target gas can dissociate spontaneously to smaller fragments in a process that does not involve metal anions. Also, the deprotonated fragment can form a dimer in collision with the neutral organic target gas. Dehydrogenation and bisdehydrogenation reactions are the most informative reactions of metal anions for two reasons. First, the products of these reactions are metal-containing anions, which proves that the metal anions have an important role in this reaction and they can insert into a C-H bond. Second, metal anions have the potential to convert hydrocarbons to olefins as a valuable starting material for the petroleum industry.

The enthalpies of the dehydrogenation reaction for studied metal anions is plotted against studied metal anions (Figure 59).

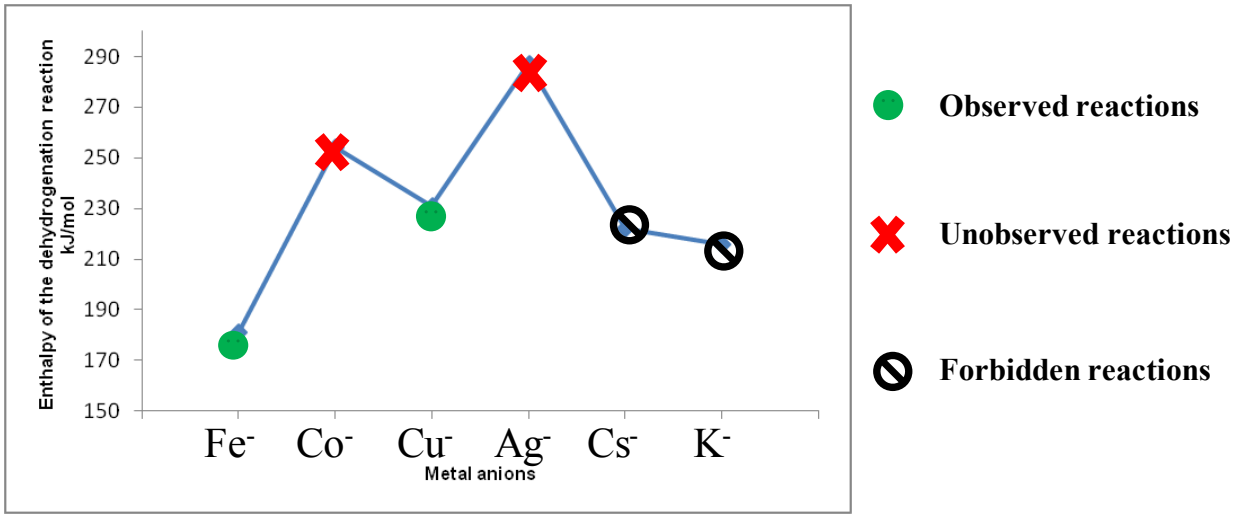

Figure 59: The plot of enthalpies of the dehydrogenation reaction of pentane for each metal anion

Fe^- and Cu^- have lower enthalpy of the dehydrogenation and they show the dehydrogenation reaction. Co^- and Ag^- have higher enthalpy of the dehydrogenation and they do not show the dehydrogenation reaction. Although the enthalpy values of the dehydrogenation reactions for Cs^- and K^- are in such values that they might show the dehydrogenation reaction, they do not; Cs^- and K^- are alkali metal anions and they do not have accessible d orbitals to form an intermediate in this reaction.

In addition to the enthalpies, the hydrogen affinities of metals is plotted for each metal anion (Figure 60).

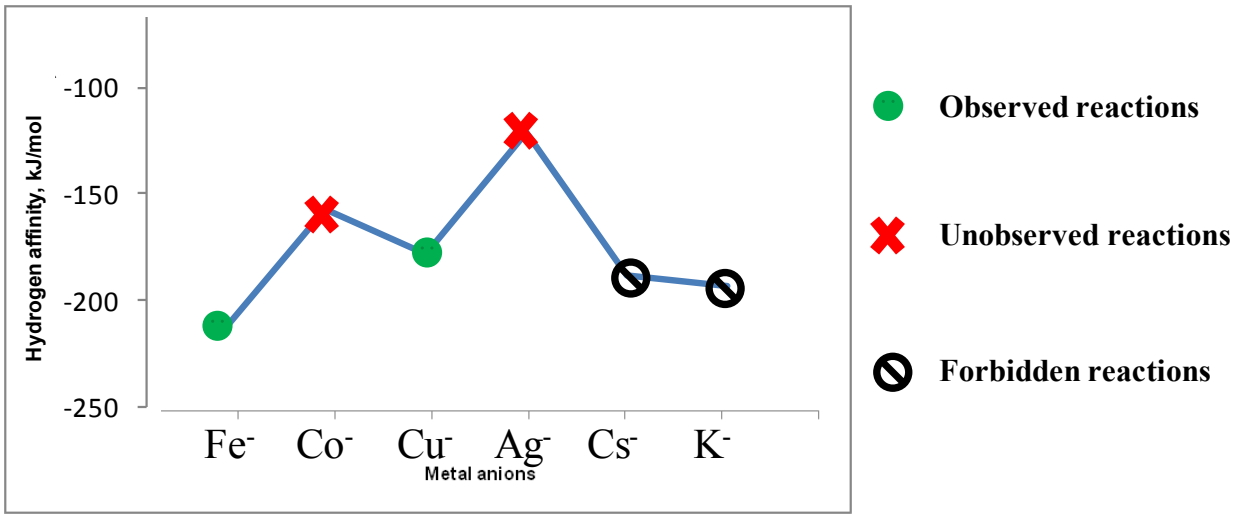

Figure 60: The plot of the hydrogen affinities for each metal anion

Hydrogen affinity values show the similar result of enthalpies. Fe^- and Cu^- have lower hydrogen affinity and they show the dehydrogenation reaction. Co^- and Ag^- have higher hydrogen affinity and they do not show the dehydrogenation reaction. Although the hydrogen affinity values for Cs^- and K^- are in such values that they might show the dehydrogenation reaction, they do not; Cs^- and K^- are alkali metal anions and they do not have accessible d orbitals to form an intermediate in this reaction.

There is a novel mechanism for reactions of metal carbonyl anions in the literature that may be similar to that used by metal anions. The first step of the mechanism is the formation of a three centre two electron bond between the metal anion and the C-H bond of hydrocarbons to form the intermediate complex. In the second step of the mechanism, the negative charge is transferred from the metal anion to an anti-bonding orbital of the C-H bond, causing the breakage of the C-H bond and formation of the intermediate. The exothermicity of electron transfer step depends on the electronegativity of the attached functional group to C. The more electronegative the functional group, the more exothermic is the electron transfer step. H has a low electronegativity and, consequently, dehydrogeation and bisdehydrogenation reactions of hydrocarbons are endothermic and need energy to occur. The third step is the dissociation of the intermediate to form products that can be observed in the spectrum. The breakage of the metal-C bond in the intermediate results in the formation of the metal hydride anion. When prior to the breakage of the metal -C bond, a β-H shift takes place, the metal dihydride anion will be formed. Also, metal anions can insert into the O-

H or the C-O bond of alcohols to form metal hydride, metal dihydride, metal-alcohol comlex and metal hydroxide anions.

Comparing the reactivity of the metal anions with the reactivity of the metal cations suggests that the reactivity of metals is governed by their electronic configuration and the charge on the metal has lower influence on the reactivity. The isoelectronic metal ions show the same reactivity in the activation of the C-H bond in the gas phase. In similar energies, Co^- and Cu^+ cannot activate the C-H bond whereas Fe^- and Ni^+ can activate the C-H bond.

To expand this research, the reactivity of metal anions that were not included in this thesis study could be investigated. In addition, the reactivity of heteroatom organic compounds can be studied in order to investigate the reactivity of a variety of bonds such as the C-N, C-P and C-S bonds. The AB initio quantum chemical calculations could provide a better understanding of the energy profile of studied reactions and the role of the electronic configuration of metal anions in their reactivity.

Claim of Original Research

I declare that the studies presented in this thesis were done for the first time in Dr. Mayer's research group in the Chemistry Department of the University of Ottawa during my two years Master's thesis research in his laboratory from September 2011 to August 2013.

Further Information:

1) In my research, I reacted each of the following as outlined in my thesis:

a) pentane with Fe^-, Co^-, Cu^-, Ag^-, Cs^- and K^- and produced metal hydride anions and metal dihydride anions;

b) 1-pentene and 2-pentene with Fe^-, Co^-, Cu^-, Ag^-, Cs^- and K^- and produced metal hydride anions, metal dihydride anions and pentenyl anion;

c) 1-pentyne with Fe^-, Co^-, Cu^-, Ag^-, Cs^- and K^- and produced metal hydride anions, metal dihydride anions and pentynyl anion;

d) 1-butanol with Fe^-, Co^-, Cu^-, Ag^-, Cs^- and K^- and produced metal hydride anions, metal dihydride anions, metal hydroxide anions, metal oxide anions and 1-butanyl anion;

e) 2-butanol with Fe^-, Co^-, Cu^-, Ag^-, Cs^- and K^- and produced metal hydride anions, metal dihydride anions, metal hydroxide anions, metal oxide anions and 2-butanyl anion;

f) 2-methyl-2-propanol with Fe^-, Co^-, Cu^-, Ag^-, Cs^- and K^- and produced metal hydride anions, metal dihydride anions, metal hydroxide anions, metal oxide anions and 2-methyl-2-propanyl anion;

2) In addition, I reacted selective hydrocarbons and alcohols and pentane-d12 and 1-butanol-d10 with Fe^-, Co^-, Cu^-, Ag^- for confirmation and comparison purposes.

3) From the relevant values of heats of formation of fragments presented by Holmes and in the NIST webbook and the Gas-Phase Ion and Neutral Thermochemistry Book (see References 18 and 19), I calculated the enthalpy of the reactions outlined in the thesis.

4) Dr. Mayer's group suggested that the mechanism of the reactions outlined in this thesis is a metal insertion mechanism similar to that suggested by Dr. Alison (see reference 14).

References

(1) Weisshaar, J. C. *Accounts of Chemical Research* **1993**, *26*, 213.

(2) Holmes, J. L.; Aubry, C.; Mayer, P. M. *Assigning Structures to Ions in Mass Spectrometry*; CRC Press, 1968.

(3) Mayer, P. M. P., Clement *Mass Spectrometry Reviews* **2009**.

(4) Curtis, S.; Renaud, J.; Holmes, J. L.; Mayer, P. M. *Journal of the American Society for Mass Spectrometry* **2010**, *21*, 1944.

(5) Curtis, S.; DiMuzio, J.; Mungham, A.; Roy, J.; Hassan, D.; Renaud, J.; Mayer, P. M. *The Journal of Physical Chemistry A* **2011**, *115*, 14006.

(6) Attygalle, A. B.; Axe, F. U.; Weisbecker, C. S. *Rapid Communications in Mass Spectrometry* **2011**, *25*, 681.

(7) Blackwell, A. D. M. a. A. W. *Compendium of Chemical Terminology*; 2nd ed.; Blackwell Scientific Publications, 1997.

(8) Schröder, D.; Schwarz, H. *Proceedings of the National Academy of Sciences* **2008**, *105*, 18114.

(9) Hall, C.; Perutz, R. N. *Chemical Reviews* **1996**, *96*, 3125.

(10) Huang, S.; Holman, R. W.; Gross, M. L. *Organometallics* **1986**, *5*, 1857.

(11) Roithová, J.; Schröder, D. *Chemical Reviews* **2009**, *110*, 1170.

(12) Blomberg, M. R. A.; Siegbahn, P. E. M.; Svensson, M. *The Journal of Physical Chemistry* **1994**, *98*, 2062.

(13) Squires, R. R. *Chemical Reviews* **1987**, *87*, 623.

(14) McElvany, S. W.; Allison, J. *Organometallics* **1986**, *5*, 416.

(15) www.micromass.co.uk.

(16) http://quantummechanics.ucsd.edu/ph130a/130_notes/img3413.png 2013.

(17) Steinfeld, J. I.; Francisco, J. S.; Hase, W. L.; Prentice Hall (Upper Saddle River, NJ): 1999.

(18) http://webbook.nist.gov/chemistry/ 2013.

(19) Sharon G. Lisa, J. E. B., Joel F. Liebman, John L. Holmes, Rhoda D. Levin, and W. Gary Mallard *Journal of Physical and Chemical Reference Data* **1988**, *17*.

(20) Houriet, R.; Stahl, D.; Winkler, F. J. *Environmental health perspectives* **1980**, *36*, 63.

Appendix 1: Table of enthalpies of reactions

The reaction	The reaction number	Enthalpy kJ/mol
Reactions of pentane		
$C_5H_{12} + Fe^- \rightarrow C_5H_{11} + FeH^-$	21	176
$C_5H_{12} + Fe^- \rightarrow C_5H_{10} + FeH_2^-$	20	-124
$C_5H_{12} + Fe^- \rightarrow C_5H_{11}^- + FeH$	101	204
$C_5H_{12} + Co^- \rightarrow C_5H_{11} + CoH^-$	102	248
$C_5H_{12} + Co^- \rightarrow C_5H_{10} + CoH_2^-$	103	-114
$C_5H_{12} + Co^- \rightarrow C_5H_{11}^- + CoH$	104	270
$C_5H_{12} + Cu^- \rightarrow C_5H_{11} + CuH^-$	22	226
$C_5H_{12} + Cu^- \rightarrow C_5H_{10} + CuH_2^-$	23	-87
$C_5H_{12} + Cu^- \rightarrow C_5H_{11-} + CuH$	105	207
$C_5H_{12} + Ag^- \rightarrow C_5H_{11} + AgH^-$	106	282
$C_5H_{12} + Ag^- \rightarrow C_5H_{10} + AgH_2^-$	107	-38
$C_5H_{12} + Ag^- \rightarrow C_5H_{11-} + AgH$	108	258
$C_5H_{12} + Cs^- \rightarrow C_5H_{11} + CsH^-$	109	217
$C_5H_{12} + Cs^- \rightarrow C_5H_{10} + CsH_2^-$	110	11
$C_5H_{12} + Cs^- \rightarrow C_5H_{11-} + CsH$	111	224
$C_5H_{12} + K^- \rightarrow C_5H_{11} + KH^-$	112	211
$C_5H_{12} + K^- \rightarrow C_5H_{10} + KH_2^-$	113	-1516
$C_5H_{12} + K^- \rightarrow C_5H_{11-} + KH$	114	217
Reactions of pentene		
$C_5H_{10} + Fe^- \rightarrow C_5H_9 + FeH^-$	24	107
$C_5H_{10} + Fe^- \rightarrow C_5H_8 + FeH_2^-$	25	-141
$C_5H_{10} + Fe^- \rightarrow C_5H_9^- + FeH$	26	20
$C_5H_{10} + Co^- \rightarrow C_5H_9 + CoH^-$	115	179
$C_5H_{10} + Co^- \rightarrow C_5H_8 + CoH_2^-$	116	-131
$C_5H_{10} + Co^- \rightarrow C_5H_9^- + CoH$	117	86
$C_5H_{10} + Cu^- \rightarrow C_5H_9 + CuH^-$	28	157
$C_5H_{10} + Cu^- \rightarrow C_5H_8 + CuH_2^-$	27	-104
$C_5H_{10} + Cu^- \rightarrow C_5H_9^- + CuH$	118	23
$C_5H_{10} + Ag^- \rightarrow C_5H_9 + AgH^-$	119	213
$C_5H_{10} + Ag^- \rightarrow C_5H_8 + AgH_2^-$	120	-55
$C_5H_{10} + Ag^- \rightarrow C_5H_9^- + AgH$	121	74
$C_5H_{10} + Cs^- \rightarrow C_5H_9 + CsH^-$	122	148
$C_5H_{10} + Cs^- \rightarrow C_5H_8 + CsH_2^-$	123	-6
$C_5H_{10} + Cs^- \rightarrow C_5H_{9-} + CsH$	124	40
$C_5H_{10} + K^- \rightarrow C_5H_9 + KH^-$	125	142
$C_5H_{10} + K^- \rightarrow C_5H_8 + KH_2^-$	126	-1533
$C_5H_{10} + K^- \rightarrow C_5H_{9-} + KH$	127	33

Reactions of 1-pentyne		
$C_5H_8 + Fe^- \rightarrow C_5H_7 + FeH^-$	33	98
$C_5H_8 + Fe^- \rightarrow C_5H_6 + FeH_2^-$	34	-126
$C_5H_8 + Fe^- \rightarrow C_5H_7^- + FeH$	35	128
$C_5H_8 + Co^- \rightarrow C_5H_7 + CoH^-$	128	170
$C_5H_8 + Co^- \rightarrow C_5H_6 + CoH_2^-$	36	-116
$C_5H_8 + Co^- \rightarrow C_5H_7^- + CoH$	37	194
$C_5H_8 + Cu^- \rightarrow C_5H_7 + CuH^-$	129	148
$C_5H_8 + Cu^- \rightarrow C_5H_6 + CuH_2^-$	38	-89
$C_5H_8 + Cu^- \rightarrow C_5H_7^- + CuH$	39	131
$C_5H_8 + Ag^- \rightarrow C_5H_7 + AgH^-$	130	204
$C_5H_8 + Ag^- \rightarrow C_5H_6 + AgH_2^-$	131	-40
$C_5H_8 + Ag^- \rightarrow C_5H_7^- + AgH$	42	182
$C_5H_8 + Cs^- \rightarrow C_5H_7 + CsH^-$	132	139
$C_5H_8 + Cs^- \rightarrow C_5H_6 + CsH_2^-$	133	9
$C_5H_8 + Cs^- \rightarrow C_5H_7^- + CsH$	43	148
$C_5H_8 + K^- \rightarrow C_5H_7 + KH^-$	134	133
$C_5H_8 + K^- \rightarrow C_5H_6 + KH_2^-$	135	-1518
$C_5H_8 + K^- \rightarrow C_5H_7^- + KH$	44	141
Reactions of 1-butanol		
$C_4H_{10}O + Fe^- \rightarrow C_4H_9O + FeH^-$	45	192
$C_4H_{10}O + Fe^- \rightarrow C_4H_8O + FeH_2^-$	46	-172
$C_4H_{10}O + Fe^- \rightarrow C_4H_9O^- + FeH$	47	110
$C_4H_{10}O + Co^- \rightarrow C_4H_9O + CoH^-$	136	264
$C_4H_{10}O + Co^- \rightarrow C_4H_8O + CoH_2^-$	137	-162
$C_4H_{10}O + Co^- \rightarrow C_4H_9O^- + CoH$	138	176
$C_4H_{10}O + Cu^- \rightarrow C_4H_9O + CuH^-$	139	242
$C_4H_{10}O + Cu^- \rightarrow C_4H_8O + CuH_2^-$	52	-135
$C_4H_{10}O + Cu^- \rightarrow C_4H_9O^- + CuH$	53	113
$C_4H_{10}O + Ag^- \rightarrow C_4H_9O + AgH^-$	140	298
$C_4H_{10}O + Ag^- \rightarrow C_4H_8O + AgH_2^-$	141	-86
$C_4H_{10}O + Ag^- \rightarrow C_4H_9O^- + AgH$	57	164
$C_4H_{10}O + Cs^- \rightarrow C_4H_9O + CsH^-$	142	233
$C_4H_{10}O + Cs^- \rightarrow C_4H_8O + CsH_2^-$	143	-37
$C_4H_{10}O + Cs^- \rightarrow C_4H_9O^- + CsH$	61	130
$C_4H_{10}O + K^- \rightarrow C_4H_9O + KH^-$	144	227
$C_4H_{10}O + K^- \rightarrow C_4H_8O + KH_2^-$	145	-1564
$C_4H_{10}O + K^- \rightarrow C_4H_9O^- + KH$	65	123
Reactions of 2-butanol		
$C_4H_{10}O + Fe^- \rightarrow C_4H_9O + FeH^-$	66	203
$C_4H_{10}O + Fe^- \rightarrow C_4H_8O + FeH_2^-$	67	-185
$C_4H_{10}O + Fe^- \rightarrow C_4H_9O^- + FeH$	68	105
$C_4H_{10}O + Co^- \rightarrow C_4H_9O + CoH^-$	146	275

$C_4H_{10}O + Co^- \rightarrow C_4H_8O + CoH_2^-$	147	-175
$C_4H_{10}O + Co^- \rightarrow C_4H_9O^- + CoH$	89	171
$C_4H_{10}O + Cu^- \rightarrow C_4H_9O + CuH^-$	148	253
$C_4H_{10}O + Cu^- \rightarrow C_4H_8O + CuH_2^-$	76	-148
$C_4H_{10}O + Cu^- \rightarrow C_4H_9O^- + CuH$	77	108
$C_4H_{10}O + Ag^- \rightarrow C_4H_9O + AgH^-$	149	309
$C_4H_{10}O + Ag^- \rightarrow C_4H_8O + AgH_2^-$	150	-99
$C_4H_{10}O + Ag^- \rightarrow C_4H_9O^- + AgH$	83	159
$C_4H_{10}O + Cs^- \rightarrow C_4H_9O + CsH^-$	151	244
$C_4H_{10}O + Cs^- \rightarrow C_4H_8O + CsH_2^-$	152	-50
$C_4H_{10}O + Cs^- \rightarrow C_4H_9O^- + CsH$	84	125
$C_4H_{10}O + K^- \rightarrow C_4H_9O + KH^-$	153	238
$C_4H_{10}O + K^- \rightarrow C_4H_8O + KH_2^-$	154	-1577
$C_4H_{10}O + K^- \rightarrow C_4H_9O^- + KH$	85	118
Reactions of 2-methyl-2-propanol		
$C_4H_{10}O + Fe^- \rightarrow C_4H_9O + FeH^-$	86	200
$C_4H_{10}O + Fe^- \rightarrow C_4H_8O + FeH_2^-$	155	-197
$C_4H_{10}O + Fe^- \rightarrow C_4H_9O^- + FeH$	87	106
$C_4H_{10}O + Co^- \rightarrow C_4H_9O + CoH^-$	156	272
$C_4H_{10}O + Co^- \rightarrow C_4H_8O + CoH_2^-$	157	-187
$C_4H_{10}O + Co^- \rightarrow C_4H_9O^- + CoH$	89	172
$C_4H_{10}O + Cu^- \rightarrow C_4H_9O + CuH^-$	158	250
$C_4H_{10}O + Cu^- \rightarrow C_4H_8O + CuH_2^-$	159	-160
$C_4H_{10}O + Cu^- \rightarrow C_4H_9O^- + CuH$	90	109
$C_4H_{10}O + Ag^- \rightarrow C_4H_9O + AgH^-$	160	306
$C_4H_{10}O + Ag^- \rightarrow C_4H_8O + AgH_2^-$	161	-111
$C_4H_{10}O + Ag^- \rightarrow C_4H_9O^- + AgH$	94	160
$C_4H_{10}O + Cs^- \rightarrow C_4H_9O + CsH^-$	162	241
$C_4H_{10}O + Cs^- \rightarrow C_4H_8O + CsH_2^-$	163	-62
$C_4H_{10}O + Cs^- \rightarrow C_4H_9O^- + CsH$	96	126
$C_4H_{10}O + K^- \rightarrow C_4H_9O + KH^-$	164	235
$C_4H_{10}O + K^- \rightarrow C_4H_8O + KH_2^-$	165	-1589
$C_4H_{10}O + K^- \rightarrow C_4H_9O^- + KH$	99	119

Appendix 2: Calculation of reaction enthalpies

All reaction enthalpies of reactions indicated in this thesis study are derived from the known values of heats of formation of fragments in the literature. The value indicated

under each fragment in each reaction is the heat of formation of that fragment. The enthalpy of a reaction is the sum of the heats of formation of products subtracted by the sum of heats of formation of starting materials. For example, for the dehydrogenation reaction of pentane with Fe^-, the enthalpy Δ_rH is derived as follows:

$\Delta_fH_{(C5H12)}$ = -147

$\Delta_fH_{(Fe-)}$ = 402

$\Delta_fH_{(C5H11)}$ = 50

$\Delta_fH_{(FeH-)}$ = 381

$C_5H_{12} + Fe^- \rightarrow C_5H_{11} + FeH^-$

-147 402 50 381

Δ_rH= [(50) + (381)] - [(-147) + (402)] = 176

All of the heats of formation and the enthalpy values are in kJ/mol.

Reactions of pentane with Fe^- ;

$C_5H_{12} + Fe^- \rightarrow C_5H_{11} + FeH^-$ Δ_rH= 176

-147 402 50 381

$C_5H_{12} + Fe^- \rightarrow C_5H_{10} + FeH_2^-$ Δ_rH= -124

-147 402 -32 163

$C_5H_{12} + Fe^- \rightarrow C_5H_{11}^- + FeH$ Δ_rH= 204

-147 402 -12 471

Reactions of pentane with Co^- ;

$C_5H_{12} + Co^- \rightarrow C_5H_{11} + CoH^-$ Δ_rH= 248

-147 361 50 412

$C_5H_{12} + Co^- \rightarrow C_5H_{10} + CoH_2^-$ $\Delta_rH = -114$

-147 361 -32 132

$C_5H_{12} + Co^- \rightarrow C_5H_{11}^- + CoH$ $\Delta_rH = 270$

-147 361 -12 496

Reactions of pentane with Cu^- ;

$C_5H_{12} + Cu^- \rightarrow C_5H_{11} + CuH^-$ $\Delta_rH = 226$

-147 219 50 248

$C_5H_{12} + Cu^- \rightarrow C_5H_{11}^- + CuH$ $\Delta_rH = 207$

-147 219 -12 291

$C_5H_{12} + Cu^- \rightarrow C_5H_{10} + CuH_2^-$ $\Delta_rH = -87$

-147 219 -32 17

Reactions of pentane with Ag^- ;

$C_5H_{12} + Ag^- \rightarrow C_5H_{11} + AgH^-$ $\Delta_rH = 282$

-147 159 5 244

$C_5H_{12} + Ag^- \rightarrow C_5H_{11}^- + AgH$ $\Delta_rH = 258$

-147 159 -12 282

$C_5H_{12} + Ag^- \rightarrow C_5H_{10} + AgH_2^-$ $\Delta_rH = -28$

-147 159 -32 6

Reactions of pentane with Cs^- ;

$C_5H_{12} + Cs^- \rightarrow C_5H_{11} + CsH^-$ $\Delta_rH = 217$

-147 31 50 51

$C_5H_{12} + Cs^- \rightarrow C_5H_{11}^- + CsH$ $\Delta_rH = 224$

-147 31 -12 120

$C_5H_{12} + Cs^- \rightarrow C_5H_{10} + CsH_2^-$ $\Delta_rH = 11$

-147 31 -32 -73

Reactions of pentane with K^- ;

$C_5H_{12} + K^- \rightarrow C_5H_{11} + KH^-$ $\Delta_rH = 211$

-147 41 50 55

$C_5H_{12} + K^- \rightarrow C_5H_{11}^- + KH$ $\Delta_rH = 217$

-147 41 -12 123

$C_5H_{12} + K^- \rightarrow C_5H_{10} + KH_2^-$ $\Delta_rH = -1516$

-147 41 -32 -1590

Reactions of 1-pentene with Fe^- ;

$C_5H_{10} + Fe^- \rightarrow C_5H_9 + FeH^-$ $\Delta_rH = 107$

-22 402 106 381

$C_5H_{10} + Fe^- \rightarrow C_5H_8 + FeH_2^-$ $\Delta_rH = -141$

-22 402 76 163

$C_5H_{10} + Fe^- \rightarrow C_5H_9^- + FeH$ $\Delta_rH = 20$

-22 402 -71 471

Reactions of 1-pentene with Co^- ;

$C_5H_{10} + Co^- \rightarrow C_5H_9 + CoH^-$ $\Delta_rH = 179$

-22 361 106 412

$C_5H_{10} + Co^- \rightarrow C_5H_8 + CoH_2^-$ $\Delta_rH = -131$

-22 361 76 132

$C_5H_{10} + Co^- \rightarrow C_5H_9^- + CoH$ $\Delta_rH = 86$

-22 361 -71 496

Reactions of 1-pentene with Cu^- ;

$C_5H_{10} + Cu^- \rightarrow C_5H_9 + CuH^-$ $\Delta_rH = 157$

-22 219 106 248

$C_5H_{10} + Cu^- \rightarrow C_5H_8 + CuH_2^-$ $\Delta_rH = -104$

-22 219 76 17

$C_5H_{10} + Cu^- \rightarrow C_5H_9^- + CuH$ $\Delta_rH = 23$

-22 219 -71 291

Reactions of 1-pentene with Ag^- ;

$C_5H_{10} + Ag^- \rightarrow C_5H_9 + AgH^-$ $\Delta_rH = 213$

-22 159 106 244

$C_5H_{10} + Ag^- \rightarrow C_5H_9^- + AgH$ $\Delta_rH = 74$

-22 159 -71 282

$C_5H_{10} + Ag^- \rightarrow C_5H_8 + AgH_2^-$ $\Delta_rH = -55$

-22 159 76 6

Reactions of 1-pentene with Cs^-

$C_5H_{10} + Cs^- \rightarrow C_5H_9 + CsH^-$ $\Delta_rH = 148$

-22 31 106 51

$C_5H_{10} + Cs^- \rightarrow C_5H_{9-} + CsH$ $\Delta_rH = 40$

-22 31 -71 120

$C_5H_{10} + Cs^- \rightarrow C_5H_8 + CsH_2^-$ $\Delta_rH = -6$

-22 31 76 -73

Reactions of 1-pentene with K^- ;

$C_5H_{10} + K^- \rightarrow C_5H_9 + KH^-$ $\Delta_rH = 142$

-22 41 106 55

$C_5H_{10} + K^- \rightarrow C_5H_{9-} + KH$ $\Delta_rH = 33$

-22 41 -71 123

$C_5H_{10} + K^- \rightarrow C_5H_8 + KH_2^-$ $\Delta_rH = -1533$

-22 41 76 -1590

Reactions of 1-pentyne with Fe^- ;

$C_5H_8 + Fe^- \rightarrow C_5H_7 + FeH^-$ $\Delta_rH = 98$

144 402 263 381

$C_5H_8 + Fe^- \rightarrow C_5H_6 + FeH_2^-$ $\Delta_rH = -126$

144 402 257 163

$C_5H_8 + Fe^- \rightarrow C_5H_7^- + FeH$ $\Delta_rH = 128$

144 402 203 471

Reactions of 1-pentyne with Co^- ;

$C_5H_8 + Co^- \rightarrow C_5H_6 + CoH_2^-$ $\Delta_rH = -116$

144 361 257 132

$C_5H_8 + Co^- \rightarrow C_5H_7^- + CoH$ $\Delta_rH = 194$

144 361 203 496

$C_5H_8 + Co^- \rightarrow C_5H_7 + CoH^-$ $\Delta_rH = 170$

144 361 263 412

Reactions of 1-pentyne with Cu^- ;

$C_5H_8 + Cu^- \rightarrow C_5H_7 + CuH^-$ $\Delta_rH = 148$

144 219 263 248

$C_5H_8 + Cu^- \rightarrow C_5H_6 + CuH_2^-$ $\Delta_rH = -89$

144 219 257 17

$C_5H_8 + Cu^- \rightarrow C_5H_7^- + CuH$ $\Delta_rH = 131$

144 219 203 291

Reactions of 1-pentyne with Ag^- ;

$C_5H_8 + Ag^- \rightarrow C_5H_7^- + AgH$ $\Delta_rH = 182$

144 159 203 282

$C_5H_8 + Ag^- \rightarrow C_5H_7 + AgH^-$ $\Delta_rH = 204$

144 159 263 244

$C_5H_8 + Ag^- \rightarrow C_5H_6 + AgH_2^-$ $\Delta_rH = -40$

144 159 257 6

Reactions of 1-pentyne with Cs^- ;

$C_5H_8 + Cs^- \rightarrow C_5H_7^- + CsH$ $\Delta_rH = 148$

144 31 203 120

$C_5H_8 + Cs^- \rightarrow C_5H_7 + CsH^-$ $\Delta_rH= 139$

144 31 263 51

$C_5H_8 + Cs^- \rightarrow C_5H_6 + CsH_2^-$ $\Delta_rH= 9$

144 31 257 -73

Reactions of 1-pentyne with K^- ;

$C_5H_8 + K^- \rightarrow C_5H_7^- + KH$ $\Delta_rH= 141$

144 41 203 123

$C_5H_8 + K^- \rightarrow C_5H_7 + KH^-$ $\Delta_rH= 133$

144 41 263 55

$C_5H_8 + K^- \rightarrow C_5H_6^{\cdot} + KH_2^-$ $\Delta_rH= -1518$

144 41 257 -1590

Reactions of 1-butanol with Fe^- ;

$C_4H_{10}O + Fe^- \rightarrow C_4H_9O + FeH^-$ $\Delta_rH= 192$

-275 402 -62 381

$C_4H_{10}O + Fe^- \rightarrow C_4H_8O + FeH_2^-$ $\Delta_rH= -172$

-275 402 -208 163

$C_4H_{10}O + Fe^- \rightarrow C_4H_9O^- + FeH$ $\Delta_rH= 110$

-275 402 -234 471

Reactions of 1-butanol with Co^-

$C_4H_{10}O + Co^- \rightarrow C_4H_8O + CoH_2^-$ $\Delta_rH= -162$

-275 361 -208 132

$C_4H_{10}O + Co^- \rightarrow C_4H_9O^- + CoH$ $\Delta_rH = 176$

-275 361 -234 496

$C_4H_{10}O + Co^- \rightarrow C_4H_9O + CoH^-$ $\Delta_rH = 264$

-275 361 -62 412

Reactions of 1-butanol with Cu^- ;

$C_4H_{10}O + Cu^- \rightarrow C_4H_8O + CuH_2^-$ $\Delta_rH = -135$

-275 219 -208 17

$C_4H_{10}O + Cu^- \rightarrow C_4H_9O + CuH^-$ $\Delta_rH = 242$

-275 219 -62 248

$C_4H_{10}O + Cu^- \rightarrow C_4H_9O^- + CuH$ $\Delta_rH = 113$

-275 219 -234 291

Reactions of 1-butanol with Ag^- ;

$C_4H_{10}O + Ag^- \rightarrow C_4H_9O^- + AgH$ $\Delta_rH = 164$

-275 159 -234 282

$C_4H_{10}O + Ag^- \rightarrow C_4H_9O + AgH^-$ $\Delta_rH = 298$

-275 159 -62 244

$C_4H_{10}O + Ag^- \rightarrow C_4H_8O + AgH_2^-$ $\Delta_rH = -86$

-275 159 -208 6

Reactions of 1-butanol with Cs^- ;

$C_4H_{10}O + Cs^- \rightarrow C_4H_9O^- + CsH$ $\Delta_rH = 130$

-275 31 -234 120

$C_4H_{10}O + Cs^- \rightarrow C_4H_9O + CsH^-$ $\Delta_rH= 233$

-275 31 -62 51

$C_4H_{10}O + Cs^- \rightarrow C_4H_8O + CsH_2^-$ $\Delta_rH= -37$

-275 31 -208 -73

Reactions of 1-butanol with K^- ;

$C_4H_{10}O + K^- \rightarrow C_4H_9O^- + KH$ $\Delta_rH= 123$

-275 41 -234 123

$C_4H_{10}O + K^- \rightarrow C_4H_9O + KH^-$ $\Delta_rH= 227$

-275 41 -62 55

$C_4H_{10}O + K^- \rightarrow C_4H_8O + KH_2^-$ $\Delta_rH= -1564$

-275 41 -208 -1590

Reactions of 2-butanol with Fe^- ;

$C_4H_{10}O + Fe^- \rightarrow C_4H_9O + FeH^-$ $\Delta_rH= 203$

-295 402 -71 381

$C_4H_{10}O + Fe^- \rightarrow C_4H_8O + FeH_2^-$ $\Delta_rH= -185$

-295 402 -241 163

$C_4H_{10}O + Fe^- \rightarrow C_4H_9O^- + FeH$ $\Delta_rH= 105$

-295 402 -259 471

Reactions of 2-butanol with Co^- ;

$C_4H_{10}O + Co^- \rightarrow C_4H_8O + CoH_2^-$ $\Delta_rH= -175$

-295 361 -241 132

$C_4H_{10}O + Co^- \rightarrow C_4H_9O^- + CoH$ $\Delta_rH = 171$

-295 361 -259 496

$C_4H_{10}O + Co^- \rightarrow C_4H_9O + CoH^-$ $\Delta_rH = 275$

-295 361 -71 412

Reactions of 2-butanol with Cu^- ;

$C_4H_{10}O + Cu^- \rightarrow C_4H_8O + CuH_2^-$ $\Delta_rH = -148$

-295 219 -241 17

$C_4H_{10}O + Cu^- \rightarrow C_4H_9O + CuH^-$ $\Delta_rH = 253$

-295 219 -71 248

$C_4H_{10}O + Cu^- \rightarrow C_4H_9O^- + CuH$ $\Delta_rH = 108$

-295 219 -259 291

Reactions of 2-butanol with Ag^- ;

$C_4H_{10}O + Ag^- \rightarrow C_4H_9O^- + AgH$ $\Delta_rH = 159$

-295 159 -259 282

$C_4H_{10}O + Ag^- \rightarrow C_4H_9O + AgH^-$ $\Delta_rH = 309$

-295 159 -71 244

$C_4H_{10}O + Ag^- \rightarrow C_4H_8O + AgH_2^-$ $\Delta_rH = -99$

-295 159 -241 6

Reactions of 2-butanol with Cs^- ;

$C_4H_{10}O + Cs^- \rightarrow C_4H_9O^- + CsH$ $\Delta_rH = 125$

-295 31 -259 120

$C_4H_{10}O + Cs^- \rightarrow C_4H_9O + CsH^-$ $\Delta_rH= 244$

-295 31 -71 51

$C_4H_{10}O + Cs^- \rightarrow C_4H_8O + CsH_2^-$ $\Delta_rH= -50$

-295 31 -241 -73

Reactions of 2-butanol with K^- ;

$C_4H_{10}O + K^- \rightarrow C_4H_9O^- + KH$ $\Delta_rH= 118$

-295 41 -259 123

$C_4H_{10}O + K^- \rightarrow C_4H_9O + KH^-$ $\Delta_rH= 238$

-295 41 -71 55

$C_4H_{10}O + K^- \rightarrow C_4H_8O + KH_2^-$ $\Delta_rH= -1577$

-295 41 -241 -1590

Reactions of 2-methyl-2-propanol with Fe^- ;

$C_4H_{10}O + Fe^- \rightarrow C_4H_9O + FeH^-$ $\Delta_rH= -200$

-312 402 -91 381

$C_4H_{10}O + Fe^- \rightarrow C_4H_8O + FeH_2^-$ $\Delta_rH= -197$

-312 402 -270 163

$C_4H_{10}O + Fe^- \rightarrow C_4H_9O^- + FeH$ $\Delta_rH= 106$

-312 402 -275 471

Reactions of 2-methyl-2-propanol with Co^- ;

$C_4H_{10}O + Co^- \rightarrow C_4H_8O + CoH_2^-$ $\Delta_rH= -187$

-312 361 -270 132

$C_4H_{10}O + Co^- \rightarrow C_4H_9O^- + CoH$ $\Delta_rH= 172$

-312 361 -275 496

$C_4H_{10}O + Co^- \rightarrow C_4H_9O + CoH^-$ $\Delta_rH= 272$

-312 361 -91 412

Reactions of 2-methyl-2-propanol with Cu^- ;

$C_4H_{10}O + Cu^- \rightarrow C_4H_8O + CuH_2^-$ $\Delta_rH= -160$

-312 219 -270 17

$C_4H_{10}O + Cu^- \rightarrow C_4H_9O + CuH^-$ $\Delta_rH= 250$

-312 219 -91 248

$C_4H_{10}O + Cu^- \rightarrow C_4H_9O^- + CuH$ $\Delta_rH= 109$

-312 219 -275 291

Reactions of 2-methyl-2-propanol with Ag^- ;

$C_4H_{10}O + Ag^- \rightarrow C_4H_9O^- + AgH$ $\Delta_rH= 160$

-312 159 -275 282

$C_4H_{10}O + Ag^- \rightarrow C_4H_9O + AgH^-$ $\Delta_rH= -306$

-312 159 -91 244

$C_4H_{10}O + Ag^- \rightarrow C_4H_7O^- + AgH_2$ $\Delta_rH= -111$

-312 159 -270 6

Reactions of 2-methyl-2-propanol with Cs^- ;

$C_4H_{10}O + Cs^- \rightarrow C_4H_9O^- + CsH$ $\Delta_rH= 126$

-312 31 -275 120

$C_4H_{10}O + Cs^- \rightarrow C_4H_9O + CsH^-$ $\Delta_rH= 241$

-312 31 -91 51

$C_4H_{10}O + Cs^- \rightarrow C_4H_8O + CsH_2^-$ Δ_rH= -62

-312 31 -270 -73

Reactions of 2-methyl-2-propanol with K^- ;

$C_4H_{10}O + K^- \rightarrow C_4H_9O^- + KH$ Δ_rH= 119

-312 41 -275 123

$C_4H_{10}O + K^- \rightarrow C_4H_9O + KH^-$ Δ_rH= 235

-312 41 -91 55

$C_4H_{10}O + K^- \rightarrow C_4H_8O + KH_2^-$ Δ_rH= -1589

-312 41 -270 -1590

Appendix 3: Calculation of hydrogen affinity of metal anions

$Fe^- + H \rightarrow FeH^-$

The enthalpy of this reaction is calculated from the heats of formation of fragments as:

H^- + Fe → FeH^- Δ_rH= -179.2 (166)

145.2 415 381

In addition, there are two electron affinity reactions as:

$H^- + Fe \rightarrow FeH^-$ Δ_rH= -179.2 (166)

$Fe^- \rightarrow Fe + e^-$ -EA(Fe) = 0.31^96.5= 29.91 (167)

$H + e^- \rightarrow H^-$ EA(H) = -0.754^96.5= -72.76 (168)

The sum of reactions 166, 167 and 168 produces reaction 169 which defines the hydrogen affinity of iron:

$Fe^- + H \rightarrow FeH^-$ $\Delta_rH = -222.05$ (169)

$Co^- + H \rightarrow CoH^-$

The enthalpy of this reaction is calculated from the enthalpies of fragments as:

H^- + Co → CoH^- $\Delta_rH = -159.8$ (170)

145.2 426.6 412

In addition, there are two electron affinity reactions as:

$H^- + Co \rightarrow CoH^-$ $\Delta_rH = -159.8$ (170)

$Co^- \rightarrow Co + e^-$ -EA(Co) =0.663^96.5= 63.97 (171)

$H + e^- \rightarrow H^-$ EA(H)= -0.754^96.5= -72.76 (172)

The sum of reactions 170, 171 and 172 produces reaction 173 which defines the hydrogen affinity of cobalt:

$Co^- + H \rightarrow CoH^-$ $\Delta_rH = -168.59$ (173)

$Cu^- + H \rightarrow CuH^-$

The enthalpy of this reaction is calculated from the enthalpies of fragments as:

H^- + Cu → CuH^- $\Delta_rH = -234.5$ (174)

145.2 337.4 248.1

In addition, there are two electron affinity reactions as:

$H^- + Cu \rightarrow CuH^-$ $\Delta_rH = -234.5$ (174)

$Cu^- \rightarrow Cu + e^-$ -EA(Cu)= 1.236^96.5= 119.2 (175)

$H + e^- \rightarrow H^-$ EA(H)= -0.754^96.5= -72.76 (176)

The sum of reactions 174, 175 and 176 produces reaction 177 which defines the hydrogen affinity of copper:

$Cu^- + H \rightarrow CuH^-$ $\Delta_r H$= -188.06 (177)

$Ag^- + H \rightarrow AgH^-$

The enthalpy of this reaction is calculated from the enthalpies of fragments as:

H^- + Ag → AgH^- $\Delta_r H$= -186.1 (178)

145.2 284.9 244

In addition, there are two electron affinity reactions as:

$H^- + Ag \rightarrow AgH^-$ $\Delta_r H$= -186.1 (178)

$Ag^- \rightarrow Ag + e^-$ -EA(Ag)= 1.304^96.5= 125.8 (179)

$H + e^- \rightarrow H^-$ EA(H)= -0.754^96.5= -72.76 (180)

The sum of reactions 178, 179 and 180 produces reaction 181 which defines the hydrogen affinity of silver:

$Ag^- + H \rightarrow AgH^-$ $\Delta_r H$= -133.024 (181)

$Cs^- + H \rightarrow CsH^-$

The enthalpy of this reaction is calculated from the enthalpies of fragments as:

H^- + Cs → CsH^- $\Delta_r H$= -170.7 (182)

145.2 76.5 51

In addition, there are two electron affinity reactions as:

$H^- + Cs \rightarrow CsH^-$ $\Delta_r H = -170.7$ (182)

$Cs^- \rightarrow Cs + e^-$ -EA(Cs)= 0.47^96.5= 45.355 (183)

$H + e^- \rightarrow H^-$ EA(H)= -0.754^96.5= -72.76 (184)

The sum of reactions 182, 183 and 184 produces reaction 185 which defines the hydrogen affinity of cesium:

$Cs^- + H \rightarrow CsH^-$ $\Delta_r H = -198.105$ (185)

$K^- + H \rightarrow KH^-$

The enthalpy of this reaction is calculated from the enthalpies of fragments as:

$H^- + K \rightarrow KH^-$ $\Delta_r H = -179.2$ (186)

145.2 89 55

In addition, there are two electron affinity reactions as:

$H^- + K \rightarrow KH^-$ $\Delta_r H = -179.2$ (186)

$K^- \rightarrow K + e^-$ -EA(K)= 0.501^96.5= 48.34 (187)

$H + e^- \rightarrow H^-$ EA(H)= -0.754^96.5= -72.76 (188)

The sum of reactions 186, 187 and 188 produces reaction 189 which defines the hydrogen affinity of potassium,

$K^- + H \rightarrow KH^-$ $\Delta_r H = -203.62$ (189)

Appendix 4: Table of heats of formation of metal-containing fragments

Fragment	$\Delta_f H$, (kJ/mol)	Electron affinity, (eV)	Gas phase acidity, (kJ/mol)
Fe	415.47[18]	0.1510[18]	
Fe	416[19]		
Fe^-	401.75[18]		
Fe^-	402	0.151[19]	1461[19]
FeH	471 (Calculated)	0.934[18]	
FeH^-	381[18]	0.934[19]	
FeH_2	414 (Calculated)		
FeH_2^-	163 (Calculated)	1.049[19]	
Co	426.68[18]	0.6633[18]	
Co	425[19]		
Co^-	360.7[18]		
Co^-	361[19]	0.662[19]	1437[19]
CoH	496[19]	0.671[18]	
CoH^-	412[18]		
CoH^-	412[19]	0.671[19]	
CoH_2	272 (Calculated)		
CoH_2^-	132 (Calculated)	1.45[19]	
Cu	337.6[18]	1.236[18]	
Cu	338.2[19]		

Cu^-	219[18]		
Cu^-	220[19]	1.228[19]	1459[19]
Cu^-	219 (Calculated)		
CuH	291[19]	0.444[18]	
CuH^-	248 (Calculated)		
CuH_2	268 (Calculated)		
CuH_2^-	17 (Calculated)	2.6[18]	
Ag	248.9[18]	1.304[18]	
Ag	284.6[19]		
Ag^-	159[18]		
Ag^-	159[19]	1.302[19]	
AgH	282[19]		
AgH	283 (Calculated)		
AgH^-	244 (Calculated)		
AgH_2	274 (Calculated)		
AgH_2^-	6 (Calculated)		
Cs	76.5[18]	0.471[18]	
Cs	76.1[19]	0.47[19]	
Cs^-	31[19]	0.472[19]	
CsH	120 (Calculated)		
CsH^-	51 (Calculated)		
CsH_2	81 (Calculated)		
CsH_2^-	-73 (Calculated)		
K	89[18]		

K	89[19]		
K^-	41[19]	0.501[18]	
K^-		0.501[19]	1448[19]
KH	123.01[18]		
KH	123[19]		
KH^-	55 (Calculated)		
KH_2	-1445 (Calculated)		
KH_2^-	-1590 (Calculated)		

Appendix 5: Table of heats of formation of organic fragments

Fragment	Structure	$\Delta_f H$, (kJ/mol)	Electron affinity, (eV)	Gas phase acidity, (kJ/mol)
C_5H_6	$CH{\equiv}C\text{-}CH{=}CH\text{-}CH_3$	257[19]		
$C_5H_6^-$				
C_5H_7	$HC{\equiv}CC(CH_3)_2$	263[19]		
C_5H_7	More			
$C_5H_7^-$	nprC≡C$^-$	203[19]	2.85[19]	1589[19]
$C_5H_7^-$	nprC≡C$^-$		2.9[18]	
$C_5H_7^-$	$CH_2{=}C(CH{=}CH_2)CH_2^-$	159[19]		1614[19]
$C_5H_7^-$	Pentadienide-	118[19]	0.91[19]	1542[19]

$C_5H_7^-$		203 (Calculated)		
C_5H_8	1-pentyne	144.3[18]		
C_5H_8	2-pentyne	128.9[18]		
C_5H_8	$C_3H_7C{\equiv}CH$	144[19]		
C_5H_8	$C_2H_5C{\equiv}CCH_3$	128[19]		
C_5H_8	$(CH_3)_2CHC{\equiv}CH$	136[19]		
C_5H_8	$CH_2{=}CH\text{-}CH{=}CH\text{-}CH_3$	76[19]		
$C_5H_8^-$				
C_5H_9	$CH_2{=}CHCHCH_2CH_3$	106[19]		
C_5H_9	$CH_3CHCH{=}CHCH_3$	92[19]		
C_5H_9	$(CH_3)_2CCH{=}CH_2$	81[19]		
C_5H_9	Cyclopentyl radical		0.27[18]	
$C_5H_9^-$		-71(Calculated)		
C_5H_{10}	1-pentene	-22[18]		
C_5H_{10}	1-C_5H_{10}	-21.4[19]		
C_5H_{10}	2-(Z)-C_5H_{10}	-26.5[19]		
C_5H_{10}	2-(E)-C_5H_{10}	-31.5[19]		
C_5H_{10}	$(CH_3)_2CHCH{=}CH_2$	-27.4[19]		
C_5H_{10}	$C_2H_5C(CH_3){=}CH_2$	-35.6[19]		
C_5H_{10}	$(CH_3)_2C{=}CHCH_3$	-42.1[19]		
$C_5H_{10}^-$				
C_5H_{11}	1-C_5H_{11}	56[19]		
C_5H_{11}	$CH_3CH_2CH_2CHCH_3$	50[19]		
C_5H_{11}	$(CH_3)_2CCH_2CH_3$	27[19]		

C_5H_{11}	$(CH_3)_3CCH_2$	33[19]	0.23[18]	
$C_5H_{11}^-$		-11 (Calculated)		
C_5H_{12}	pentane	-146.8[18]		
C_5H_{12}	neopentane	-167.9[18]		
C_5H_{12}		-146.5[19]		
$C_5H_{12}^-$				
C_4H_8O		-211.8[18]		
C_4H_8O	C_3H_7-CHO	-207.5[19]		
C_4H_8O	C_2H_5-CO-CH_3	-240.8[19]		
C_4H_8O	$(CH_3)_3CO$	-270 (Estimated)		
$C_4H_8O^-$				
C_4H_9O	n-C_4H_9O	-69[19]	1.78[18]	
C_4H_9O	n-C_4H_9O	-62 (Calculated)		
C_4H_9O	s-C_4H_9O	-71 (Calculated)		
C_4H_9O	t-C_4H_9O	-91 (Calculated)		
$C_4H_9O^-$	$iBuO^-$	-246[19]	1.87[19]	1568[19]
$C_4H_9O^-$	$nBuO^-$	-234[19]	1.78[19]	1571[19]
$C_4H_9O^-$	$sBuO^-$	-259[19]	1.95[19]	1566[19]
$C_4H_9O^-$	$tBuO^-$	-275[19]	1.91[19]	1567[19]
$C_4H_{10}O$	n-C_4H_9OH	-275[19]		
$C_4H_{10}O$		-277[18]		
$C_4H_{10}O$	Se-C_4H_9OH	-295[19]		
$C_4H_{10}O$	Iso-C_4H_9OH	-284[19]		

$C_4H_{10}O$	Tert-C_4H_9OH	-312[19]		
$C_4H_{10}O^-$				

Appendix 6: Calculations of heats of formation of some fragments

All unknown heats of formation of fragments are derived from the known values of heats of formation in the literature. All energy values are in kJ/mol.

FeH

$FeH + e^- \rightarrow FeH^-$, EA = -0.934 eV ^ 96.48 kJ/mol/eV = -90.11, $\Delta_fH(FeH^-)$= 381

$\Delta_fH(FeH)$= 471

$Fe^- + H^+ \rightarrow FeH$ $\Delta_{acid}H$= -1461 , $\Delta_fH(Fe^-)$ = 402 , $\Delta_fH(H^+)$ = 1530[19]

$\Delta_fH(FeH)$= 471

$C_5H_{11}^-$

$C_5H_{11} + e^- \rightarrow C_5H_{11}^-$ EA= -0.7 ^ 96.48 = -67.5 , EA ($C_4H_9^-$, $C_3H_7^-$)= -0.7[19], $\Delta_fH(C_5H_{11})$= 56

$\Delta_fH(C_5H_{11}^-)$= -11.5

$C_5H_9^-$

$C_5H_9 + e^- \rightarrow C_5H_9^-$ EA = -0.36 ^ 96.48 = -35 , EA ($C_4H_7^-$ and $C_3H_5^-$) = -0.36[19] , $\Delta_fH(C_5H_9)$ = 106

$\Delta_fH(C_5H_9^-)$ = -71

n-C4H9O

$C_4H_9O + e^- \rightarrow C_4H_9O^-$,EA = -1.78 ^ 96.48 = -172 , Δ_fH ($C_4H_9O^-$) = -234

Δ_fH (C_4H_9O) = -62

s-C4H9O

$C_4H_9O + e^- \rightarrow C_4H_9O^-$,EA = -1.95 ^ 96.48 = -188 , Δ_fH ($C_4H_9O^-$) = -259

Δ_fH (C_4H_9O) = -71

t-C4H9O

$C_4H_9O + e^- \rightarrow C_4H_9O^-$,EA = -1.91 ^ 96.48 = -184 , Δ_fH ($C_4H_9O^-$) = -275

Δ_fH(C_4H_9O) = -91

CuH^-

$CuH + e^- \rightarrow CuH^-$ EA = -o.444 ^ 96.48 = -42.83 Δ_fH(CuH) = 291

$\Delta_fH(CuH^-)$ = 248

Cu^-

$Cu + e^- \rightarrow Cu^-$ EA = -1.236 ^ 96.48 = -119 , Δ_fH(Cu) = 338

$\Delta_fH(Cu^-)$ = 219

CuH_2

$CuH^- + H^+ \rightarrow CuH_2$

($\Delta_{acid}H$ (FeH_2)= -1497 and $\Delta_{acid}H$(FeH)= -1439 and $\Delta_{acid}H$(CuH)= -1451) so $\Delta_{acid}H(CuH_2)$= -1510 , Δ_fH (CuH^-) = 248

Δ_fH(CuH_2)= 268

CuH_2^-

$CuH_2 + e^- \rightarrow CuH2^-$ EA= -2.6 ^ 96.48 = -251 , $\Delta_fH(CuH_2) = 268$

$\Delta_fH(CuH_2^-) = 17$

FeH_2

$FeH^- + H^+ \rightarrow FeH_2$ $\Delta_{acid}H\ (FeH_2)$= -1497 , $\Delta_fH(\ FeH^-\ ) =$ 381 , $\Delta_fH(\ H^+\ ) =$ 1530

$\Delta_fH\ (FeH_2) =$ 414

FeH_2^-

$FeH_2 + e^- \rightarrow FeH_2^-$

(EA(CuH)= -0.44 and EA(CuH_2)= -2.6 and EA(FeH) = -0.934) so
EA(FeH_2) = -2.6 , $\Delta_fH(\ FeH_2) = 414$

$\Delta_fH\ (FeH_2^-) =$ 163

CoH_2

$CoH^- + H^+ \rightarrow CoH_2$

($\Delta_{acid}H$ (FeH)= 1439 and $\Delta_{acid}H$ CoH= 1411 and $\Delta_{acid}H(\ FeH_2)$= 1497) so
$\Delta_{acid}H\ (CoH_2)$=1470

$\Delta_fH\ (CoH^-)$= 412 , $\Delta_fH(\ H^+) = 1530$

$\Delta_fH\ (CoH_2)$= 272

CoH_2^-

$CoH_2 + e^- \rightarrow CoH_2^-$ EA= -1.45^96.48= -140 $\Delta_fH(CoH_2)$= 272

$\Delta_fH(\ CoH_2^-)$= 132

$FeH_2^- \rightarrow FeH^- + H$

$FeH_2^- \rightarrow FeH^- + H$ $\Delta_fH(FeH_2^-) = 163$, $\Delta_fH(FeH^-) = 381$, $\Delta_fH(H) = 218$

$\Delta_rH = 436$

HCs

$Cs^- + H^+ \rightarrow HCs$, $\Delta_rH = -1441$, $\Delta_fH(Cs^-) = 31$, $\Delta_fH(H^+) = 1530$

$\Delta_fH(HCs) = 120$

AgH

$Ag^- + H^+ \rightarrow AgH$, $\Delta_rH = -1406$, $\Delta_fH(Ag^-) = 159$, $\Delta_fH(H^+) = 1530$

$\Delta_fH(AgH) = 283$

AgH^-

$AgH + e^- \rightarrow AgH^-$, EA = -0.4 ^ 96.48 = - 39 , $\Delta_fH(AgH) = 283$

$\Delta_fH(AgH^-) = 244$

CsH^-

$CsH + e^- \rightarrow CsH^-$, EA = -0.72 ^ 96.48 = -69 , $\Delta_fH(CsH) = 120$

$\Delta_fH(CsH^-) = 51$

KH^-

$KH + e^- \rightarrow KH^-$, EA = - 0.7 ^ 96.48 = -68 , $\Delta_fH(KH) = 123$

$\Delta_fH(KH^-) = 55$

AgH_2

$AgH^- + H^+ \rightarrow AgH_2$, $\Delta_{acid}H = -1500$, $\Delta_fH\ (AgH^-) = 244$, $\Delta_fH\ (H^+) = 1530$

$\Delta_fH\ (AgH_2) = 274$

AgH_2^-

$AgH_2 + e^- \rightarrow AgH_2^-$, EA = -2.9 ^ 96.48 = -278 , $\Delta_fH\ (AgH_2) = 274$,

$\Delta_fH\ (AgH_2^-) = 6$

CsH_2

$CsH^- + H^+ \rightarrow CsH_2$, $\Delta_rH = -1500$, $\Delta_fH(CsH^-) = 51$, $\Delta_fH\ (H^+) = 1530$

$\Delta_fH\ (CsH_2) = 81$

CsH_2^-

$CsH_2 + e^- \rightarrow CsH_2^-$, EA = -1.6 ^ 96.48 = -154 , $\Delta_fH\ (CsH_2) = 81$

$\Delta_fH\ (CsH_2^-) = -73$

KH_2

$KH^- + H^+ \rightarrow KH_2$, $\Delta rH = -1500$, $\Delta_fH\ (KH^-) = 55$, $\Delta_fH\ (H^+) = 1530$

$\Delta_fH\ (KH_2) = -1445$

KH_2^-

$KH_2 + e^- \rightarrow KH_2^-$, EA = -1.5 ^ 96.48 = -145 , $\Delta_fH\ (KH_2) = -1445$

$\Delta_fH\ (KH_2^-) = -1590$

Some electron affinities of fragments were estimated, according to known electron affinities, to complete the calculations of enthalpies (Table 23).[18,19] The estimated electron affinities are indicated by 'Estimated' in this table.

Table 13: The literature and the estimated values for electron affinities of fragments

Fragment	Electron affinity, eV	Fragment	Electron affinity, eV	Fragment	Electron affinity, eV
Fe	0.151	FeH	0.934	FeH2	1.049
Co	0.663	CoH	0.671	CoH2	1.45
Cu	1.236	CuH	0.444	CuH2	2.60
Ag	1.304	AgH	Estimated 0.40	AgH2	Estimated 2.90
Cs	0.471	CsH	Estimated 0.72	CsH2	Estimated 1.60
K	0.501	KH	Estimated 0.70	KH2	Estimated 1.50

Appendix 7: Enthalpies of some reactions

Reaction	Enthalpy (kJ/mol)
$Fe^- + H^+ \rightarrow HFe$	1439[18]
$Cu^- + H^+ \rightarrow HCu$	1451[18]
$Co^- + H^+ \rightarrow HCo$	1411[18]
$Ag^- + H^+ \rightarrow HAg$	1406[18]
$Cs^- + H^+ \rightarrow HCs$	1441[18]
$K^- + H^+ \rightarrow HK$	1439[18]
$HFe^- + H^+ \rightarrow H_2Fe$	1497[18]
$C_5H_{10} + H_2 \rightarrow C_5H_{12}$	-126.6[18]
$C_5H_{11}^- + H^+ \rightarrow C_5H_{12}$	1720[18]
$C_5H_9^- + H^+ \rightarrow$ ⌂	1750[18]
$C_5H_7^- + H^+ \rightarrow CH_3CH_2CH_2C{\equiv}CH$	1589[18]

Appendix 8: MassLynx settings

a) Below are guideline settings for an all RF experiment:

Source		**Analyzer**		**Acquire**	
Capillary	2.95 kV	LM Res 1	15	Function	MS
Cone	60 V	HM Res 1	15	Data Format	Continuum
Extractor	7 V	Energy 1	2	Set Mass	
RF Lens	0.2 V	Entrance	50	Start Mass	5 amu
Source Block Temp.	80 ˚c	Collision	0	End Mass	300 amu
Desolvation Temp.	170 ˚c	Exit	50	Scope Gain	32
		LM Res 2	15	Scan Time	2 sec.
		HM Res 2	15	Inter Scan Time	0.25 sec.
		Energy 2	2	Run Duration	200 min.
		Multiplier 2	650 V		

b) Below are guideline settings for a CID experiment:

Source		**Analyzer**		**Acquire**	
Capillary	2.95 kV	LM Res 1	12	Function	Daughter
Cone	60 V	HM Res 1	12	Data Format	Continuum
Extractor	7 V	Energy 1	2	Set Mass	56
RF Lens	0.2 V	Entrance	50	Start Mass	5 amu
Source Block	80 ˚c	Collision	0	End Mass	100 amu

Temp.					
Desolvation Temp.	170 ˚c	Exit	50	Scope Gain	32
		LM Res 2	12	Scan Time	2 sec.
		HM Res 2	12	Inter Scan Time	0.25 sec.
		Energy 2	2	Run Duration	200 min.
		Multiplier 2	650 V		

c) Below are guideline settings for a reaction experiment:

Source		**Analyzer**		**Acquire**	
Capillary	2.95 kV	LM Res 1	12	Function	Daughter
Cone	60 V	HM Res 1	12	Data Format	Continuum
Extractor	7 V	Energy 1	2	Set Mass	56
RF Lens	0.2 V	Entrance	50	Start Mass	5 amu
Source Block Temp.	80 ˚c	Collision	0	End Mass	200 amu
Desolvation Temp.	170 ˚c	Exit	50	Scope Gain	32
		LM Res 2	12	Scan Time	2 sec.
		HM Res 2	12	Inter Scan Time	0.25 sec.
		Energy 2	2	Run Duration	200 min.
		Multiplier 2	650 V		